T.C.
MARMARA UNIVERSITY
FACULTY OF ENGINEERING
MECHANICAL ENGINEERING DEPARTMENT

EXPERIMENTAL STUDY AND NUMERICAL SIMULATION OF CI ENGINE

Serhat Selim BALSEVEN

Advisor:
Ass. Prof. Dr. Mustafa YILMAZ

İSTANBUL 2014

T.C.
MARMARA UNIVERSITY
FACULTY OF ENGINEERING
MECHANICAL ENGINEERING DEPARTMENT

EXPERIMENTAL STUDY AND NUMERICAL SIMULATION OF CI ENGINE

Serhat Selim BALSEVEN

Advisor	Head of Department
Ass. Prof. Dr. Mustafa YILMAZ	Prof. Dr. AbdülKerim KAR
…….	…….

İSTANBUL 2014

ABSTRACT

In this project, worked on the four cylinder four stroke diesel engine experiment system and measured some values like intake air temperature, intake manifold pressure, air-mass, injected fuel quantity, oil temperature, exhaust gas temperature depending on engine speed with using of different sensor types. After that, some theoretical diesel cycle calculation are made and 1D simulation is performed on the GT Power simulation program. Finally, evaluation of data from the simulation is compared the results between the theoretical, numerical and experimental.

ACKNOWLEDGEMENT

I thank to my advisor Ass. Prof. Dr. Mustafa YILMAZ, Mechanical Engineering Department Researcher Hasan KÖTEN and also, Technology Faculty Mechanical Engineering Department Researcher İlker Turgut YILMAZ.

TABLE OF CONTENT page

LIST OF TABLES **page**

LIST OF FIGURES **page**

NOMENCLATURE

$\bar{U}_P$	=	Average piston speed (m/s)
$\dot{W}_b$	=	Brake power (kj/s)
$\dot{m}_a$	=	Mass flow rate of air (kg/s)
$\dot{m}_f$	=	Mass flow rate of fuel (kg/s)
$\bar{y}_i$	=	Average Numerical Value
ρ_a	=	Air density (kg/m^3)
A_p	=	Piston cross-sectional area (m^2)
$\dot{W}$	=	Power (kj/s)
c_p	=	Specific heat at constant pressure (kj/kg*K)
c_v	=	Specific heat at constant volume (kj/kg*K)
$\dot{m}$	=	Mass flow rate (kg/s)
m_a	=	Mass of air (kg)
m_f	=	Mass of fuel (kg)
r_c	=	Compression ratio
w_T	=	Temperature Determination Error Ratio
w_p	=	Pressure Determination Error Ratio
w_λ	=	Excess Air Coefficient Measurement Error Ratio

w_τ = Ignition Delay Error Ratio

y_{gi} = Numerical Value

y_i = Theoretical Value

η_c = Combustion efficiency

η_t = Thermal efficiency

η_v = Volumetric efficiency

$\bar{\sigma}$ = Percentage Mean Deviation

Δh = Change in enthalpy from standard conditions (kj/kg mole)

Δv = Change in the volume (L)

a = Crank Offset (cm)

AF = Air fuel ratio (kg_a/kg_f)

B = Bore (cm)

bmep = Break mean effective pressure (kpa)

bsfc = Break specific fuel consumption (kg/kj)

E = Activation Energy (j/mole)

F = y dependent variables is dependent on the variable number

Isfc = Indicated specific fuel consumption (kg/kj)

k = Ratio of specific heats

mep = Mean effective pressure (kpa)

N = Engine Speed (RPM)

n = Number of revolution per cycle

P = Pressure (kpa)

Q = Heat transfer (kj)

q = Heat transfer per unit mass (kj/kg)

r = Connecting Rod Length (cm)

R = Gas constant (kj/kg*K)

R = Ratio of connecting rod length to crank offset

S	=	Stroke (cm)
s	=	Distance between wrist pin and crank shaft axis (cm)
sfc	=	Specific fuel consumption (kg/kj)
T	=	Temperature (K) (℃)
t	=	Time (s)
T_i	=	Intake temperature (K) (℃)
u	=	Specific ınternal energy (kj/kg)
U_p	=	Piston speed (m/s)
V	=	Cylinder Volume (m^3)
V_{BDC}	=	Cylinder volume at bottom dead center (L)
V_c	=	Clearance Volume (L)
V_d	=	Displacement Volume (L)
V_{TDC}	=	Cylinder volume at bottom dead center (L)
w	=	Specific work (kj/kg)
W	=	Work (kj)
W_b	=	Brake power (kj)
w_b	=	Break specific work (kj/kg)
W_f	=	Friction work (kj)
W_i	=	Indıcated work (kj)
z	=	Number of Experiment
β	=	Cutoff ratio
ɵ	=	Crank Angle
m	=	Mass (kg)
σ	=	Percentage Deviation
τ	=	Torque (N-M)
π	=	3.14159…..

1.INTRODUCTION

The performance of a gas-fuelled diesel engine (dual fuel) is examined at light load and an effective threshold limit to the combustion of the gaseous fuel through bulk flame spread is specified. The relationship of such a limit to some of the key operating parameters is then discussed. A contrasting between the measured values of the limit with those agrement to the lower flammability limits of the gaseous fuel when assessed under the dominant cylinder conditions during pilot diesel fuel ignition displayed similar mode. It is suggested that such a similarity may form a basis for estimating the lean functional limits for dual fuel combustion in engines. A simple approach for estimating the limiting equivalence ratio for the clear bulk flame spread limit is described for a methane-fuelled dual fuel engine (O. Badr, G.A. Karim, et al,1998). The present contribution describes an experimental investigation conducted on a single cylinder DI Diesel engine, which has been properly modified to operate under dual fuel conditions. The primary amount of fuel is the gaseous one, which is ignited by a pilot Diesel liquid injection. Comparative results are given for various engine speeds and loads for conventional Diesel and dual fuel operation, revealing the effect of dual fuel combustion on engine performance and exhaust emissions (R.G. Papagiannakis, D.T. Hountalas, 2003). The authors research work concerns the use of biogas in dual-fuel diesel engines. It examines engine performance using simulated biogas of varying quality representing the range of methane: carbon dioxide composition which may be encountered in gas from different sources. The total programme includes the effects of biogas quality and of the proportion of energy from pilot fuel injection over a range of speeds and loads, in vestigations into the performance parameters over a range of compositions of gaseous mixture. A two cylinder, indirect-injection diesel engine of stationary type is being used as the first experimental test bed in this work and the variation of quality is provided by mixing natural gas and carbon dioxide. A data acquisition system for in-cylinder pressure and crank angle is being used successfully and some emissions measurements are also available, particularly for CO and O2. One of the authors is from India where there is thought to be considerable potential for exploiting the gaseous products from resources such as biogas, landfill and sewage gas through small stationary dual-fuel engines for irrigation and CHP applications. The nature of combustion process in the dual-fuel engine is examined by the authors through pressure-crank angle data and studies of characteristics affecting engine efficiency (A. Henham and M. K. Makkar, 1998). It is well known that the operation of dual fuel engines at lower loads suffers from lower thermal efficiency and higher unburned percentages of fuel. To rectify this problem, tests have been conducted on a special single cylinder compression ignition research engine (Ricardo E6) to investigate the effect of pilot fuel quantity on the performance of an indirect injection diesel engine fuelled with gaseous fuel. Diesel fuel was used as the pilot fuel and methane or propane was used as the main fuel which was inducted into the intake manifold to mix with the intake air. Through experimental investigations, it is shown that, the low efficiency and excess emissions at light loads can be improved significantly by increasing the amount of pilot fuel, while increasing the amount of pilot fuel at high loads led to early knocking (G.H. Abd Alla, H.A. Soliman, et al,1998). Methane and carbon dioxide are the two main constituents of biogas. Biogas also contains traces of nitrogen, hydrogen, oxygen and hydrogen sulphide. When diesel engine runs on biogas, the combustion is poor as comuared

to diesel fuel. One of the reason of poor combustion is the presence of carbon dioxide in the biogas. Percentage of methane and carbon dioxide in biogas varies with the maturities of feed stock, temperature, water content, loading rate of raw material and bacterial actions. We see that, the effect of variations of carbon dioxide in biogas on the performance of the engine to simulate the performance of the engine running with biogas from different sources (varying proportion of methane and carbon dioxide) (Saiful Bari,1996). An analysis of the cycle-to-cycle combustion variation as reflected in the combustion pressure data of a single cylinder, naturally aspirated, four stroke, Ricardo E6 engine converted to run as dual fuel engine on diesel and gaseous fuel of LPG or methane. A measuring set-up consisting of a piezo-electric pressure transducer with charge amplifier and fast data acquisition card installed on an IBM microcomputer was used to gather the data of up to 1200 consecutive combustion cycles of the cylinder under various combination of engine operating and design parameters. These parameters included type of gaseous fuel, engine load, compression ratio, pilot fuel injection timing, pilot fuel mass, and engine speed. The data for each operating conditions were analyzed for the maximum pressure, the maximum rate of pressure rise representing the combustion noise, and indicated mean effective pressure. The cycle-to-cycle variation is expressed as the mean value, standard deviation, and coefficient of variation of these three parameters. It was found that the type of gaseous fuel and engine operating and design parameters affected the combustion noise and its cyclic variation and these effects have been presented (Mohamed Y.E. Selim, 2004). Nuclear power plants used uranium as fuel, and are not renewable, that has revealed as wastes constitute a serious concern for the environment. Today in the world with 350 GW installed capacity of nuclear power plants, approximately 10 thousand tons of used fuel, ie, "nuclear waste" is produced. Today the amount of accumulated nuclear waste has exceeded 250 thousand tons. In countries with nuclear power plants, storage of used fuel is a growing problem the urgency. If this problem cannot be resolved, some of the reactors will be forced to shut down. Because these reactors, the amount of waste which they produce throughout the operating life is not capable to store all (IEA, 2009). In this study, Combustion and emission characteristics of dual-fuel engines which use natural gas, biogas, producer gas, methane, liquefied petroleum gas, propane, etc. as gaseous fuel. It reveals that ‘dualfuel concept’ is a promising technique for controlling both NOx and soot emissions even on existing diesel engine. But, HC, CO emissions and ‘bsfc’ are higher for part load gas diesel engine operations. Thermal efficiency of dual-fuel engines improve either with increased engine speed, or with advanced injection timings, or with increased amount of pilot fuel. The ignition characteristics of the gaseous fuels need more research for a long-term use in a dual-fuel engine. It is found that, the selection of engine operating and design parameters play a vital role in minimizing the performance divergences between an existing diesel engine and a ‘gas diesel engine’ (B.B. Sahoo, N. Sahoo, et al, 2008). Combustion pressure rise rate and thermal efficiency data are measured and presented for a dual fuel engine running on a dual fuel of Diesel and compressed natural gas and utilizing exhaust gas recirculation (EGR). The maximum pressure rise rate during combustion is presented as a measure of combustion noise. The experimental investigation on the dual fuel engine revealed the noise generated from combustion and the thermal efficiency at different EGR ratios. A Ricardo E6 Diesel version engine is converted to run on a dual fuel of Diesel and compressed natural gas and having an exhaust gas recycling system is used throughout the work. The engine is fully

computerized, and the cylinder pressure data and crank angle data are stored in a PC for offline analysis. The effects of EGR ratio, engine speeds, loads, temperature of recycled exhaust gases, intake charge pressure and engine compression ratio on combustion noise and thermal efficiency are examined for the dual fuel engine. The combustion noise and thermal efficiency of the dual fuel engine are found to be affected when EGR is used in the dual fuel engine (Mohamed Y.E. Selim, 2001). This study Investigates the effect of variation in LPG composition on emissions and performance characteristics in a dual fuel engine run on diesel fuel and five gaseous fuel of LPG with different composition. To quantify the best LPG composition for dual fuel operation especially in order to improve the exhaust emissions quality while maintaining high thermal efficiency comparable to a conventional diesel engine, a two-cylinder, naturally aspirated, four-stroke, DI diesel engine converted to run as pilot-injected dual fuel engine. The tests and data collection were performed under various conditions of load at constant engine speed. From the results, it is observed that the exhaust emissions and fuel conversion efficiency of the dual fuel engine are found to be affected when different LPG composition is used as higher butane content lead to lower NOx levels while higher propane content reduces CO levels. Fuel #3 (70% propane, 30% butane) with mass fraction 40% substitution of the diesel fuel was the best LPG composition in the dual fuel operation except that at part loads. Also, tests were made for fuel #3-diesel blend in the dual fuel operation at part loads to improve the engine performances and exhaust emissions by using the Exhaust Gas Recirculation (EGR) method (H.E. Saleh, 2007). The result of this study describes the obtained from CI engine performance running on dual fuel mode at fixed engine speed and four loads, varying the mixing system and pilot fuel quality, associated with fuel composition and cetane number. The experiments were carried out on a power generation diesel engine at 1500 m above sea level, with simulated biogas (60% CH4–40% CO2) as primary fuel, and diesel and palm oil biodiesel as pilot fuels. Dual fuel engine performance using a naturally aspirated mixing system and diesel as pilot fuel was compared with engine performance attained with a supercharged mixing system and biodiesel as pilot fuel. For all loads evaluated, was possible to achieve full diesel substitution using biogas and biodiesel as power sources. Using the supercharged mixing system combined with biodiesel as pilot fuel, thermal efficiency and substitution of pilot fuel were increased, whereas methane and carbon monoxide emissions were reduced (Iván Darío Bedoya, et al, 2008). At the spark-ignition engines burned biogas (65% CH4+ 35% CO2) in the form of experimental data and computer simulation analysis is performed (Stone, C. R., Gould, et al, 1993). In the effort to reduce pollutant emissions from diesel engines various solutions have been proposed, one of which is the use of natural gas as supplement to liquid diesel fuel, with these engines referred to as fumigated, dual fuel, compression ignition engines. One of the main purposes of using natural gas in dual fuel (liquid and gaseous one) combustion systems is to reduce particulate emissions and nitrogen oxides. Natural gas is a clean burning fuel; it possesses a relatively high auto-ignition temperature, which is a serious advantage over other gaseous fuels since then the compression ratio of most conventional direct injection (DI) diesel engines can be maintained high. In the present work, an experimental investigation has been conducted to examine the effects of the total air–fuel ratio on the efficiency and pollutant emissions of a high speed, compression ignition engine located at the authors' laboratory, where liquid diesel fuel is partially substituted by natural gas in various proportions, with the natural gas

fumigated into the intake air. The experimental results disclose the effect of these parameters on brake thermal efficiency, exhaust gas temperature, nitric oxide, carbon monoxide, unburned hydrocarbons and soot emissions, with the beneficial effect of the presence of natural gas being revealed. Given that the experimental measurements cover a wide range of liquid diesel supplementary ratios without any appearance of knocking phenomena, the belief is strengthened that the findings of the present work can be very valuable if opted to apply this technology on existing DI diesel engines (R.G. Papagiannakis, C.D. Rakopoulos, 2009). This study perforn of Investigate the effect of premixed fuel ratio on the combustion and emission characteristics in diesel engine by the experimental and numerical method. In order to investigate the effect of various factors such as the premixed ratio, EGR rate, and equivalence ratio on the exhaust gas from the premixed charge compression ignition diesel engine, the injection amount of premixed fuel is controlled by electronic port injection system. The range of premixed ratio between dual fuels used in this study is between 0 and 0.85, and the exhaust gas is recirclulated up to 30 percent of EGR rate (Chang Sik Lee, et al, 2002). A single-cylinder diesel engine has been converted into a dual-fuel engine to operate with natural gas together with a pilot injection of diesel fuel used to ignite the CNG–air charge. The CNG was injected into the intake manifold via a gas injector on purpose designed for this application. The main performance of the gas injector, such as flow coefficient, instantaneous mass flow rate, delay time between electrical signal and opening of the injector, have been characterized by testing the injector in a constant-volume optical vessel. The CNG jet structure has also been characterized by means of shadowgraphy technique. The engine, operating in dual-fuel mode, has been tested on a wide range of operating conditions spanning different values of engine load and speed. For all the tested operating conditions, the effect of CNG and diesel fuel injection pressure, together with the amount of fuel injected during the pilot injection, were analyzed on the combustion development and, as a consequence, on the engine performance, in terms of specific emission levels and fuel consumption (A.P. Carlucci, A. de Risi, et al, 2006). The present contribution is mainly concerned, with an experimental investigation of the characteristics of dual fuel operation when liquid diesel is partially replaced with natural gas under ambient intake temperature in a DI diesel engine. Results are given revealing the effect of liquid fuel percentage replacement by natural gas on engine performance and emissions (R.G. Papagiannakis, D.T. Hountalas, 2002). The aim of the this paper is to investigate the emission and performance characteristics of a commercial diesel engine (Deutz FL8 413F) being operated on natural gas with pilot diesel ignition. A computer program has been developed to model the experimental data usinga chemical kinetic reaction mechanism of the Gas–Diesel (dual-fuel) combustion. A detailed chemical kinetic reaction mechanisms of natural gas and NOx were used to predict the main combustion characteristics (temperature, pressure and species concentrations) under the conditions of this study. The followingse ctions include a description of the experimental facilities, discussion of numerical simulation and engine test results. The performance in terms of accuracy of the networks is assessed by comparison with the experiments. A reasonably good prediction of performance and emission was obtained by computation covering the whole range of the engine operating conditions (Cheikh Mansour, Abdelhamid Bounif, et al, 1999). Combustion pressure data are measured and presented for a dual fuel engine running on dual fuel of diesel and compressed natural gas, and compared to the diesel engine case. The maximum pressure rise rate during

combustion is presented as a measure of combustion noise. Experimental investigation on diesel and dual fuel engines revealed the noise generated from combustion in both cases. A Ricardo E6 diesel version engine is converted to run on dual fuel of diesel and compressed natural gas and is used throughout the work. The engine is fully computerized and the cylinder pressure data, crank angle data are stored in a PC for off-line analysis. The effect of engine speeds, loads, pilot injection angle, and pilot fuel quantity on combustion noise is examined for both diesel and dual engine. Maximum pressure rise rate and some samples of ensemble averaged pressure–crank angle data are presented in the present work. The combustion noise, generally, is found to increase for the dual fuel engine case as compared to the diesel engine case (Mohamed Y.E. Selim, 2000). The paper describes some aspects of the findings of an investigation which was initiated mainly to obtain a better understanding of the phenomenon of knock under dual-fuel operation and to determine the effect of various operating parameters on the knock-free performance limits and the nature of these limits. Some common gaseous fuels such as methane, propane, ethylene, acetylene, hydrogen and somc of their mixtures were used as the main fuels. A method is suggested to relate changes in the knock-limited power output of a dual-fuel engine with the intake temperature of the charge and the nature of the main fuel used (G. A. Karim, A.M.I, et al, 1966). A thermodynamic multizone model incorporating detailed kinetic schemes has been developed for the prediction of the combustion processes in dual-fuel engines and some of their performance features. The consequences of the interaction between the gaseous and the diesel fuels and the resulting modification to the combustion processes are considered. A reacting zone has been incorporated in the model to describe the partial oxidation of the gaseous fuel–air mixture. The associated formation and concentrations of exhaust emissions are correspondingly established. The model can predict the onset of knock as well as the operating features and emissions for the more demanding case of light load performance. Predicted values for methane operation show good agreement with corresponding experimental values (Z Liu, G A Karim, 1996). The combustion characteristics of a turbocharged natural gas and diesel dual-fuelled compression ignition engine are investigated. With the measured cylinder pressures of the engine operated on pure diesel and dual fuel, the ignition delay, effects of pilot diesel and engine load on combustion characteristics are analysed. Emissions of HC, CO, NOx and smoke are measured and studied too. The results show that the quantity of pilot diesel has important effects on the performance and emissions of a dual-fuel engine at low-load operating conditions. Ignition delay varies with the concentration of natural gas. Smoke is much lower for the developed dual-fuel engine under all the operating conditions (Liu Shenghua, Zhou Longbao, et al, 2002). A direct-injection CI engine, was fuelled with three different gaseous fuels: methane, propane, and butane. The engine performance at various gaseous concentrations was recorded at 1500 r/min and quarter, half, and three-quarters relative to full a load of 18.7 kW. In order to investigate the combustion performance, a novel three-zone heat release rate analysis was applied to the data. The resulting heat release rate data are used to aid understanding of the performance characteristics of the engine in dual-fuel mode. Data are presented for the heat release rates, effects of engine load and speed, brake specific energy consumption of the engine, and combustion phasing of the three different primary gaseous fuels. Methane permitted the maximum energy substitution, relative to diesel, and yielded the most significant reductions in

CO2. However, propane also had significant reductions in CO2 but had an increased diffusional combustion stage which may lend itself to the modern high-speed direct-injection engine (J Stewart, A Clarke, et al, 2006). Engine performance, diesel fuel substitution, energy consumption and long term use have been concerned. The attained results show that biogas–diesel dual fuelling of this engine revealed almost no deterioration in engine performance but lower energy conversion efficiency which was offset by the reduced fuel cost of biogas over diesel. The long term use of this engine with biogas– diesel dual fuelling is feasible with some considerations (Phan Minh Duc, Kanit Wattanavichien, 2006). Many of these studies were carried out for automotive applications. In this thesis, without going on too much of a spark-ignited engine modifications are discussed in the experimental biogas hydrogen mixtures. Content of biogas is %65 CH4+ % 35% CO2, 60% CH4+ % 40CO2 and 55% CH4+, 45% CO2 and in the case of a 15% hydrogen addition to biogas engine performance and emissions are discussed. Experiments have been repeated for the different excess air factor and different engine speeds. Energy is an essential element of social life for the prosperity of people and to lead a more comfortable life. In the historical period, the using of the energy begins with human existence. Since first ancient times, people have benefitted from the power of fire and animals when there was not enough energy to do their job. The coal was used a primary energy sources until the 19th century on the steam machines and the heating purposes after the finding by Chinese. The discovery of oil in the State of Pennsylvania in America, natural gas, fuel oil and oil derivatives used as gasoline fossil origin and has up to the present (Gezgin E., 2003). Combustion noise, knock and ignition limits data are measured and presented for a dual fuel engine running on dual fuels of Diesel and three gaseous fuels separately. The gaseous fuels used are liquefied petroleum gas, pure methane and compressed natural gas mixture. The maximum pressure rise rate during combustion is presented as a measure of combustion noise, and the knocking and ignition limits are presented as torque output at the onset of knocking and ignition failure. Experimental investigation on the dual fuel engine revealed the noise generated from combustion, knocking and ignition limits for all gases at different design and operating conditions. A Ricardo E6 Diesel version engine is converted to run on dual fuel of Diesel and the tested gaseous fuel and is used throughout the work. The engine is fully computerized, and the cylinder pressure data, crank angle data and engine operating variables are stored in a PC for off line analysis. The effects of engine speeds, loads, pilot injection angle, pilot fuel quantity and compression ratio on combustion noise, knocking torque, thermal efficiency and maximum pressure are examined for the dual engine running on the three gaseous fuels separately. The combustion noise, knocking and ignition limits are found to relate to the type of gaseous fuels and to the engine design and operating parameters (Mohamed Y.E. Selim, 2002). The depletion of fossil fuels is understood by most energy users to be an inevitability. Researchers all over the world focus their attention on the development of various alternative fuels. It is believed that the use of compressed natural gas (CNG), as an alternative to conventional fuels will result in low levels of emissions. However, the use of CNG as the main fuel in a diesel engine with the diesel fuel used as an igniter has always been associated with some problems. The main problem in such a dual-fuel engine is the increased tendency toward detonation because of the high compression ratio of the engine. The current work is an experimental investigation of such a problem. An extensive experimental program was carried out on a variable compression ratio Recardo E6 engine.

The results of the current investigation indicate that the dual-fuel engine can operate detonation-free for a compression ratio of 16.5. The results also indicate that dual-fuel engines are lower than diesel engines in brake thermal efficiency, brake power, and brake mean effective pressure at all loads. On the other hand, CO and NO emissions are higher at high loads. However, at low loads, dual-fuel engines give lower NO (M. G. Galal, M.M. Abdel Aal, et al, 2002). This papers examine the exhaust waste heat recovery potential of a high-efficiency, low-emissions dual fuel low temperature combustion engine using an Organic Rankine Cycle (ORC). Potential improvements in fuel conversion efficiency (FCE) and specific emissions (NOx and CO2) with hot exhaust gas recirculation (EGR) and ORC turbocompounding were quantified over a range of injection timings and engine loads. With hot EGR and ORC turbocompounding, FCE improved by an average of 7 percentage points for all injection timings and loads while NOx and CO2 emissions recorded an 18 percent (average) decrease. From pinch-point analysis of the ORC evaporator, ORC heat exchanger effectiveness (3), percent EGR, and exhaust manifold pressure were identified as important design parameters. Higher pinch point temperature differences (PPTD) uniformly yielded greater exergy destruction in the ORC evaporator, irrespective of engine operating conditions. Increasing percent EGR yielded higher FCEs and stable engine operation but also increased exergy destruction in the ORC evaporator. It was observed that hot EGR can prevent water condensation in the ORC evaporator, thereby reducing corrosion potential in the exhaust piping. Higher 3 values yielded lower PPTD and higher exergy efficiencies while lower 3 values decreased post-evaporator exhaust temperatures below water condensation temperatures and reduced exergy efficiencies (Kalyan K. Srinivasan, Pedro J. Mago, et al, 2009). In addition, the establishment of a nuclear power plant and the dismantling of the facility are quite expensive when compared to other energy sources. All of these developments and concerns about the future, the search for alternative energy sources to renewable energy sources in the world has started directly. Renewable energy source is defined as", "in their cycles of nature, the next day the same energy source that may be present. By definition, conventional energy sources are not considered as a renewable energy source. During 2008-2030, world energy demand is estimated to be 1.6% of the average annual surplus. At the end of this period, by the year 2030, total energy demand is expected to be 45% (Görez, T., Alkan, A.).In this study, experiments were performed on 4 cylinder turbocharged, intercooled with 62.5 kW gen-set diesel engine by using hydrogen, liquefied petroleum gas (LPG) and mixture of LPG and hydrogen as secondary fuels. The experiments were performed to measure ignition delay period at different load conditions and various diesel substitutions. The experimental results have been compared with ignition delay correlation laid down by other researchers for diesel and dual fuel diesel engine. It is found that ignition delay equation based on pressure, temperature and oxygen concentration for a dual fuel diesel engine run on dieselebiogas gives variation up to 6.56% and 14.6% from the present experimental results,while ignition delay equation for a pure diesel engine gives 7.55%and 33.3% variation at lower and higher gaseous fuel concentrations, respectively. It is observed that the ignition delay of dual fuel engine depends not only on the type of gaseous fuels and their concentrations but also on charge temperature, pressure and oxygen concentration (D.B. Lata, Ashok Misra, 16 October 2010). This study Investigated the combustion and emissions characteristics of a compression-ignition engine using a dual-fuel

approach with ammonia and diesel fuel. Ammonia can be regarded as a hydrogen carrier and used as a fuel, and its combustion does not produce carbon dioxide. Ammonia vapor was introduced into the intake manifold and diesel fuel was injected into the cylinder to initiate combustion. The test engine was a four-cylinder, turbocharged diesel engine with slight modifications to the intake manifold for ammonia induction. An ammonia fueling system was developed, and various combinations of ammonia and diesel fuel were successfully tested. One scheme was to use different combinations of ammonia and diesel fuel to achieve a constant engine power. The other was to use a small quantity of diesel fuel and vary the amount of ammonia to achieve variable engine power. Under the constant engine power operation, in order to achieve favorable fuel efficiency, the preferred operation range was to use 40–60% energy provided by diesel fuel in conjunction with 60–40% energy supplied by ammonia. Exhaust carbon monoxide and hydrocarbon emissions using the dual-fuel approach were generally higher than those of using pure diesel fuel to achieve the same power output, while NOx emissions varied with different fueling combinations. NOx emissions could be reduced if ammonia accounted for less than 40% of the total fuel energy due to the lower combustion temperature resulting in lower thermal NOx. If ammonia accounted for the majority of the fuel energy, NOx emissions increased significantly due to the fuel-bound nitrogen. On the other hand, soot emissions could be reduced significantly if a significant amount of ammonia was used due to the lack of carbon present in the combination of fuels. Despite the overall high ammonia conversion efficiency (nearly 100%), exhaust ammonia emissions ranged from 1000 to 3000 ppmV and further after-treatment will be required due to health concerns. On the other hand, the variable engine power operation resulted in relatively poor fuel efficiency and high exhaust ammonia emissions due to the lack of diesel energy to initiate effective combustion of the lean ammonia-air mixture. The in cylinder pressure history was also analyzed, and results indicated that ignition delay increased with increasing amounts of ammonia due to its high resistance to autoignition. The peak cylinder pressure also decreased because of the lower combustion temperature of ammonia. It is recommended that further combustion optimization using direct ammonia/diesel injection strategies be performed to increase the combustion efficiency and reduce exhaust ammonia emissions (Aaron J. Reiter, Song-Charng Kong, 2010). Human beings have to seek new sources of energy because of fossil fuels damage the environment and the reserves of this resource is limited. Today, the world of nuclear energy as well as new and clean sources of energy called geothermal, solar, wind and biogas energy in recent years focus on the most researched subject, and constitute (Kum. H., 1999). The results of an extensive experimental campaign about dual fuel combustion development and the related pollutant emissions are reported, paying particular attention to the effect of both the in-cylinder charge bulk motion and methane supply method. A diesel common rail research engine was converted to operate in dual fuel mode and, by activating/deactivating the two different inlet valves of the engine (i.e. swirl and tumble), three different bulk flow structures of the charge were induced inside the cylinder. A methane port injection method was proposed, in which the gaseous fuel was injected into the inlet duct very close to the intake valves, in order to obtain a stratified-like air–fuel mixture up to the end of the compression stroke. For comparison purposes, a homogeneous-like air–fuel mixture was obtained injecting methane more upstream the intake line. Combining the different positions of the methane injector and the three possible bulk

flow structures, seven different engine inlet setup were tested. In this way, it was possible to evaluate the effects on dual fuel combustion due to the interaction between methane injector position and charge bulk motion. In addition, methane injection pressure and diesel pilot injection parameters were varied setting the engine at two operating conditions. For some interesting low load tests, the combustion development was studied more in detail by means of direct observation of the process, using an in-cylinder endoscope and a digital CCD camera. Each combustion image was post-processed by a dedicated software, in order to extract only those portions with flame presence and to calculate an average luminance value over the whole frame. These luminance values, chosen as indicators of the combustion intensity, were represented over crank angle position and, then, an analysis of the resulting curves was performed. Results showed that the charge bulk motion associated to the swirl port, improving the charge mixing of the diesel spray and the propagation of the turbulent flame fronts, is capable to enhance the oxidation of air–methane mixture, both at low and high engine loads. Furthermore, at low loads, the analysis of combustion images and luminance curves showed that methane port injection can significantly affect the intensity and the spreading of the flame during dual fuel combustion, especially when a suitable in-cylinder bulk motion is obtained. Concerning the engine emissions, some correlations with what observed during the analysis of the combustion development were found. Furthermore, it was revealed that, for several combinations of the engine operating parameters, methane port injection was always associated to the lowest emission levels, demonstrating that this methane supply method is a very effective strategy to reduce unburned hydrocarbons and nitric oxides concentrations, especially when implemented with variable intake geometry systems (Antonio P. Carlucci, Domenico Laforgia, et al, 2010). A single cylinder direct injection diesel research engine was modified to operate as the DDF engine. A gas mixer was installed on the intake manifold to supply natural gas to the engine. Test runs of normal and abnormal conditions were investigated and these include i) determination of diesel engine and DDF engine performance, ii) varying ratios of natural gas and diesel fuel while keeping constant engine speed and torque, iii) varying intake temperature while keeping constant engine speed and amount of natural gas and diesel fuel, and iv) varying amount of natural gas while keeping constant speed and amount of diesel fuel. Operating parameters such as engine speed, torque, and intake temperature, were controlled and recorded. The average cylinder pressure-time data were recorded and analyzed for all test conditions (Krisada Wannatong, Nirod Akarapanyavit, et al, 2007). In order to meet the energy requirements, there has been growing interest in alternative fuels like biodiesels, methyl alcohol, ethyl alcohol, biogas, hydrogen and producer gas to provide a suitable diesel oil substitute for internal combustion engines. Biomass is basically composed of carbon, hydrogen and oxygen. A proximate analysis of biomass indicates the volatile matter to be between 60–80% and 20–25% carbon and the rest, ash. The first part of sub-stoichiometric oxidation leads to the loss of volatiles from biomass and is exothermic; it results in peak temperatures of 1400–1500 K and generation of gaseous products like carbon monoxide, hydrogen in some proportions and carbon dioxide and water vapor, which in turn are reduced in part to carbon monoxide and hydrogen by the hot bed of charcoal generated during the process of gasification. Therefore, solid biomass can be converted into a mixture of combustible gases, and subsequently utilized for combustion in a CI engine. Producer gas, if used in dual fuel mode, is an excellent substitute for reducing the

amount of diesel consumed by the CI engine. Downdraft moving bed gasifiers coupled with an IC engine are a good choice for moderate quantities of available biomass, up to 500 kW of electric power. Vegetable oils present a very promising alternative to diesel oil since they are renewable and have similar properties. Vegetable oils offer almost the same power output with slightly lower thermal efficiency when used in diesel engines. Research in this direction with edible oils have yielded encouraging results, but their use as fuel for diesel engines has limited applications due to higher domestic requirement. In view of this, Honge oil (Pongamia Pinnata Linn) is selected and its viscosity is reduced by the transesterification process to obtain Honge oil methyl ester (HOME). Since vegetable oils produce higher smoke emissions, dual fuel operation could be adopted in order to improve their performance. A gas carburetor was suitably designed to maximize the engine performance in dual fuel mode with Honge oil–producer gas and HOME–producer gas respectively. Thus bio-derived gas and vegetable oil, when used in a dual fuel mode with carburetor, resulted in better performance with reduced emissions (N.R. Banapurmat, P.G. Tewari, 2008). The next 100 years is expected to run out of oil, coal and gas as the fossil origin considered as an alternative to conventional energy sources and nuclear power plants that began to be established in 170 the fast upward trend seems to be lost (Saygın, H., 2004). Dual fuel engines at part load inevitably suffer from lower thermal efficiency and higher emission of carbon monoxide and unburned fuel. The conducted to investigate the combustion characteristics of a dual fuel (Diesel–gas) engine at part loads using a single zone combustion model with detailed chemical kinetics for combustion of natural gas fuel. In this home made software, the presence of the pilot fuel is considered as a heat source that is deriving form two superposed Wiebe's combustion functions to account for its contribution to ignition of the gaseous fuel and the rest of the total released energy. The chemical kinetics mechanism consists of 112 reactions with 34 species. This combustion model is able to establish the development of the combustion process with time and the associated important operating parameters, such as pressure, temperature, heat release rate (HRR) and species concentration. Therefore, this work is an attempt to investigate the combustion phenomenon at part load and using exhaust gas recirculation (EGR) to improve the above mentioned problems. Also, the results of this work show that each of the different cases of EGR (thermal, chemical and radical cases) has an important role on the combustion process in dual fuel engines at part loads. It is found that all the different cases of EGR have positive effects on the performance and emission parameters of dual fuel engines at part loads despite the negative effect of some diluent gases in the chemical case, which moderates too much the positive effects of the thermal and radical cases of EGR. Predicted values show good agreement with corresponding experimental values over the whole range of engine operating conditions (V. Pirouzpanah, R. Khoshbakhti Saray, et al, 2007). The drawback of lean operation with hydrocarbon fuels is a reduced power output. Lean operation of hydrocarbon engines has additional drawbacks. Lean mixtures are hard to ignite, despite the mixture being above the low fire (point) limit of the fuel. This results in misfire, which increases un-burned hydrocarbon emissions, reduces performance and wastes fuel. Hydrogen can be used in conjunction with compact liquid fuels such as gasoline; alcohol or diesel provided each is stored separately. Mixing hydrogen with other hydrocarbon fuels reduces all of these drawbacks. Hydrogen's low ignition energy limit and high burning speed makes the hydrogen/hydrocarbon mixture easier to ignite, reducing misfire and thereby

improving emissions, performance and fuel economy. Regarding power output, hydrogen augments the mixture's energy density at lean mixtures by increasing the hydrogen-to-carbon ratio, and thereby improves torque at wide-open throttle conditions. The simulation program for determining the mole fraction of each of the exhaust species when the hydrogen is burnt along with diesel and the results are presented. The proportion of hydrogen in the hydrogen–diesel blend affecting the mole fraction of the exhaust species is also simulated. Experimental investigations were carried out, in hydrogen–diesel dual fuel mode, which showed a good agreement between the predicted and experimental results. The program code developed is valid for any combination of dual fuels (M. Masood, M.M. Ishrat, 2007). The limitations of an existing characteristic–time combustion (CTC) model are explored and a new combustion model is developed and applied to simulate combustion in dual-fuel engines in which the premixed natural gas is ignited by the combustion flame initiated by a diesel spray. The model consists of a diesel auto-ignition model and a flame propagation model. A G-equation-based model previously developed to simulate SI engine combustion was incorporated with an auto-ignition model to simulate the flame propagation process in partially premixed environments. The computer code is based on the KIVA-3V code and consists of updated sub-models to simulate more accurately the fuel spray atomization, auto-ignition, combustion, and emissions processes. Modifications were made to implement the level set G-equation approach and to track the location of the flame as a function of the turbulent flame speed, flame curvature, flow velocity, and the movement of the computational mesh in the engine environment. Good agreement with engine experiments was obtained by using the present model (S Singh, L Liang, et al, 2005). Experimental results of rapeseed methyl ester (RME) and diesel fuel used separately as pilot fuels for dual-fuel compression–ignition (CI) engine operation with hydrogen gas and natural gas (the two gaseous fuels are tested separately). During hydrogen dual-fuel operation with both pilot fuels, thermal efficiencies are generally maintained. Hydrogen dual-fuel CI engine operation with both pilot fuels increases NOx emissions, while smoke, unburnt HC and CO levels remain relatively unchanged compared with normal CI engine operation. During hydrogen dual-fuel operation with both pilot fuels, high flame propagation speeds in addition to slightly increased ignition delay result in higher pressure-rise rates, increased emissions of NOx and peak pressure values compared with normal CI engine operation. During natural gas dual-fuel operation with both pilot fuels, comparatively higher unburnt HC and CO emissions are recorded compared with normal CI engine operation at low and intermediate engine loads which are due to lower combustion efficiencies and correspond to lower thermal efficiencies. This could be due to the pilot fuel failing to ignite the natural gas–air charge on a significant scale. During dual-fuel operation with both gaseous fuels, an increased overall hydrogen–carbon ratio lowers CO2 emissions compared with normal engine operation. Power output (in terms of brake mean effective pressure, BMEP) as well as maximum engine speed achieved are also limited. This results from a reduced gaseous fuel induction capability in the intake manifold, in addition to engine stability issues (i.e. abnormal combustion). During all engine operating modes, diesel pilot fuel and RME pilot fuel performed closely in terms of exhaust emissions. Overall, CI engines can operate in the dual-fuel mode reasonably successfully with minimal modifications. However, increased NOx emissions (with hydrogen use) and incomplete combustion at low and intermediate loads (with natural gas use) are concerns; while port gaseous fuel induction limits power output at

high speeds (T. Korakianitis, A.M. Namasivayam, et al, 2011). As of the 2050, only 10% of fossil-based energy even in the case of the provision of nuclear energy, about 1,000 new nuclear power plants are to be established. However, even today there are 436 nuclear power plants around the world. Although it is possible the establishment of a new power plant to be built in 1000, even it will take dozens of years. The uranium reserves run out of quickly when the so many central are established. The International Atomic Energy Agency (IAEA), the global warming and climate change are required to intervene quickly to stop, but there is no way this fast dissemination of nuclear energy. Because the establishment of the first nuclear power plant to produce electricity takes at least 10 years (IEA, 2009).Depletion of fossils fuels and environmental degradation have prompted researchers throughout the world to search for a suitable alternative fuel for diesel engine. One such step is to utilize renewable fuels in diesel engines by partial or total replacement of diesel in dual fuel mode. In this study, acetylene gas has been considered as an alternative fuel for compression ignition engine, which has excellent combustion properties. Investigation has been carried out on a single cylinder, air cooled, direct injection (DI), compression ignition engine designed to develop the rated power output of 4.4 kW at 1500 rpm under variable load conditions, run on dual fuel mode with diesel as injected primary fuel and acetylene inducted as secondary gaseous fuel at various flow rates. Acetylene aspiration resulted in lower thermal efficiency. Smoke, HC and CO emissions reduced, when compared with baseline diesel operation. With acetylene induction, due to high combustion rates, NOx emission significantly increased. Peak pressure and maximum rate of pressure rise also increased in the dual fuel mode of operation due to higher flame speed. It is concluded that induction of acetylene can significantly reduce smoke, CO and HC emissions with a small penalty on efficiency (T. Lakshmanan, G. Nagarajan, 2009). The increase in demand and decrease in availability of fossil fuels with more stringent emission norms have led to research in finding an alternative fuel for internal combustion (IC) engines. Among the alternative fuels, gaseous fuels find a great potential. The gaseous fuel taken up for the present study is acetylene, which possesses excellent combustion properties. Preignition is the major problem with this fuel. In the present study, timed manifold injection technique is adopted to induct the fuel into the IC engine. A four-stroke, 4.4 kW diesel engine is selected, with slight modification in intake manifold for holding the gas injector, which is controlled by an electronic control unit (ECU). By using an ECU, an optimized injection timing of 10o after top dead center and 90o crank angle duration are arrived. At this condition, experiments were conducted for the various gas flow rates of 110 g/s, 180 g/s and 240 g/s. The performance was nearer to diesel at full load. Oxides of nitrogen, hydrocarbon and carbon monoxide emission decreased due to lean operation with marginal increase in smoke emission. To conclude, a safe operation of acetylene replacement up to 24% was possible with reduction in emission parameters (T. Lakshmanan, G. Nagarajan, 2010). An experimental investigation was performed to study the influence of dual-fuel combustion characteristics on the exhaust emissions and combustion performance in a diesel engine fueled with biogas–biodiesel dualfuel. In this work, the combustion pressure and the rate of heat release were evaluated under various conditions in order to analyze the combustion and emission characteristics for single-fuel (diesel and biodiesel) and dual-fuel (biogas–diesel and biogas–biodiesel) combustion modes in a diesel engine. In addition, to compare the engine performances and exhaust emission characteristics with combustion mode, fuel consumption,

exhaust gas temperature, efficiency, and exhaust emissions were also investigated under various test conditions. For the dual-fuel system, the intake system of the test engine was modified to convert into biogas and biodiesel of a dual-fueled combustion engine. Biogas was injected during the intake process by two electronically controlled gas injectors, which were installed in the intake pipe. The results of this study showed that the combustion characteristics of single-fuel combustion for biodiesel and diesel indicated the similar patterns at various engine loads. In dual-fuel mode, the peak pressure and heat release for biogas–biodiesel were slightly lower compared to biogas–diesel at low load. At 60% load, biogas–biodiesel combustion exhibited the slightly higher peak pressure, rate of heat release (ROHR) and indicated mean effective pressure (IMEP) than those of diesel. Also, the ignition delay for biogas–biodiesel indicated shortened trends compared to ULSD dual-fueling due to the higher cetane number (CN) of biodiesel. Significantly lower NOx emissions were emitted under dual-fuel operation for both cases of pilot fuels compared to single-fuel mode at all engine load conditions. Also, biogas–biodiesel provided superior performance in reductions of soot emissions due to the absence of aromatics, the low sulfur, and oxygen contents for biodiesel (Seung Hyun Yoon, Chang Sik Lee, 2011). A dual fuel engine is an internal combustion engine where the primary gaseous fuel source is pre-mixed with air as it enters the combustion chamber. This homogenous air fuel mixture is ignited by a small quantity of diesel known as the 'pilot' that is injected towards the end of the compression stroke. The diesel fuel ignites in the same way as in compression ignition (CI) engines, and the gaseous fuel is consumed by flame propagation in a similar manner to spark ignited engines. The motivation to dual-fuel a CI engine is partly economic due to the lower cost of the primary fuel, and partly environmental as some emissions characteristics are improved. A direct injection four cylinder CI engine, typically used in genset applications, was fuelled with three different gaseous fuels; methane, propane and butane. The performance and emissions (NOx and smoke) characteristics of various gaseous concentrations were recorded at 1500rpm (synchronous speed) and at ¼, ½, and ¾ load. In order to invest igate the combustion performance under these different conditions, a three zone heat release rate analysis is proposed an applied to the data. The resulting mass burned rate, ignition delay and combustion duration are used to explain the emissions and performance characteristics of the engine. The shown that the highest gas substitution levels were achieved when using methane under all test conditions, but emissions of NOx and smoke were lower when using propane. Butane proved to be the most unsatisfactory of the three primary fuels, with the highest emissions of NOx and smoke (J. Patterson, A. Clarke, et al, 2006). The first dual fuel measurements with pure jatropha oil and biogas, using a 12 kW diesel engine generator. Reference tests are done with pure jatropha oil and with diesel to characterize the engine's thermal efficiency nt, volumetric efficiency nv and air-excess ratio k versus output power. An extensive parameter study is done to predict/explain the effect of dual fuel operation on nv and k. Dual fuel experiments, adding different qualities (CH_4/CO_2 ratios) of synthetic biogas to the intake air, show that thermal efficiency is hardly affected for higher loads. For lower loads, biogas addition results in a decrease up to 10% in thermal efficiency, independent of biogas quality. Both nv and k decrease with addition of biogas, in quantitative agreement with predictions. The engine runs well up to a certain heat release fraction of methane; at higher fractions irregularities are observed, probably attributable to light end-gas knock (C.C.M.

Luijten, E. Kerkhof, 2010). The combustion knock characteristics of diesel engines running on natural gas using pilot injection as means of initiating combustion. The diesel engines knock under normal operating conditions but the knock referred to in this study is an objectionable one. In the dual-fuel combustion process we have the ignition stage followed by the combustion stage. There are three types of knock: diesel knock, spark knock and knock due to secondary ignition delay of the primary fuel (erratic knock). Several factors have been noted to feature in defining knock characteristics of dual-fuel engines that include ignition delay, pilot quantity, engine load and speed, turbulence and gas flow rate (O. Mınwafor, 2001). An alternative fuel such as natural gas may be used in a dual-fuel engine for both economic reasons and emission advantages. However, the performance at relatively light load and idling conditions has been quite poor, while at very high load, engine knock is often encountered. The studying of this way, a three-dimensional, dual-fuel, in-cylinder model has now been developed. This is used to provide an improved understanding of the operational features arising from the interaction between the gaseous fuel and the pilot fuel, the preignition processes, and subsequent combustion of the pilot fuel and gas during the piston movement (Haiyan Miao, Brian Milton, 2005). The mathematical models to predict pressure, net heat release rate, mean gas temperature, and brake thermal efficiency for dual fuel diesel engine operated on hydrogen, LPG and mixture of LPG and hydrogen as secondary fuels are developed. In these models emphasis have been given on spray mixing characteristics, flame propagation, equilibrium combustion products and in-cylinder processes, which were computed using empirical equations and compared with experimental results. This combustion model predicts results which are in close agreement with the results of experiments conducted on a multi cylinder turbocharged, intercooled gen-set diesel engine. The predictions are also in close agreement with the results on single cylinder diesel engine obtained by other researchers. A reasonable agreement between the predicted and experimental results reveals that the presented model gives quantitatively and qualitatively realistic prediction of in-cylinder processes and engine performances during combustion.(D.B. Lata, Ashok Misra, 16 September 2010). It is essential that there is a needed to provide a fuel from internal-combustion engines to obtain mechanical energy to heat energy. A kind of Biogas gas fuel compound is a center within 60% Methane (CH4), 40% carbon dioxide (CO2), and a very small amount of other compounds. It can be used as an ideal fuel for engines, when its burned is no longer material such as ash did not set (Uyarel A.Y. , Erşan K., 1987). In the future, with these features it will be a large potential (Biogas as Vehicle Fuel, A European Overview, 2003). Analyzed CH4-CO2-air mixtures with using of laminar turbulent Bunsen flame configuration in the variable pressures. Premix calculations and experimental results has shown that decreasing speed of laminar flame progressed with increasing of the CO2 dilutions. As a result, the average fuel consumption ratio is reduced by addition of CO2 but it has increased with the pressure (Cohe, C., Chauveau, C, et al, 2009). Have produced electricity from biogas by using a bus diesel engine. Optimum engine efficiency at 1.097 lambda and the ignition advance before top dead center in the % 54o C which 28.6 %. In 134.20 kW Power generator power output and CO and NOx emission values 1.154 and 896 ppm in order to achieved (Siripornakarachai and Sucharitakul, 2007). In 1992 They analyzed methane and carbon dioxide blends as fuel. A single cylinder CFR engine used. An increasing in braking power with equivalence ratio has increased and decreased in fuel ratio and carbon

dioxide. The high carbon dioxide ratio in fuel has caused high rate of unburned methane. The average temperature of the exhaust gas has reached the maximum value and decreased with the volumetric percentage of carbon dioxide. [Karim, G. A., Wierzba]. Biogas's components, the physical and chemical characteristics and the problems encountered in the use of researched their engines. Two types of biogas engines have developed: biogas-diesel dual fuel engine generator and the spark-ignition biogas engine generator. In addition, the said that biogas used as a fuel in the vehicles with compression and ruination (Jiang, Y., Xiong, S., et al, 2012). The effects of the constant speed of a spark-ignition engine the reduction of CO2 concentration in biogas about performance, emissions and the combustion efficiency were worked experimentally. In this study, the lime water scrubber which is used to decrease CO2 level in biogas is 41 %, 30% and 20%. The Experiments were carried out different rates of equivalence, the constant engine speed 1500 rpm and compression ratio 1: 1 from the rich mixture to poor mixture. CO2 level provides significant reduction in performance and that causes an increase in poor mixture with in particular watched that reduction in HC emissions. It was seen that there was poor combustion-combustion limit. Up to 10% of the CO2-level decline while NO levels enough to reduce HC levels will be important as they detect that (Porpatham, E., Ramesh., et al, 2008). Dump gas spark-ignition engines with the usage of a research carried out. Dump gas combustion characteristics and performance have worsened when the compared to methane, increasing the compression ratio and the improved performance of the ignition time dump gas performance recovery. Also studied the effects of the addition dump gas about 30% H2. Addition of small amounts of hydrogen, such as for example 3 - 5 % poor and rich combustion conditions give better results for development of performance particularly. In addition to add hydrogen developed combustion characteristics and in particularly the dump gas observed in poor and rich mixture with cyclic variations (Bade Shrestha, Narayanan, et al, 2008). In this study, the biogas is observed as experimental in the single-cylinder SI engine. They found, Presence of CO2 in the biogas can reduce NOx emissions but, the occupying of low cylinder pressure will be formed. Power of the engine and the brake thermal efficiency were reduced and HC emission levels were increased when the compared to the other gases (Huang, Crookes, 1998). Some research were made about the using of biogas in the dual-fuel diesel engines. The engine performance was analyzed for the variable rates of methane and carbon dioxide. The data system that is obtained for Cylinder pressure and the crankshaft angle can be used in a successful way (Henham A., Makkar, 1998). In addition during the flame emissions are saved, and the homogeneity has decreased. Presence of CO2 in the biogas reduced of the combustion speed (Forsich, C., Lacknera, et al, 2004). Compression ratio range has been found as the appropriate from 11.1 to 13.1 in the experiment which is using with biogas. The compression rates can be used very high, in cases where the biogas used for fuel. High compression ratios were found to increase the levels of HC and NOx (Crookes, 2006). They have worked on a SI engine operating in a closed loop by using a combination of different biogas hydrogen mixtures and second law analysis. During the combustion process of hydrogen is burnt to different rates of gases in the burning of the spatial distribution. Biogas can be used a number of different ways. One of them, to obtain a rich methane fuel by changing the amount of CO2 in the biogas. Many of operations have shown that the improvement of engine performance parameters and emission values when the hydrogen was added (Rigopoulos, Michos, 2009).

2. THEORETICAL STUDY

2.1 ENGINE PARAMETERS

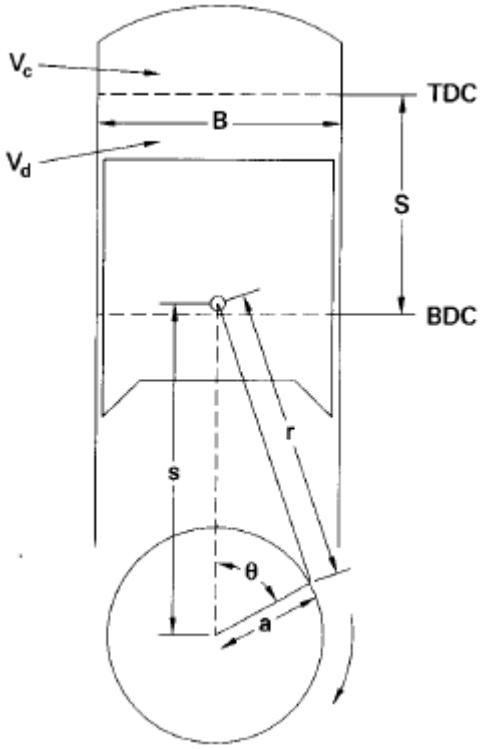

Figure 2.1. Piston and Cylinder Geometry of Reciprocating engine(Willard W. Pulkrabek)

For an engine with bore B (see Fig. 2.1), crank offset a, stroke length S, turning at an engine speed of N:

$$S = 2a \tag{2.1}$$

$$Up = 2SN \tag{2.2}$$

N is generally given in RPM (revolutions per minute), Up in m/sec, and B, a, and S in m or cm.
The distance s between crank axis and wrist pin axis is given by;

$$s = a\cos\theta + \sqrt{r^2 - \sin\theta^2} \tag{2.3}$$

The ratio of instantaneous piston speed divided by the average piston speed can be written as;

$$\frac{U_p}{\bar{U}_p} = (\pi/2)\sin\theta[1 + (\cos\theta/\sqrt{(R^2 - \sin\theta^2)}] \tag{2.4}$$

$$R=r/a \tag{2.5}$$

Displacement, or displacement volume V_d is the volume displaced by the piston as it travels from BDC to TDC;

$$V_d = V_{BDC} - V_{TDC} \tag{2.6}$$

For an engine with N_c cylinders;

$$V_d = N_c \left(\frac{\pi}{4}\right) B^2 S \tag{2.7}$$

The cylinder volume V at any crank angle is;

$$V = V_c + \left(\frac{\pi B^2}{4}\right)(r + a - s) \tag{2.8}$$

This can also be written in a non-dimensional form by dividing by V_c, substituting for r,s and a, and employing the definition of R;

$$V/V_c = 1 + 1/2(r_c - 1)[R + 1 - \cos\theta - \sqrt{R^2 - \sin\theta^2}] \tag{2.9}$$

The cross-sectional area of cylinder;

$$A_P = (\pi/4)B^2 \tag{2.10}$$

2.2 WORK

Work is the output of any heat engine, and in reciprocating IC engine this work is generated by the gases in the combustion chamber of the cylinder. Work is the result of force acting of a through distance. Force due to gas pressure on the moving piston generates the work in an IC engine cycle. The ratio of brake work at the crankshaft to indicated work in the combustion chamber defines the mechanical efficiency of an engine;

$$\eta_m = \frac{w_b}{w_i} = W_B/W_i \tag{2.11}$$

2.3 MEAN EFFECTIVE PRESSURE

Pressure in the cylinder of an engine is continuously changing during the cycle. An average or mean effective pressure(mep) is defined as;

$$w = (mep)\Delta v \tag{2.12}$$

$$mep = \frac{w}{\Delta v} = W/V_d \tag{2.13}$$

If the brake work is used, brake mean effective pressure is obtained;

$$bmep = w_b/\Delta v \tag{2.14}$$

Indicated work gives indicated mean effective pressure;

$$imep = w_i/\Delta v \tag{2.15}$$

2.4 TORQUE AND POWER

Torque is a good indicator of an engine's ability to do work. It is defined as force acting at a moment distance and has a units of N-m.

$$2\pi\tau = W_b = (bmep)V_d/n \tag{2.16}$$

For a two stroke cycle engine with one cycle for each revolution;

$$\tau = (bmep)V_d/2\pi \quad \text{two-stroke cycle} \tag{2.17}$$

For a four stroke cycle engine which takes two revolutions per cycle;

$$\tau = (bmep)V_d/4\pi \quad \text{four-stroke cycle} \tag{2.18}$$

2.5 AIR-FUEL RATIO AND FUEL-AIR RATIO

Air is used to supply oxygen needed for chemical reaction. For combustion reaction to occur, proper relative amounts of air(oxygen) fuel must be present. Air fuel ratio(AF) and fuel air ratio(FA) are parameters used to describe the mixture ratio;

$$AF = \frac{m_a}{m_f} = \dot{m}_a/\dot{m}_f \tag{2.19}$$

$$FA = \dot{m}_f/\dot{m}_a = m_f/m_a \tag{2.20}$$

2.6 SPECIFIC FUEL CONSUMPTION

Specific fuel consumption is defined by;

$$sfc = \dot{m}_f/\dot{W} \tag{2.21}$$

Brake power gives brake specific consumption;

$$bsfc = \dot{m}_f/\dot{W}_b \tag{2.22}$$

Indıcated power gives indicated specific consumption;

$$isfc = \dot{m}_f/\dot{W}_i \tag{2.23}$$

2.7 VOLUMETRIC EFFICIENY

Volumetric efficiency in the internal combustion engine design refers to the efficiency with which the engine can move the charge into and out of the cylinders.

More specifically, volumetric efficiency is a ratio (or percentage) of the quantity of air that is trapped by the cylinder during induction over the swept volume of the cylinder under static conditions. Volumetric Efficiency can be improved in a number of ways, most effectively this can be achieved by compressing the induction charge (forced induction) or by aggressive cam phasing in Normally Aspirated engines as seen in racing applications. Volumetric efficiency is defined as;

$$\eta_v = m_a/\rho_a V_d \tag{2.24}$$

$$\eta_v = nm_a/\rho_a V_d N \tag{2.25}$$

2.8 DIESEL CYCLE

Early CI engines injected fuel into the combustion chamber very late in the compression stroke. Due to ignition delay and the finite time required to inject the fuel, combustion lasted into the expansion stroke. This kept the pressure at peak levels well past TDC. This combustion process is best approximated as a constant-pressure heat input in an air-standard cycle, resulting in the Diesel cycle. The rest of the cycle is similar to the air-standard Otto cycle. The diesel cycle is sometimes called a Constant Pressure cycle.

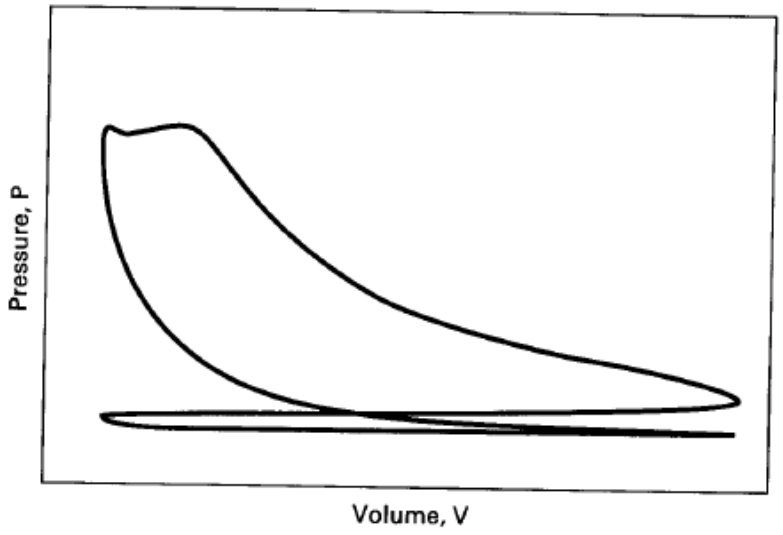

Figure 2.2. Indicator diagram of a historic CI engine operating on an early four stroke cycle (Willard W. Pulkrabek)

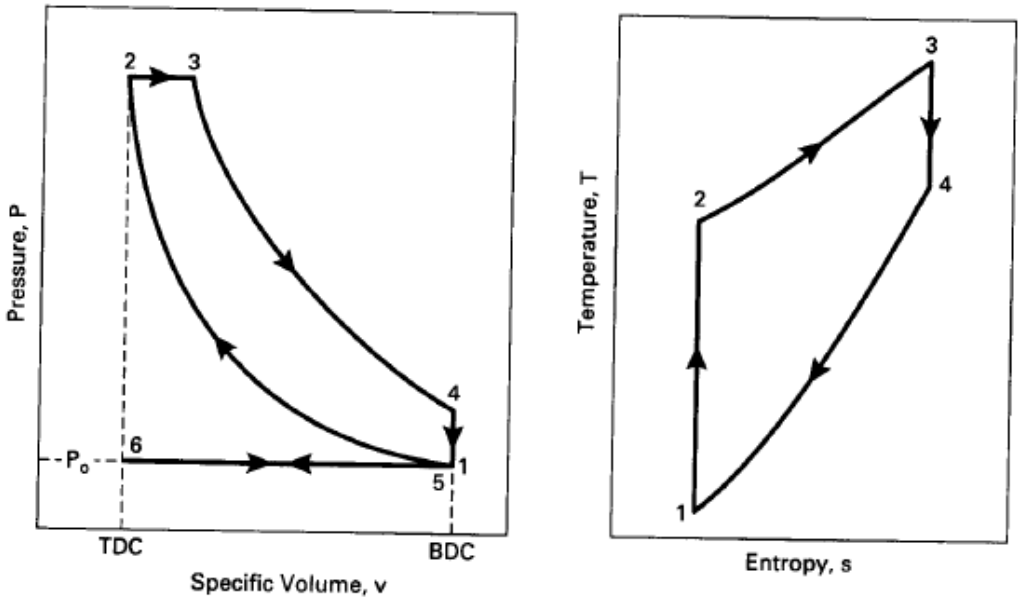

Figure 2.3. Air- Standard diesel cycle (Willard W. Pulkrabek)

Process 6-1- constant pressure intake of air at P_0, intake valve open and exhaust valve closed:

$$w_{6-1} = P_0(v_1 - v_6) \tag{2.26}$$

Process 1-2- isentropic compression stroke. All valves closed:

$$T_2 = T_1(v_1/v_2)^{k-1} = T_1(V_1/V_2)^{k-1} = T_1(r_c)^{k-1} \tag{2.27}$$

$$P_2 = P_1(v_1/v_2)^{k} = P_1(V_1/V_2)^{k} = P_1(r_c)^{k} \tag{2.28}$$

$$w_{1-2} = \frac{P_2v_2 - P_1v_1}{1-k} = R(T_2 - T_1)/(1-k) \tag{2.29}$$

Process 2-3-constant pressure heat input (combustion). All valves closed:

$$Q_{HV}\eta_c = (AF + 1)c_p(T_3 - T_2) \tag{2.30}$$

$$q_{2-3} = q_{in} = c_p(T_3 - T_2) = h_3 - h_2 \tag{2.31}$$

Cutoff ratio is defined as the change in volume that occurs during combustion, given as a ratio;

$$\beta = \frac{V3}{V_2} = \frac{v_3}{v_2} = \frac{T_3}{T_2} \tag{2.32}$$

Process 3-4-isentropic power or expansion stroke. All valves closed:

$$T_4 = T_3(v_3/v_4)^{k-1} = T_3(V_3/V_4)^{k-1} \tag{2.33}$$

$$P_4 = P_3(v_3/v_4)^{k} = P_3(V_3/V_4)^{k} \tag{2.34}$$

$$w_{3-4} = \frac{P_4v_4 - P_3v_3}{1-k} = R(T_4 - T_3)/(1-k) \tag{2.35}$$

Process 4-5-constant volume heat rejection(exhaust blowndown). Exhaust valve open and intake valve closed:

$$q_{4-5} = q_{out} = c_v(T_5 - T_4) = u_5 - u_4 = c_v(T_1 - T_4) \tag{2.36}$$

Process 5-6- constant-pressure exhaust stroke at P_0. Exhaust valve open and intake valve closed:

$$w_{5-6} = P_0(v_6 - v_5) = P_0(v_6 - v_1) \tag{2.37}$$

The thermal efficiency of diesel cycle;

$$(\eta_t) = w_{net}/q_{in} \tag{2.38}$$

$$(\eta_t) = 1 - (1/r_c)^{k-1}[(\beta^k - 1)/(k(\beta - 1))] \tag{2.39}$$

3. NUMERICAL STUDY

3.1 WHAT IS THE GT POWER PROGRAM?

In this study, I used to GT Power program for the 1D simulation. GT-SUITE includes a complete library of physics based modeling templates covering fluid flow, thermal, mechanical, electrical, magnetic, chemistry, and controls.

GT-SUITE applications include engine, aftertreatment, acoustics, cooling and vehicle thermal management, vehicle, transmission, driveline, hybrids, fuel injection and fuel systems, cranktrain, etc.

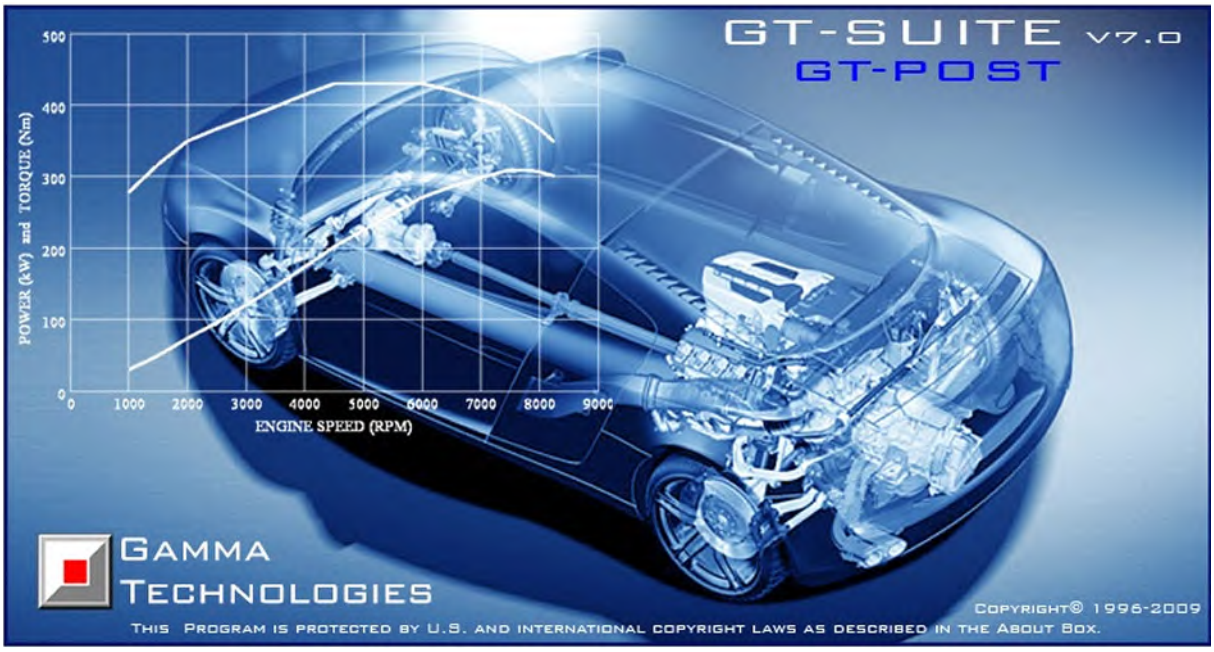

Figure 3.1. GT Power starting display

3.2 WHAT ARE THE MEANINGS OF 0D/1D-3D SIMULATION?

Simulation can be divided in 2 main categories, 3D simulation and 0D/1D simulation. 3D simulation includes all the space dimensions (X, Y, Z) and is often used to perform crash tests simulation (through Finite Element Analysis), combustion simulation, fluid flow simulation (Computational Fluid dynamics)… 3D simulation software that can be mentioned are Fluent, Radioss, IFP-C3D and many others. (www.car-engineer.com)

0D/1D simulation uses time dimension only (0D) or time and single axis dimension (1D). In both cases, software like AMESim, GT Power, Wave, etc. are often used in the automotive industry to design a thermal system, a powertrain, a fuel injection system… (www.car-engineer.com)

3.3 WHICH MODEL I USED IN THE GT POWER?

3.3.1 Heat Transfer Model

WoschniGT indicates that the in-cylinder heat transfer will be calculated by a formula which closely emulates the classical Woschni correlation without swirl.

The most important difference lies in the treatment of heat transfer coefficients during the period when the valves are open, where the heat transfer is increased by inflow velocities through the intake valves and also by backflow through the exhaust valves. This option is recommended when measured swirl data is not available. (GT Post user's manual)

3.3.2 Wiebe Combustion Model

This object imposes the combustion burn rate for spark-ignition engines using a Wiebe function. It can be used with any type of injection.

If at any instant the specified cumulative combustion exceeds the specified injected fuel fraction for a direct-injected SI (DISI) engine, the combustion rate will be limited by the amount of fuel available. (GT Post user's manual)

3.3.3 Flow Model

Flow indicates that the in-cylinder heat transfer will be calculated using flow detail provided by the 'EngCylFlow' reference object.

An effective velocity is calculated and used in the calculation of a heat transfer coefficient using the Colburn analogy. This model is recommended when swirl data is available through the 'EngCylFlow' reference object. (GT Post user's manual)

3.4 SIMULATION MODEL

The simulation model of this project shows like this. We input the bore, stroke, compression ratio, connecting rod length, inlet pressure and inlet temperature.

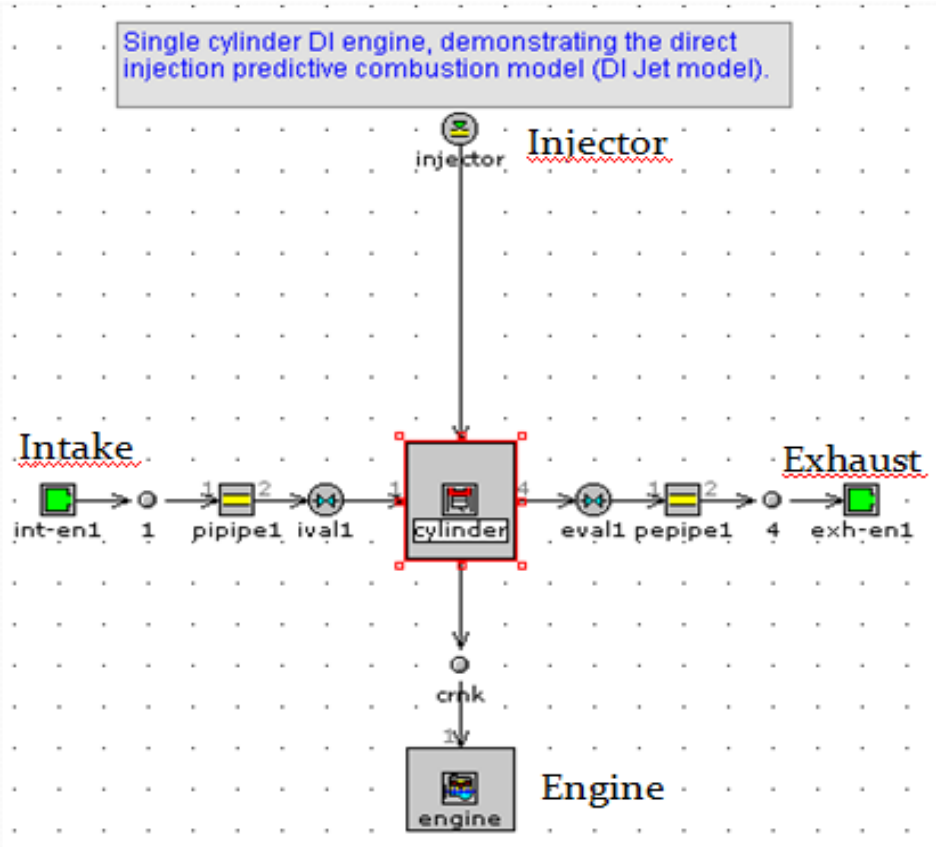

Figure 3.2. Simulation Model

3.5 GT POST

GT-POST is a powerful data analysis tool used to plot, view, and manipulate data generated either by a GT-SUITE simulation or by an external source. It offers a more efficient data analysis solution than standard spreadsheet software. By employing data pointers, the results viewed in GT-POST are updated automatically and immediately when a model is changed and a simulation is rerun. Also, GT-POST lends itself nicely to the development of portable, user-defined templates that control how results are presented. (GT Post user's manual)

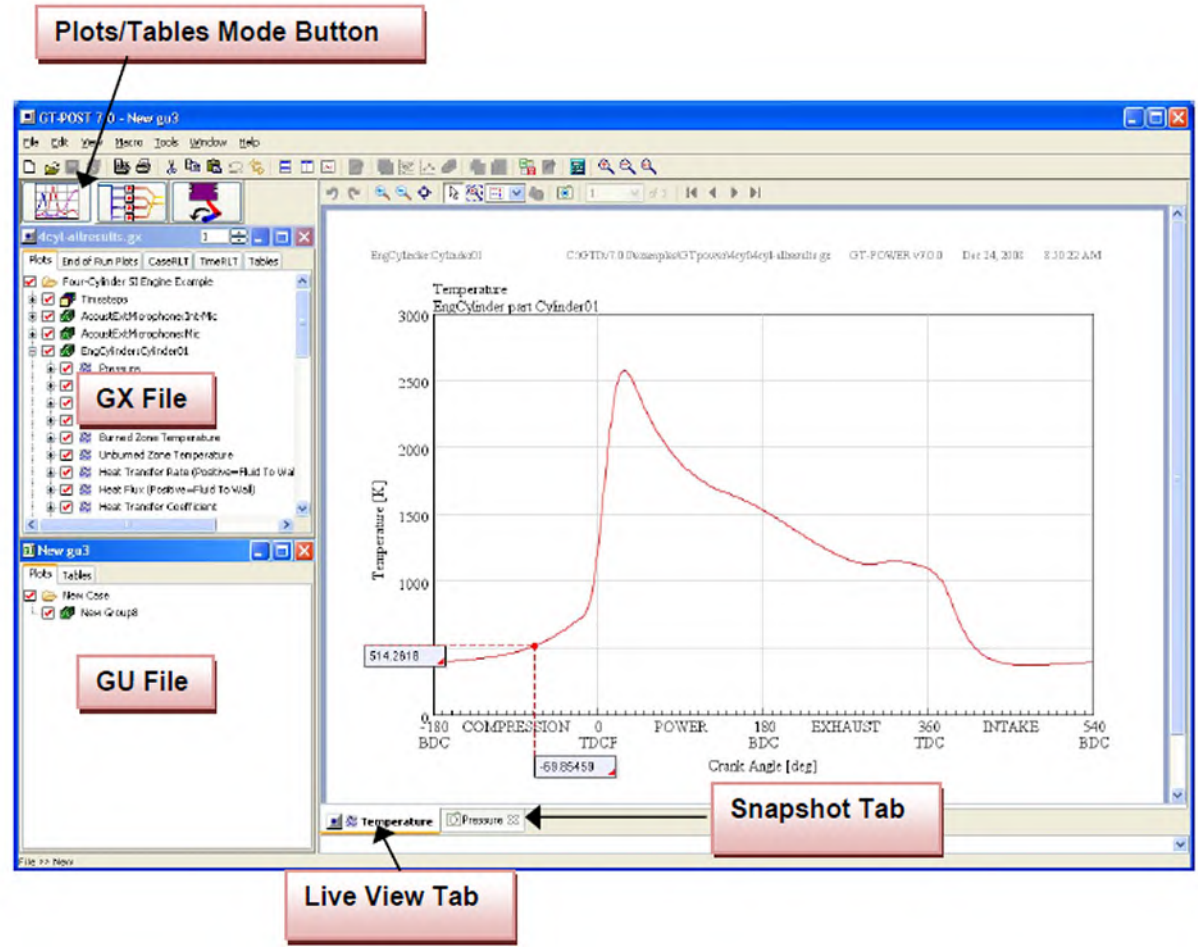

Figure 3.3. GT Post displaying

User plot files (.gu files) must be used anytime the user wishes to edit and save any plot or table found in a .gx file, or whenever the user wishes to create any new plots or tables. It is also used to compare data from different simulations or to compare simulation data to experimental data. It also allows the user to create a "template" for viewing the simulation results that are most important. (GT Post user's manual)

3.5.1 Basic Tree Operations

The various plot and table folders of each .gx or .gu file contain a hierarchical tree, organized into four levels. The highest level of this tree is referred to as the case level. For a multi-case simulation, the .gx pane will display only one case at a time. The user can switch between cases using the case selection field located at the top of the .gx pane. Within each case, there will be one or more group levels. In a .gx file this level will correspond to the parts or objects in the model for which plots have been requested. Within each group, there are one or more plots or tables containing one or more datasets. The following figure shows a typical .gx plot tree on the left and a table tree on the right demonstrating all of the levels of the tree. The plus (+) or minus (-) symbols next to each item allow the user to expand or contract each level. (GT Post user's manual)

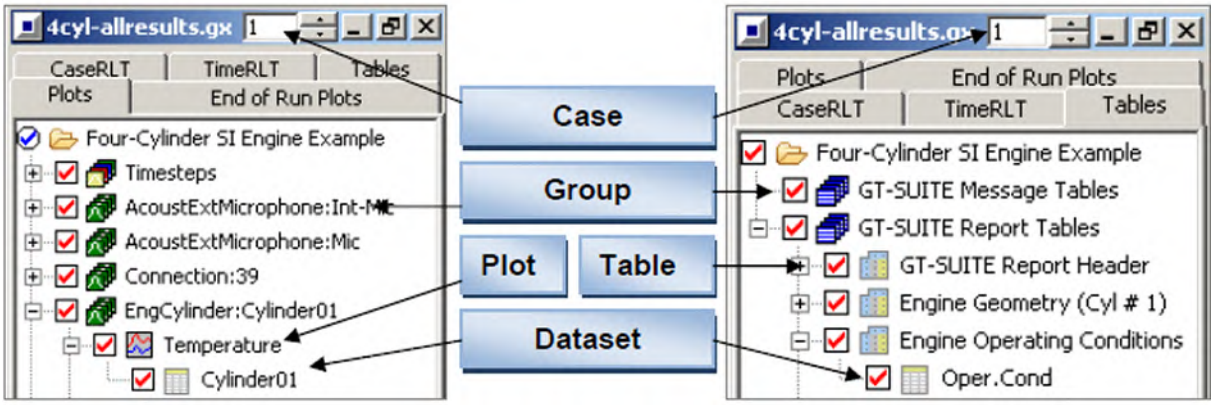

Figure 3.4. Basic Tree Definition(GT Post user's manual)

3.5.2 Viewing Data

Raw data can be viewed by right-clicking on the desired data level item and selecting View Data. In addition, the view data dialog can be launched by right clicking on the parent plot in the view pane and selecting View Data. A dialog box displays the data in array format as shown below. This data can be copied and pasted into another application. If the data is explicit (contained directly in the .gu file), the data can also be edited in this dialog box. The Export, View Even X-Increment Data, and Data Statistics options in the dialogue box are addressed in later sections. (GT Post user's manual)

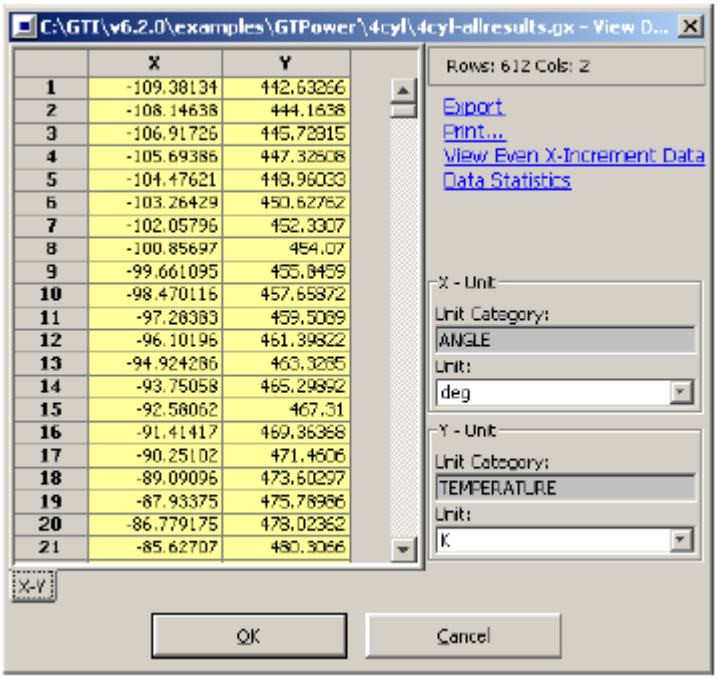

Figure 3.5. Viewing Data

3.5.3 Adding New Data

Often, it is desirable to add external data (not generated by GT-SUITE) to existing plots in a .gu file. For instance, experimental measurements are often compared with simulation results to validate a model. Data can be added to a single plot or table using the Add Data selection from the right-click menu. The dialog for adding data to an XY scatter plot is shown below. The data type must be selected from a list of the allowable data types for that plot or table type. The second option to select is the source of the data. (GT Post user's manual)

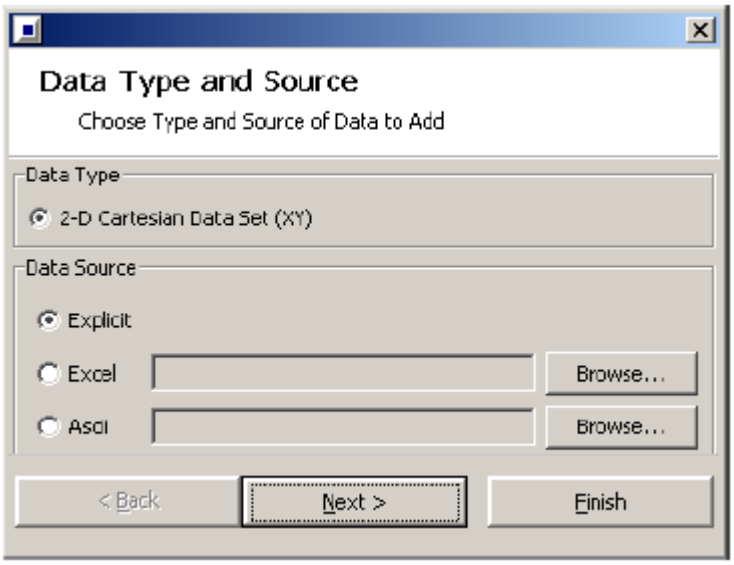

Figure 3.6. Adding New Data

The Excel or Ascii options may be used to import data directly from Excel spreadsheet or Ascii text file. The imported data may be either explicit or implicit.

If either of these options is selected, the remaining dialog screens are identical to the tool used to import multiple Excel or Ascii data sets. If the Explicit option is chosen, the remaining two screens shown below are used to define a dataset name and units and to enter (or paste in) the data.

After the data has been entered and the OK button selected, the data will be added as a new dataset within the original plot. The new data set will be "explicit", meaning that it is not tied to any GT-SUITE simulation results or to any external file. (GT Post user's manual)

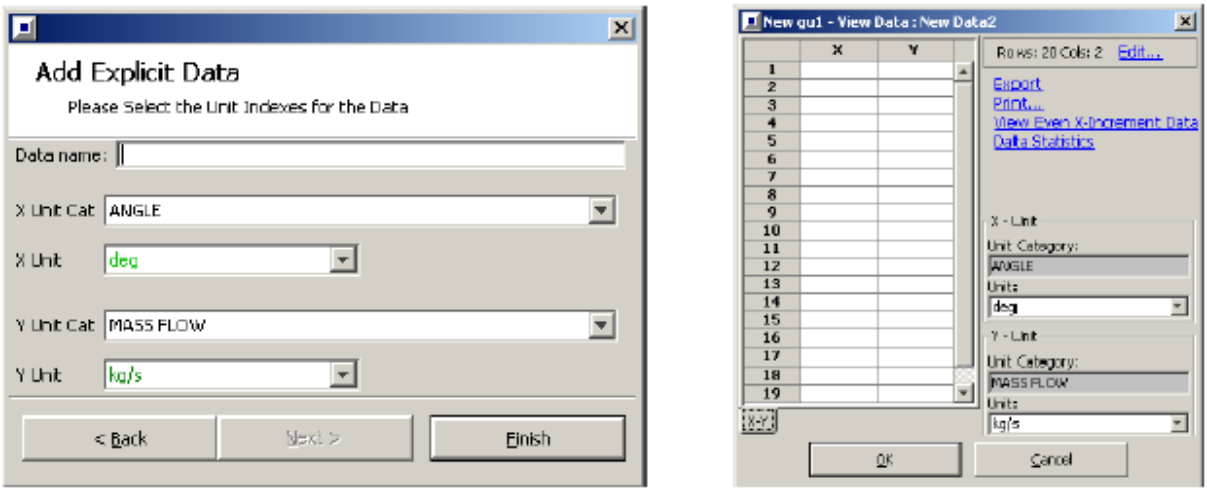

Figure 3.7. Adding Explicit Data And New gu file

3.5.4 Plot Data Combine

This macro allows any datasets that share a common unit category to be combined into a single plot. In the macro dialog, the left window is used to select the "source dataset". This is used to filter all of the datasets in the tree so that only those datasets with a matching unit are shown in the center window.

This filtered list can be further filtered by selecting either "variable" or "template" from the pull-down above the center window. These options will only show datasets with the same unit AND the same variable (i.e. pressure) or the same template (i.e. Pipe), respectively.

The desired datasets for the plot are selected in the center window and the affected cases are selected in the right window. Below the right window there are radio buttons to select whether multiple cases are combined into one plot or repeated in multiple plots. In addition, there is a field where the new plot name may be set if desired.(GT Post user's manual)

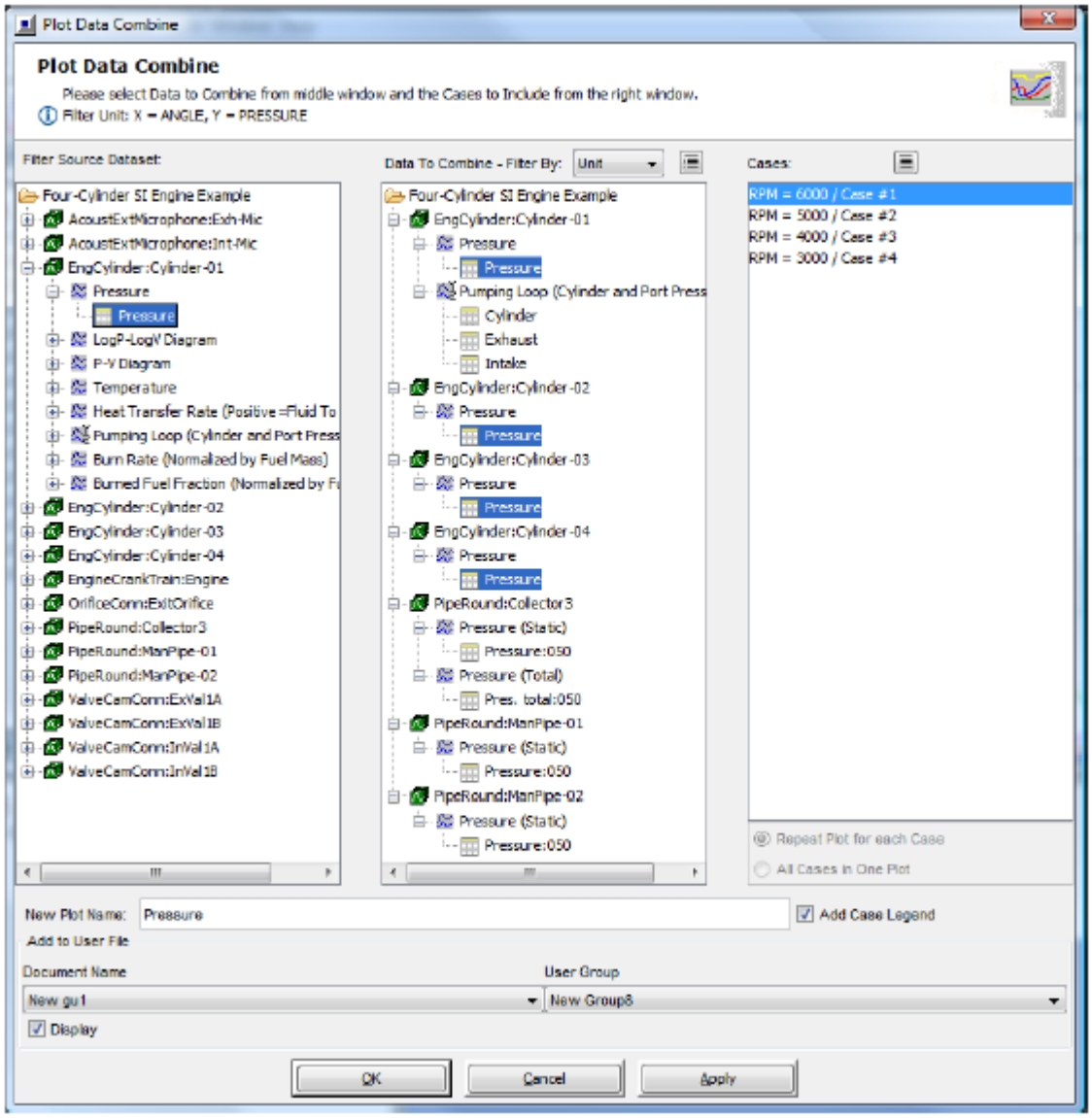

Figure 3.8. Plot Data Combine

4. EXPERIMENTAL STUDY

4.1 TEST ENGINE

The engine utilized for this research is based on a four-cylinder, turbocharged compression ignition (CI) engine with a single overhead cam (SOHC). It possesses a bore of 76 mm, a stroke of 80.5 mm, a displacement volume of 1461 cm^3 and a compression ratio of 18.25. The rated maximum power along with the maximum torque was 48 kW at 4000 rpm and 160 Nm at 2000 rpm with the boost pressure of 0.13 MPa, respectively. The detailed specifications and measurements of quality engine are summarized in Table 4.1.

Table 4.1

Engine characteristics

Model	Renault Clio II K9K700 Diesel Engine
Type	4 Cylinder-four stroke
Horse power	65hp
Bore × Stroke	76×80.5 mm
Connecting rod length	133.75mm
Displacement	1461 cm^3
Compression ratio	18.25:1
Max. Lift (exhaust)	8,6 mm
Max. Lift (intake)	8.0mm
Operation speed	1750 rpm
Maximum power	48kW at 4000 rpm
Maximum torque	160Nm at 2000 rpm

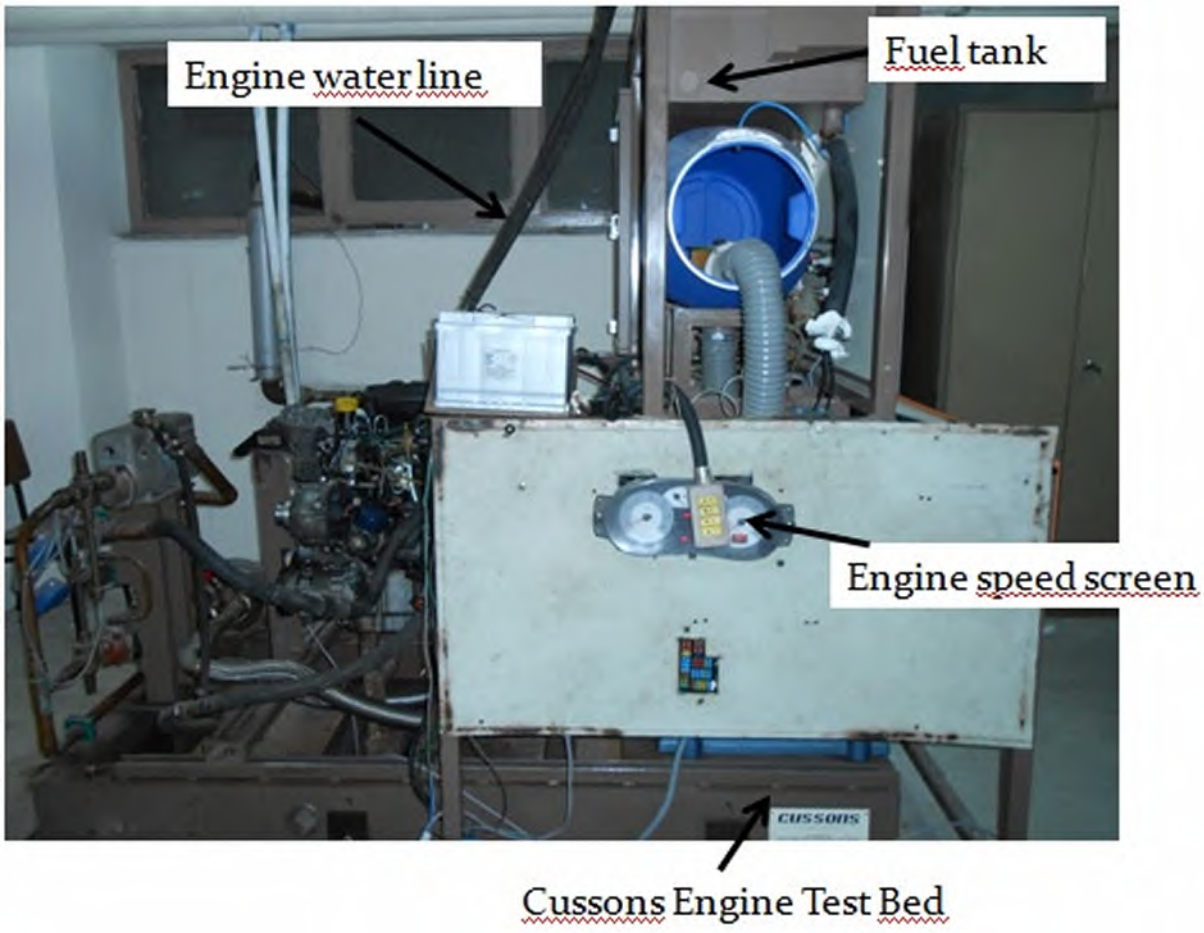

Figure 4.1 Experiment System

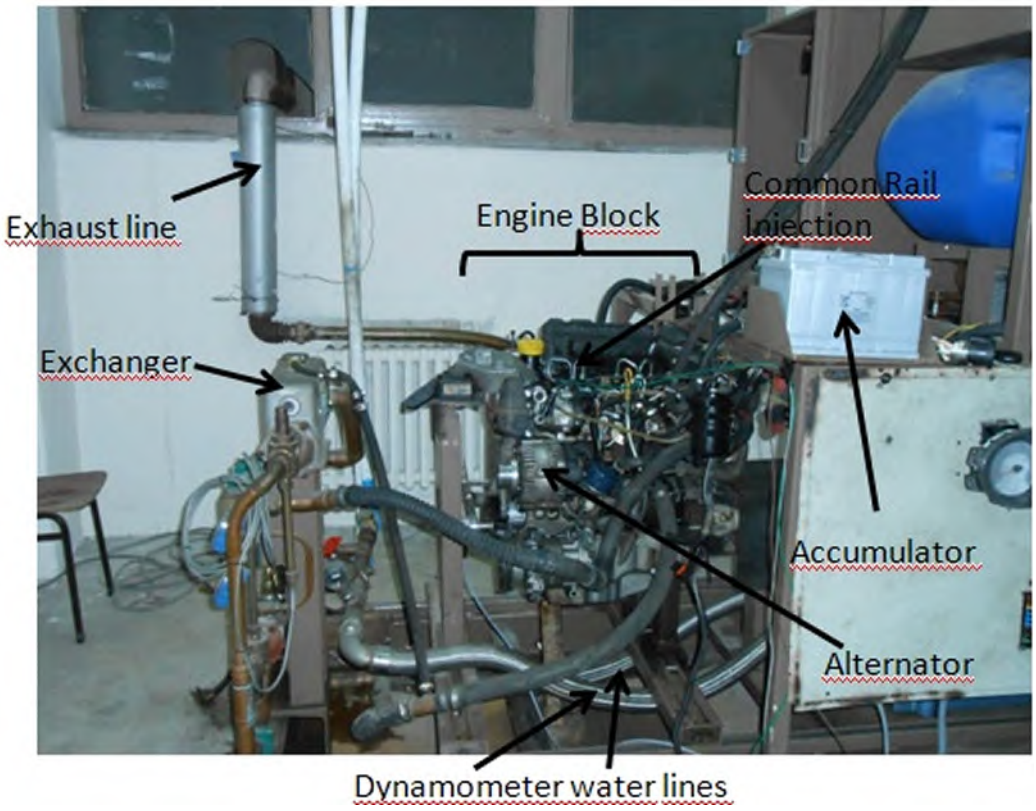

Figure 4.2. Experiment System Detailed

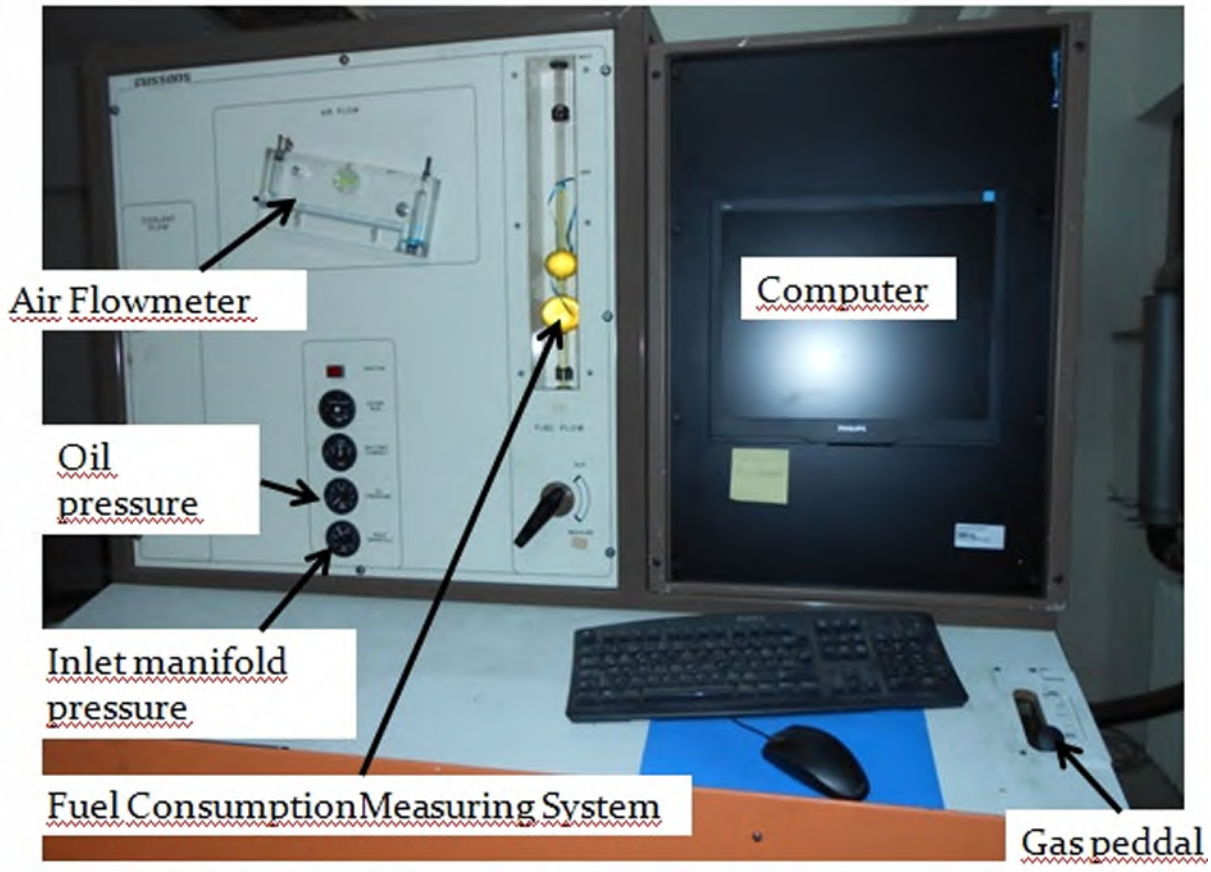

Figure 4.3. Control Panel

4.2 DYNAMOMETER

In this study, test engine is loaded to obtain the engine performance characteristics such as indicated pressure, power, torque and specific fuel consumption. In this way, engine torque on the output shaft is measured depending on the engine speed. Load systems are called as a dynamometer and force which performed on the engine output shaft is called as a load. Engine power and torque can be obtained by measuring the dynamometer torque which equaled test engine torque. Engine speed and load conditions must be controlled to obtain the engine performance and emission characteristics truly. These conditions can be controlled via CUSSONS brand four cylinder engine dynamometer as shown in figure 4.4 and figure 4.5. Break moment occurs in the torque arm which is connected to the dynamometer. This force is transmitted to the load cell by torque arm. Engine torque is calculated by determining in load cell. The engine load and speed are controlled utilizing an eddy current (EC) dynamometer system (Cussons – 1200 – 8000 rpm) this has a maximum braking power 165 kW. In this experiment, eddy-current type dynamometer consists of a rotor and carried in bearing in an outer housing or stator. The rotor has either inserted elements or teeth around its periphery similar to a coarse pitched gear wheel. Located in the outer housing are one or two circumferentially wound field coils excited by direct current. The coils do not rotate but are fixed securely in the housing which is carried upon anti-friction ball-bearing trunnions so that it is free to swivel about the same axis as the rotor assembly. Application of current to the field coil produces magnetic fields which link the rotor and stator via a small air gap which seperates these two items. The magnetic flux is distributed almost evenly along the length of the rotor teeth or inserts and through the thickness of the rotor so that, when the rotor is revolved, the interior surfaces of the stator opposite the teeth or inserts are alternately magnetized and demagnetized, thus inducing eddy currents in the stators. The magnetic fields set up by these eddy currents interact with the main field concentrations in such a manner as to oppose rotation, thus giving the machine its power absorbing capacity. The forces opposing rotation react upon the stator assembly which tends to turn upon its anti-friction trunnion bearings. This tendency is counteracted by means of a strain gauge load cell weigher system with analogue and/or digital load indication. The power absorbed by the machine can thus be measured. The dynamometers are equally efficient when being driven in either direction of rotation.(P8602 multi-cylinder engine test bed).

The energy expanded in generating the eddy currents is manifested as heat of the internal surface of the stator and this heat is carried away by cooling water which is admitted to grooves at the back of the stators. The water is carried around the hot surfaces of the inner rings and emerges through parts at the bottom of the stator, from where it flows to the dynamometer water outlet connection. (P8602 multi-cylinder engine test bed)

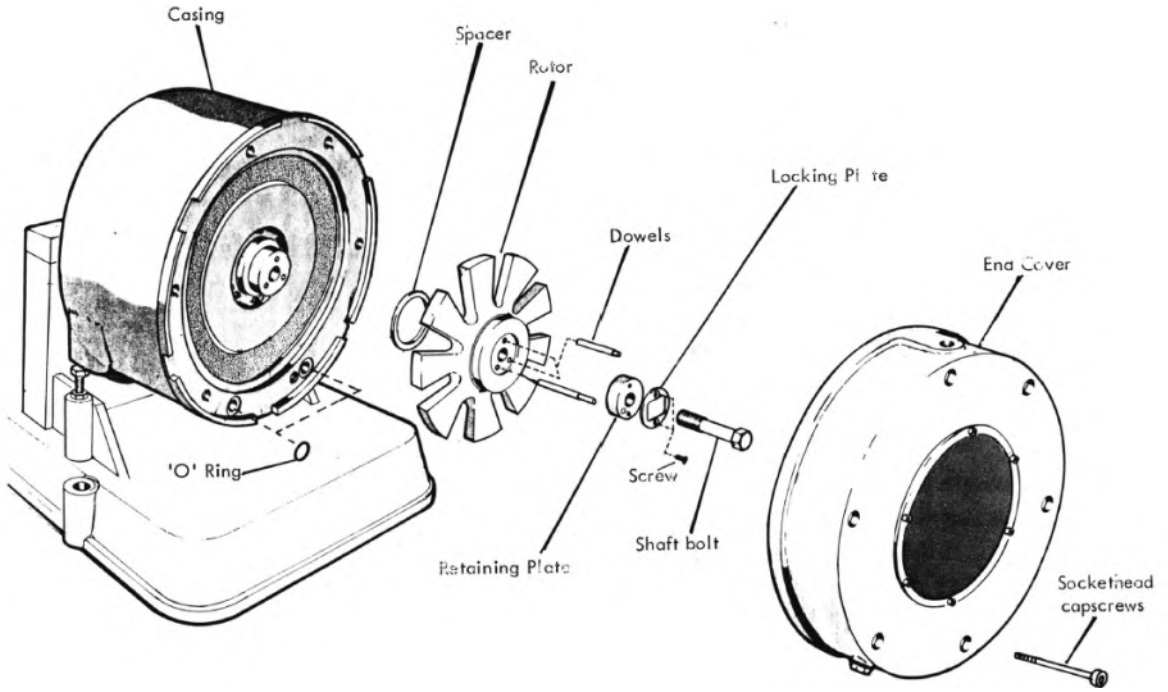

Figure 4.4. Exploeded view of items in Rotor compartment (P8602 multi-cylinder engine test bed)

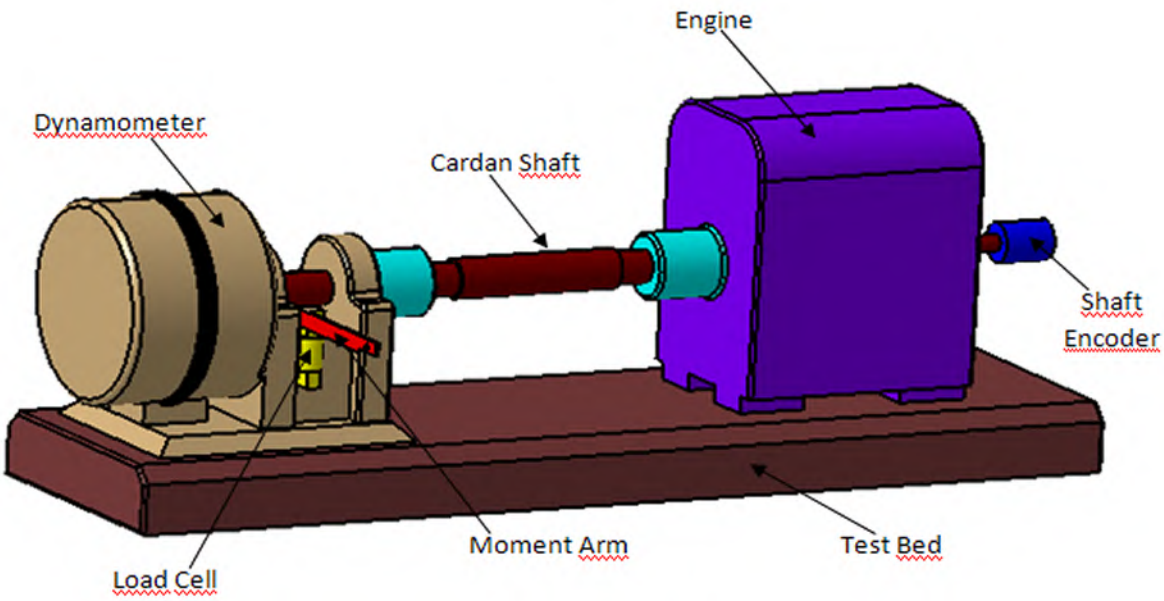

Figure 4.5. Dynamometer and Test Bed Schematic Diagram

Stator is balanced by rotor. The breaking force is measured corresponding to the moment and multiplied the moment arm length because of the breaking moment is not measured directly.. We see that in the Figure 4.6. (Turkcan A., 2006)

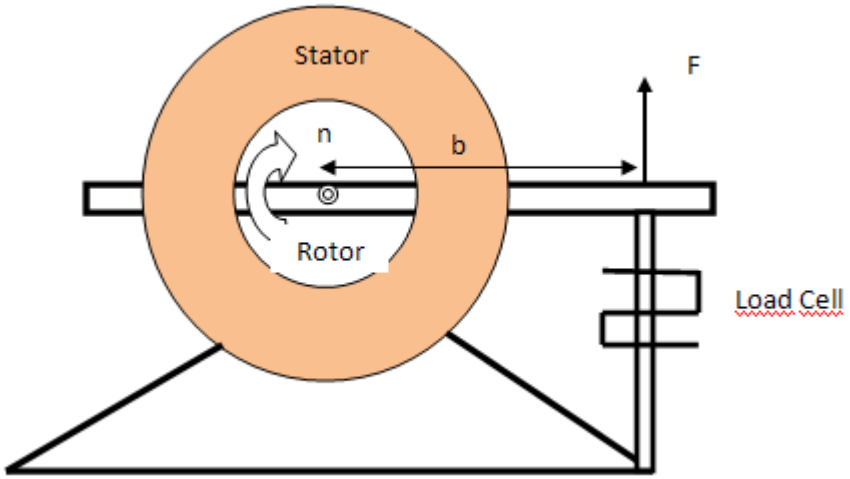

Figure 4.6. Breaking Torque Measuring Principle

If the measuring force F, engine producing torque is T (Nm):

$$T = F.b \quad (4.1)$$

Effective power producing by engine, Pe (kW) taking the n(rev/s)

$P_e=2.\pi.n.T$ equation calculated (4.2)

4.3 PRESSURE SENSORS

4.3.1 In- Cylinder Pressure Sensor

In this study, the optrand brand pressure sensor was used to measuring of the in-cylinder pressure.The sensing element is coupled via an optical fiber to an enclosure. The enclosure has four or five color-coded leads (depending upon system grounding requirements) for terminating to a power source and data acquisition system. In the table 4.2, there are some characteristics about the sensor.(AutoPSI Pressure Sensor)

Table 4.2

Sensor characteristics

Model	Optrand AutoPSI pressure sensor
Diaphragm Resonant Frequency:	120 kHz min.
Frequency Range:	1.0 Hz to 25 kHz
Fiber optic Cable Min.	
Bending Radius:	5mm (3/16”)
Sensor Type:	Sealed Gauge
Interface Unit:	Integrated with Sensor
Pressure Output Signal:	**9-18V DC input**: 0.5 – 4.5 V
(Analog) **5V DC input:**	0.5 - 4.5 V
Diagnostic Output Signal:	**9-18V DC input**: 0.5 – 2.5 V
(Analog) **5V DC input:**	0.5 – 2.5 V
Input voltage	9-18V DC
Output voltage	0.5-4.5V DC
Current Draw:	85 mA Max, 50 mA Typical
Interface Temperature Range:	**AutoPSI-S,A,TC:**-20°C to 60°C
Sensor Housing Temperature Range:	-40°C to 380°C
Cable Operating Temperature:	-40°C to 200°C
Sensitivity:	1.32mV/psi @ 200º C
Pressure range	0-3000 psi

The sensor has either four or five wires extending out of the electronic enclosure tube. The following describes the purpose of each wire:

White Wire Sensor Output Signal
Blue or Green Wire Diagnostic, Static Calibration
Red Wire Power
Black Wire Ground (Power and Signal)
Bare Wire Case (if present, otherwise case is connected to Ground)

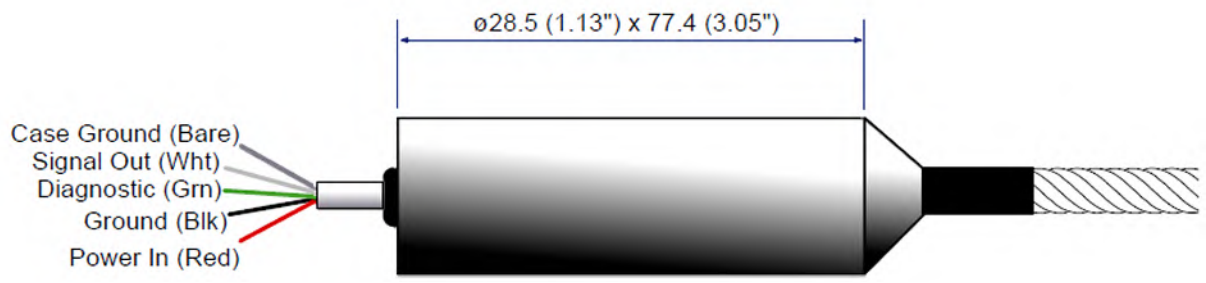

Figure 4.7. The Detail of Sensor Cable(AutoPSI Pressure Sensor)

4.3.1.1 Sensor Output Signal: Connect between the White and Black wires. The output signal is analog, 0.5 – 4.5 Volts for all sensors. The analog signal and Sensor Sensitivity Value must be used to calculate the correct pressure. (AutoPSI Pressure Sensor)

4.3.1.2 Diagnostic Output Signal: Connect between the Blue or Green wire and the Black wire. The diagnostics output signal is a DC Voltage, proportional to the LED current level, and indicates when the sensor is in or out of calibration. This voltage is typically in the 1.0 – 2.0 Volts range for all sensors and can vary from sensor to sensor. (AutoPSI Pressure Sensor)

4.3.1.3 Static Pressure Calibration: The AutoPSI sensor can measure static pressure when the diagnostic (blue or green) wire is used as input instead of an output. If the diagnostic wire is connected to a DC power source (0-2.5 volt) or a potentiometer to ground the sensor will measure static pressure. This mode is useful for calibrating the sensor with a dead weight tester or other static pressure calibration technique. (AutoPSI Pressure Sensor)

4.3.2 Fuel Line Pressure Sensor

In this study, the kistler type piezoresistive high pressure sensor with amplifier was used to measuring fuel-line pressure. The pressure to be measured acts through a rugged diaphragm on an arrangement of piezoresistive ”rods”. The pressure changes the values of the resistances diffused into the rods. These resistances are arranged in a Wheatstone bridge. The pressure sensor itself is not temperature compensated. The amplifier Type 4618A... provides temperature compensation, linearisation of the pressure signal and contains a stabilized power supply. For this reason, the sensor must always be operated with the amplifier adjusted to it. In the table 4.3, there are some chracteristics about this type sensor (Kistler).

Table 4.3

Sensor characteristics

Model	Kistler
Range	0-3000 bar
Sensitivity	3.333 mv/bar
Output impedance	10Ω
Supply (Amplifier)	18-30V DC
Thermal sensitivity shift	< ±1%
Tightening torque	15 N.m
Acceleration error	<10 mbar/g
Natural frequency	>200 kHz

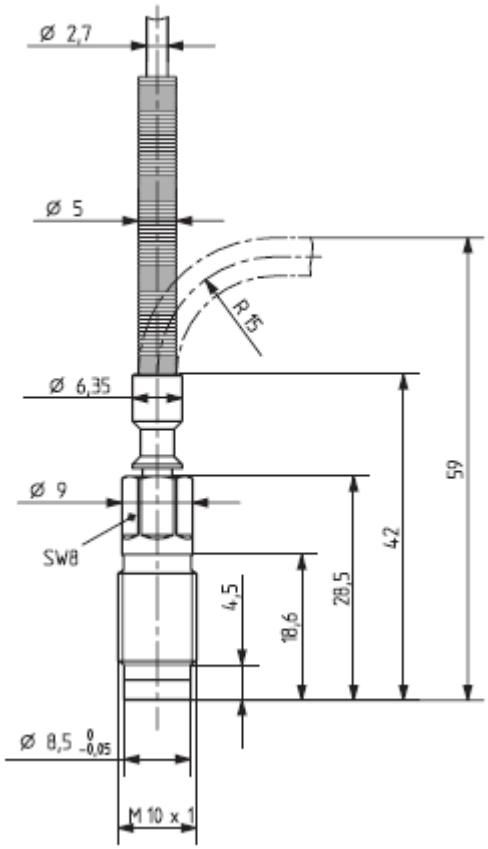

Figure 4.8. Dimensions (Kistler)

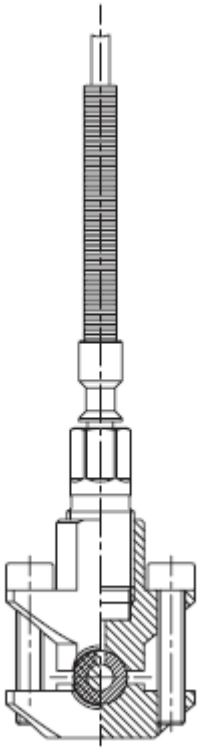

Figure 4.9.Mounting in clamp adapter(Kistler)

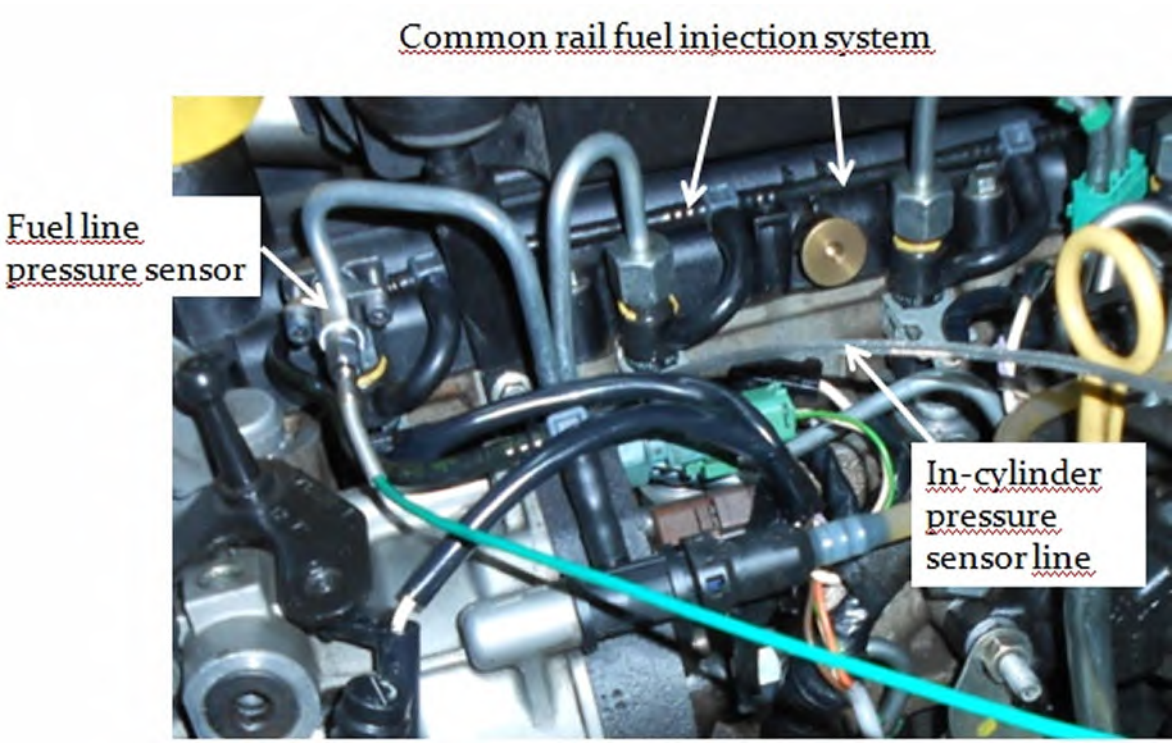

Figure 4.10. Fuel Line and In-Pressure Sensor

4.4 SOFTWARE

In this study, MOTEST was used as the programme which controls the dynamometer, engine and all devices including engine test room. MOTEST is developed by the TUZEKS. This system has completely user-specify test screen and the test procedures are designed by user. The user can edit the parameters which contain power, speed, torque, temperature, pressure, fuel consumption and emission according to his own wishes. The user can observe measurig data and prepared the report on the test screen. In the figure 4.11, example of screen is displaying. [Motest10]

In figure 4.12, It computes an excel creation which are made of tests results in the desired extent in order. In the report menu, clicking on the previously defined report gives the results depending on time and type of test condition which are determined by user. We see that in the figure 4.12, Automated test record takes the average of data which has the same functionality of automated tests. The manual test takes average of the results in the same minutes. (Motest10)

Figure 4.11 Displaying of The Test Screen

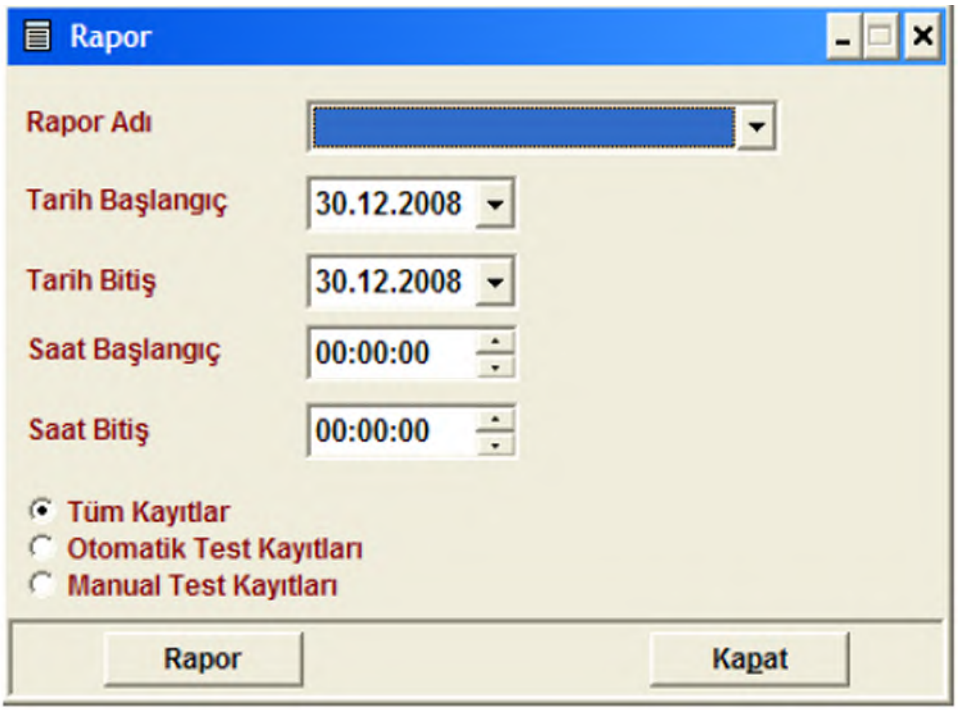

Figure 4.12. Creating a Report (Motest10)

In the figure 4.13, Calibration is operated for the defined analog channels. These are reel analog input and output channels. The calibration button which is located under the tools menu is pressed down and the calibration window appears on the screen. Channel and calibration list are listed as defined under the analogue channels (Motest10).

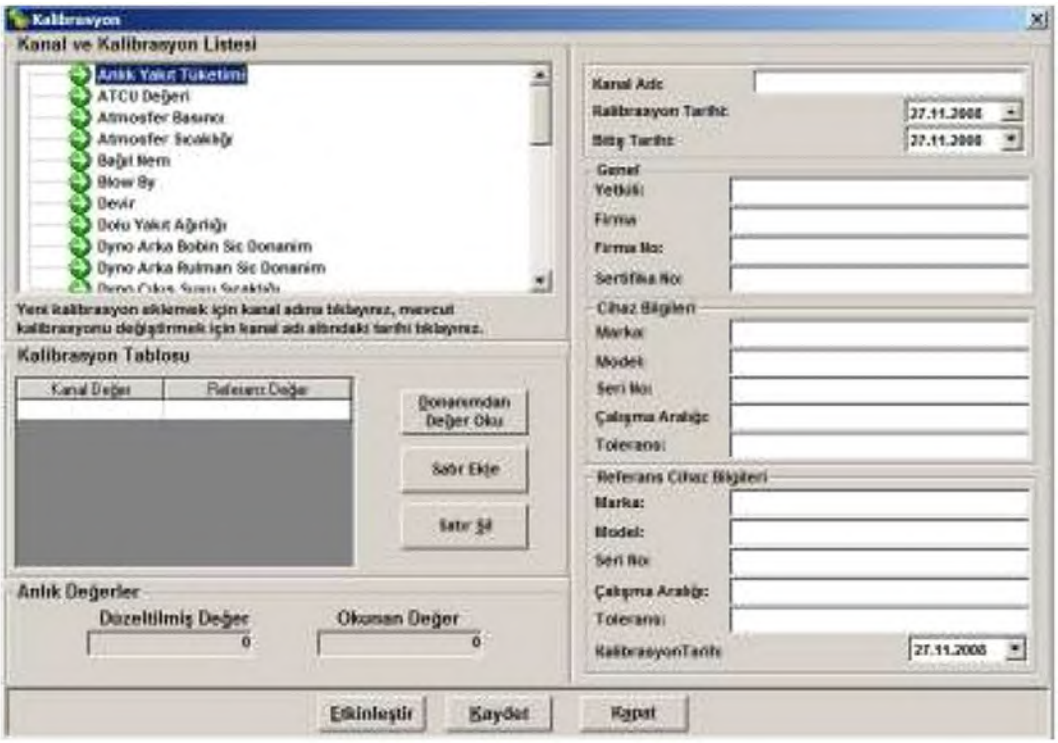

Figure 4.13 Calibration window (Motest10)

4.5 ENCODER

A rotary encoder, also called a shaft encoder, is an electro-mechanical device that converts the angular position or motion of a shaft or axle to an analog or digital code. There are two main types: absolute and incremental (relative). The output of absolute encoders indicates the current position of the shaft, making them angle transducers. The output of incremental encoders provides information about the motion of the shaft, which is typically further processed elsewhere into information such as speed, distance, and position.

Rotary encoders are used in many applications that require precise shaft unlimited rotation including industrial controls, robotics, special purpose photographic lenses, computer input devices and rotating radar platforms.(wikipedia.org)

In this study, the kübler standart optical incremental encoder was used for the rotational speed, angular displacement, acceleration and rotational motion. An optical encoder is a complex system which converts a mechanical rotary motion (angular position or speed) into a usable electrical signal. Each encoder optimizes the operating characteristics of three systems (mechanics, optics, and electronics). In the table 4.4 there are some chracteristics about encoder. (KUBLER)

Table 4.4

Encoder characteristics

Model	Kübler optical incremental encoder 5000
Working temperature range	-40ºC……+80º C
Shaft material	Stainless steel
Power supply	5…30V DC
Pulse frequency	max. 300 kHz
Shock resistance	2500m/s^2
Vibration resistance	100m/s^2

Figure 4.14. Kübler optical incremental encoder

The optical encoder's disc is made of glass or plastic with transparent and opaque areas. A light source and photo detector array reads the optical pattern that results from the disc's position at any one time. This code can be read by a controlling device, such as a microprocessor or microcontroller to determine the angle of the shaft. The absolute analog type produces a unique dual analog code that can be translated into an absolute angle of the shaft.(wikipedia.org)

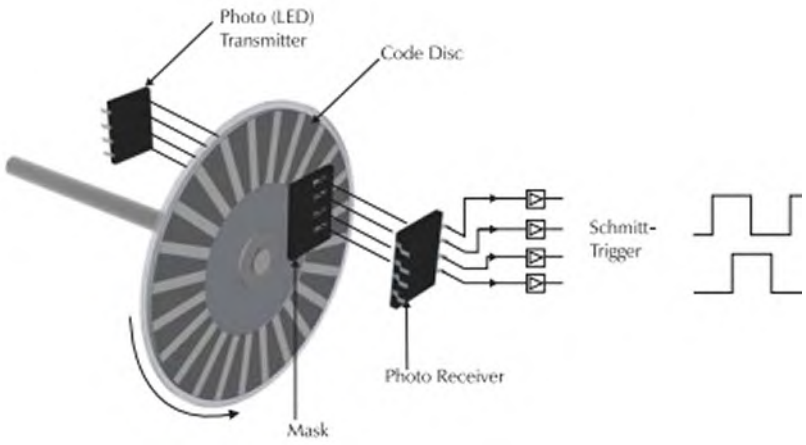

Figure 4.15.An encoder is a photoelectric emitter receiver pair looking through a slotted disk.

Light from the LED passes through the disc, the mask, and into the photo transistors. The photo transistor outputs a sine wave which corresponds to the flashing light pulses from the LED.

4.6 THERMOCOUPLE

The thermocouple is a simple, widely used component for measuring temperature. A thermocouple, shown in Figure 4.15, consists of two wires of dissimilar metals joined together at one end, called the measurement (“hot”) junction. The other end, where the wires are not joined, is connected to the signal conditioning circuitry traces, typically made of copper. This junction between the thermocouple metals and the copper traces is called the reference (“cold”) junction.

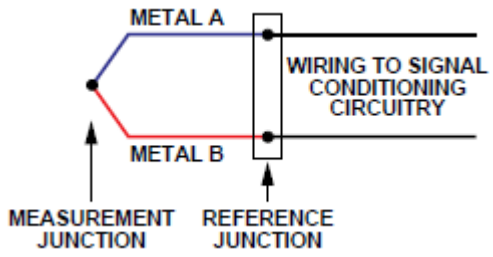

Figure 4.16 Thermocouple(www.reotemp.com)

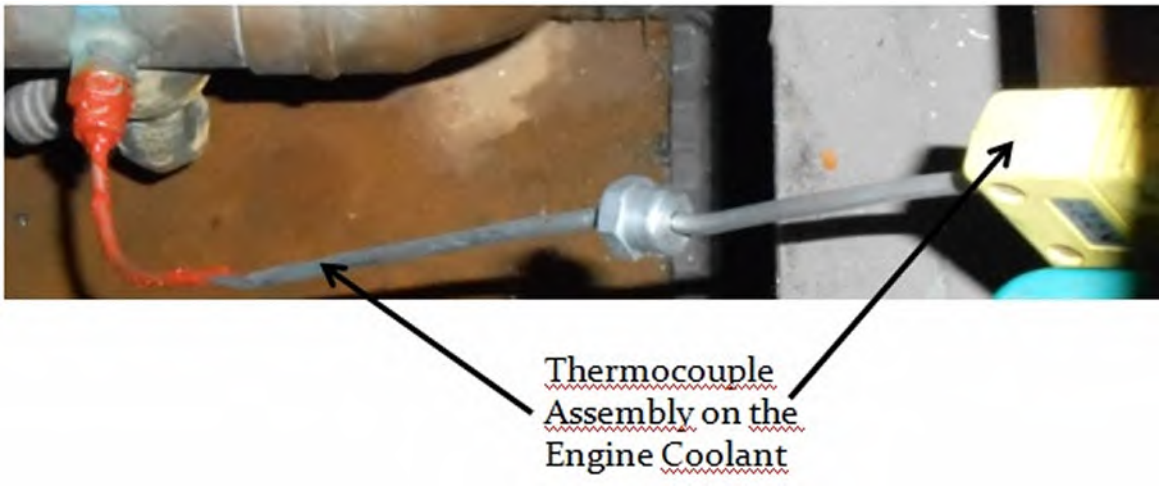

Figure 4.17 Thermocouple Assembly

The voltage produced at the reference junction depends on the temperatures at both the measurement junction and the reference junction. Since the thermocouple is a differential device rather than an absolute temperature measurement device, the reference junction temperature must be known to get an accurate absolute temperature reading. This process is known as reference junction compensation (cold junction compensation.)

Thermocouples have become the industry-standard method for cost-effective measurement of a wide range of temperatures with reasonable accuracy. They are used in a variety of applications up to approximately +2500°C in boilers, water heaters, ovens, and aircraft engines to name just a few. The most popular thermocouple is the type K, consisting of Chromium and Aluminum, with a measurement range of –200°C to +1250°C. It's inexpensive, accurate, reliable, and has a wide temperature range. (Duff M., Towey J., 2010) The type K is commonly found in nuclear applications because of its relative radiation hardness. Maximum continuous temperature is around 1100^{o} C. (www.reotemp.com)

In this study, K type thermocouple is used for the measuring of engine coolant temperature input and output, oil temperature, intake air inlet temperature, fuel temperature and exhaust gas outlet temperature.

4.7 ERROR ANALYSIS

4.7.1 Commonsense Basis Error Analysis

Analysis of the data on common sense basis has many forms. One rule of thumb that could be used is that the error in the result is equal to maximum error in any parameter used to calculate the result. Another commonsense analysis would combine all the errors in the most detrimental way in order to determine the maximum error in the final result(J.P Holman).

4.7.2 Uncertainty Analysis

The method is based on a careful specification of the uncertainties in the various primary experimental measurements. If a very careful calibration of an instrument has been performed recently, with standards of very high presicion, then the experimentalist will be justified in assigning a much lower uncertainty to measurements than if they were performed with a gage or instrument of unknown calibration history. (J.P Holman).

Suppose a set of measurements is made and the uncertainty in each measurement may be expressed with the same odds. These measurements are then used to calculate some desired result of the experiments. We wish the estimate the uncertainty in the calculated result on the basis of uncertainties in the primary measurements. The result R is a given function of the independent variables $x_{1,}x_{2,}x_3 \dots \dots \dots, x_n$ Thus,

$$R = R(x_{1,}x_{2,}x_3 \dots \dots \dots, x_n) \tag{4.3}$$

Let w_R be the uncertainty in the result and $w_1, w_2, \dots \dots w_n$ be the uncertainties in the dependent variables. If the uncertainties in the dependent variables are all given with same odds, then the uncertainty in the result having these odds,

$$w_R = \left[\left(\frac{\partial R}{\partial x_1} w_1\right)^2 + \left(\frac{\partial R}{\partial x_2} w_2\right)^2 \dots \dots + \left(\frac{\partial R}{\partial x_n} w_n\right)^2\right]^{1/2} \tag{4.4}$$

4.7.3 Uncertainty Analysis with Using of Empirical Equations

Ignition Delay Error Analysis; (Gümüş, M. 2005)

$$\tau = A\lambda^k P^{-n} exp(E/\bar{R}T) \tag{4.5}$$

Depending on the upward equation $\tau = \tau(\lambda, P, T)$ and according to uncertainty analysis, ignition delay error ratio is;

$$w_R = \left[\left(\frac{1}{z}\sum_{i=1}^{z}\left(\frac{\partial \tau}{\partial \lambda}\right)_i w_{\lambda i}\right)^2 + \left(\frac{1}{z}\sum_{i=1}^{z}\left(\frac{\partial \tau}{\partial P}\right)_i w_{pi}\right)^2 + \left(\frac{1}{z}\sum\left(\frac{\partial \tau}{\partial T}\right)_i w_{Ti}\right)^2\right]^{\frac{1}{2}} \tag{4.6}$$

In this equation;

w_λ= Excess Air Coefficient Measurement Error Ratio,
w_p= Pressure Determination Error Ratio,
w_T=Temperature Determination Error Ratio.

According to equation (4.5) ;

$$\frac{\partial \tau}{\partial \lambda} = kA\lambda^k P^{-n} exp(E/\bar{R}T) \tag{4.7}$$

$$\frac{\partial \tau}{\partial P} = -nA\lambda^k P^{-n-1} exp(E/\bar{R}T) \tag{4.8}$$

$$\frac{\partial \tau}{\partial T} = -\frac{E}{\bar{R}T} \ln (A\lambda^k P^{-n}) A\lambda^k P^{-n} exp(E/\bar{R}T) \tag{4.9}$$

are determined as.

Cylinder Pressure Level Error Analysis; (Gümüş, M. 2005)

$$L = l + pP + t\tau \tag{4.10}$$

Depending on the upward equation, $L = L(P, \tau)$ according to the uncertainty analysis, cylinder pressure level error ratio;

$$w_L = \left[\left(\frac{1}{z} \sum_{i=1}^{z} \frac{\partial L}{\partial P} w_p \right)^2 + \left(\frac{1}{z} \sum_{i=1}^{z} \frac{\partial L}{\partial \tau} w_\tau \right)^2 + \right]^{\frac{1}{2}} \tag{4.11}$$

In this equation;
w_p=Pressure Determination Error Ratio,
w_τ= Ignition Delay Error Ratio.

According the equation (4.10),

$$\frac{\partial L}{\partial P} = P \tag{4.12}$$

$$\frac{\partial L}{\partial \tau} = k \tag{4.13}$$

are determined.

The Percentages Deviation;

$$\sigma_i = \frac{y_{gi} - y_i}{y_{gi}} \times 100 \tag{4.14}$$

The Percentage Mean Deviation;

$$\bar{\sigma} = \frac{1}{z} \sum_{i=1}^{z} |\sigma_i| \tag{4.15}$$

The Correlation Coefficient;

$$R = \left(1 - \frac{(z-1)\sum_{i=1}^{z}(y_{gi} - y_i)^2}{(z-F)\sum_{i=1}^{z}(y_{gi} - \bar{y}_i)^2}\right)^{1/2} \tag{4.16}$$

z= Number of Experiment,

y_{gi}= Numerical Value,

y_i= Theoretical Value,

$\bar{y}_i = \frac{1}{z} \sum_{i=1}^{z} y_{gi}$

F= y dependent variables is dependent on the variable number (taken F=2)

For the P_3 pressure value, percentage mean deviation is calculated as 3,915 %

For the P_4 pressure value, percentage mean deviation is calculated as 19,651 %

	Numeric	Theoric	Numeric	Theoric		
Piston Speed(RPM)	P3(kpa)	P3(kpa)	P4(kpa)	P4(kpa)	Percentage Deviation for the P3	Percentage Deviation for the P4
900	6300	6556,14	530,95	672,84	4,07	26,72
1000	6302	6556,14	550,06	698,64	4,03	27,01
1100	6305	6556,14	556,32	692,67	3,98	24,51
1400	6312	6556,14	612,82	702,42	3,87	14,62
1500	6319	6556,14	622,64	690,53	3,75	10,90
1600	6314	6556,14	612,49	698,27	3,83	14,01

Table 4.5. Percentage Deviation for the P_3 and P_4 pressure

5.RESULTS

5.1 BOUNDARY CONDITIONS AND CALCULATION

Intake manifold presssure=130 kpa
Intake air temperature=305-315K
Engine Speed=800-2000 RPM
Compression Ratio=18,25
QLHV=42500 kj/kg;(Table A-2-Pulkrabek ice book)
Piston Cross Sectional Area(Ap) = 0,00509 m^2

Combustion Efficiency(nc)=1

Displacement Volume(V_d)= 0,000387 m^3 (one cylinder)

R= 3,5197(r/a)

Cv= 0,821 kj/kg.K (Table A-1-Pulkrabek ice book)

Cp=1,108 kj/kg.K (Table A-1-Pulkrabek ice book)

K=1,35 (Table A-1-Pulkrabek ice book)

Air Density= 1,181 kg/m^3 (Table A-1-Pulkrabek ice book)

R=0,287 kj/kg.K (Table A-1-Pulkrabek ice book)

Making of Theoretical Calculation for the 900 rpm;(same steps will be used for the other rpm);

T_1 =305 K given

P_1 =130 kpa given

$T_2 = T_1(r_c)^{k-1} = 305K(18{,}25)^{0.35} = 842{,}83K$

$P_2 = P_3 = P_1(r_c)^k = 130kpa(18{,}25)^{1.35} = 6556{,}14kpa$

$Q_{HV}\eta_c = (AF + 1)c_p(T_3 - T_2)$

$\left(\frac{42500kj}{kg}\right)(1) = (18{,}13 + 1)\left(\frac{1.108kj}{kgK}\right)(T_3 - 842{,}83)K$

$T_3 = 2847{,}921K$

$v_4 = v_1 = \frac{RT_1}{P_1} = \frac{0{,}287(305)}{130} = 0{,}67334\ kj/kg$

$$v_3 = \frac{RT_3}{P_3} = \frac{0{,}287(2847{,}921)}{6556{,}14} = 0{,}12466\ m^3/kg$$

$$T_4 = T_3(v_3/v_4)^{k-1} = 2847{,}921(0{,}12466/0{,}67334)^{0{,}35} = 1578{,}157K$$

$$P_4 = P_3(v_3/v_4)^{k} = 6556{,}14(0{,}12466/0{,}67334)^{1{,}35} = 672{,}61\ kpa$$

$$\beta = \frac{T_3}{T_2} = \frac{2847{,}921K}{842{,}83K} = 3{,}378$$

$$(\eta_t) = 1 - (1/r_c)^{k-1}[(\beta^k - 1)/(k(\beta - 1))]$$

$$(\eta_t) = 1 - (1/18{,}25)^{1.35-1}\left[\frac{3{,}378^{1.35} - 1}{1.35(3{,}378 - 1)}\right] = 0{,}5296 = 52{,}96\%$$

$$q_{in} = c_p(T_3 - T_2) = \frac{1{,}108kj(2847{,}921 - 842{,}83)K}{kgK} = 2221{,}64\ kj/kg$$

$$w_{net} = q_{in}\eta_t = 2221{,}64(0{,}5296) = 1176{,}75\ kj/kg$$

$$q_{out} = q_{in} - w_{net} = 2221{,}64 - 1176{,}75 = 1044{,}88\ kj/kg$$

5.2 THEORETICAL RESULTS

Engine Speed (RPM)	P1(kpa)	P2(kpa)	P3(kpa)	P4(kpa)
900	130	6556,14	6556,14	672,84
1000	130	6556,14	6556,14	698,64
1100	130	6556,14	6556,14	692,67
1400	130	6556,14	6556,14	702,42
1500	130	6556,14	6556,14	690,53
1600	130	6556,14	6556,14	698,27

Table 5.1 The Pressure Value Depending on the Engine Speed

Engine Speed (RPM)	T1(K)	T2(K)	T3(K)	T4(K)
900	305	842,83	2848,45	1578,59
1000	308	851,12	2957,76	1655,24
1100	310	856,65	2958,10	1651,75
1400	312	862,18	3008,17	1685,80
1500	313	864,94	2979,90	1662,59
1600	315	870,47	3023,80	1691,97

Table 5.2 The Temperature Value Depending on the Engine Speed

Engine Speed (RPM)	Cut off Ratio(β)	Thermal Efficiency(nt)	V1=V4(m^3/kg)	V3(m^3/kg)
900	3,38	0,5296	0,6733	0,1247
1000	3,48	0,5263	0,6800	0,1295
1100	3,45	0,5270	0,6844	0,1295
1400	3,49	0,5258	0,6888	0,1317
1500	3,45	0,5273	0,6910	0,1304
1600	3,47	0,5263	0,6954	0,1324

Table 5.3 The Thermal Efficiency, Volume and Cut off Ratio values Depending on the Engine Speed

Volumetric Efficiency is calculated as **1.0001**

Engine Speed (RPM)	Average Piston Speed (m/s)	Brake Power(kW)	Specific Power(kW/m^2)	OPD(kW/m^3)
900	2,28	12,76	627,00	8250,10
1000	2,53	14,18	696,67	9166,77
1100	2,79	15,60	766,33	10083,45
1400	3,55	19,86	975,33	12833,48
1500	3,80	21,27	1045,00	13750,16
1600	4,05	22,69	1114,67	14666,84

Table 5.4 The Average Piston Speed, Brake Power, Specific Power and OPD Values Depending on the Engine Speed

Engine Speed (RPM)	Specific Volume(1/OPD)	AF	Injected Fuel Quantity(kg/cycle)	bsfc(mf/Wb) (kg/kj)
900	0,00012121	18,13	0,00002522	0,0000019756
1000	0,00010909	17,21	0,00002670	0,0000018827
1100	0,00009917	17,25	0,00002670	0,0000017115
1400	0,00007792	16,87	0,00002744	0,0000013821
1500	0,00007273	17,14	0,00002744	0,0000012900
1600	0,00006818	16,81	0,00002818	0,0000012420

Table 5.5 The Specific Volume, Air-Fuel Ratio Injected Fuel Quantity and Break Specific Fuel Consumption Values Depending on the Engine Speed

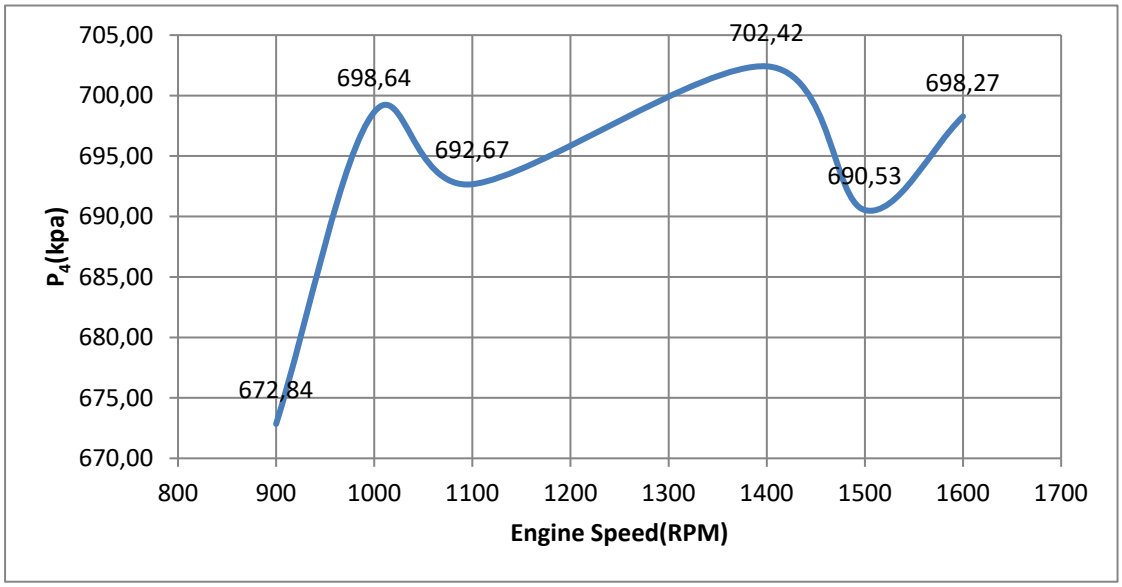

Figure 5.1. The Changing of P_4 Pressure Depending on Engine Speed

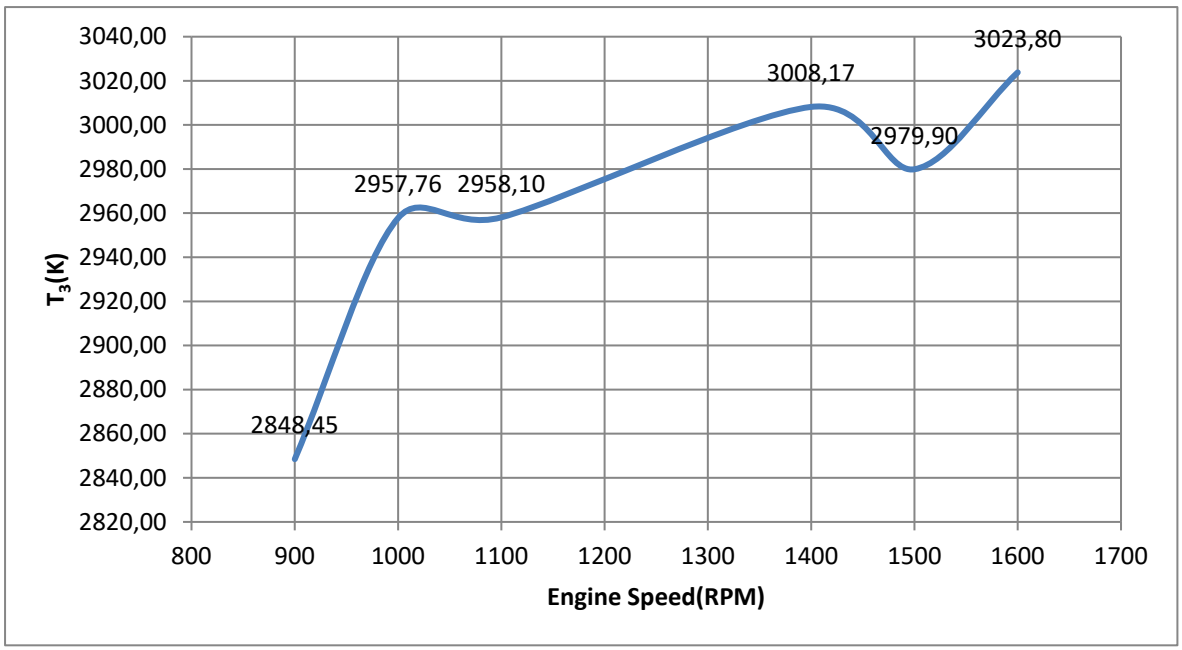

Figure 5.2. The Increasing of T_3 Temperature Depending on Engine Speed

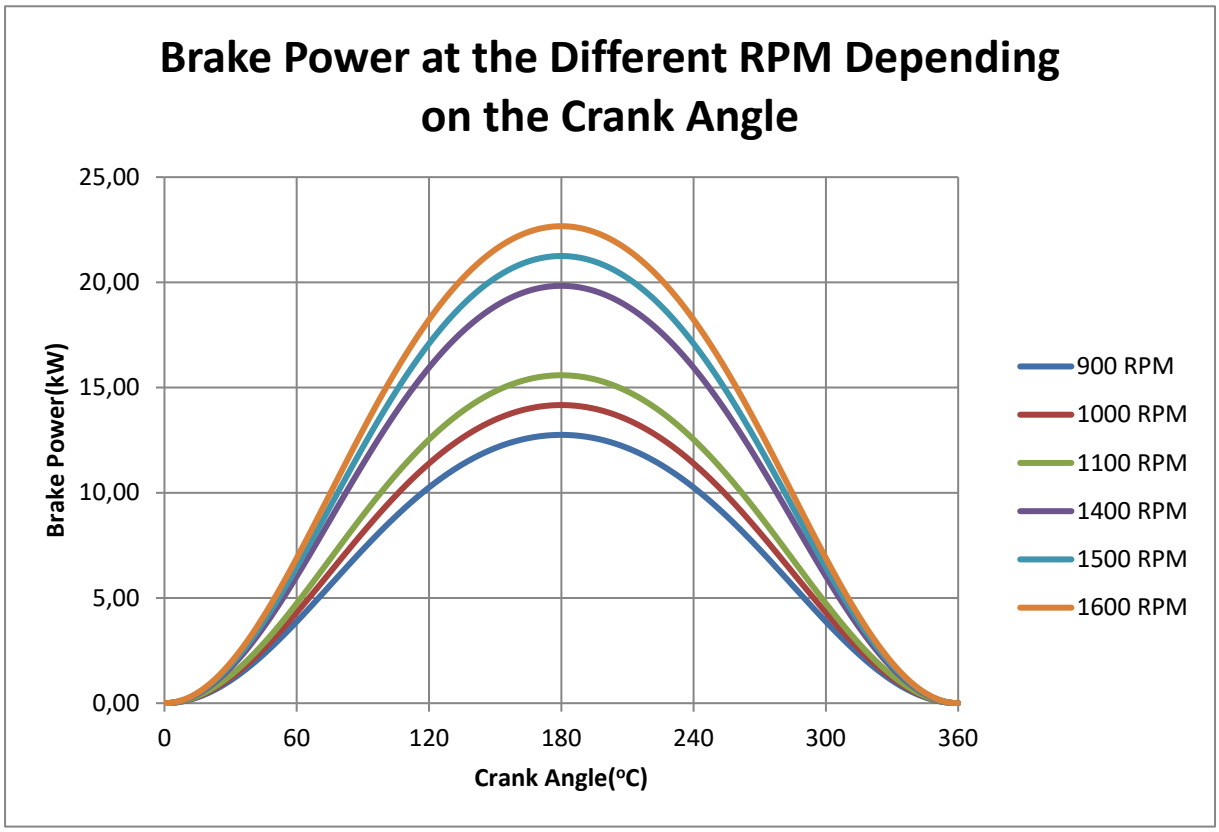

Figure 5.3. The Increasing of Brake Power Depending on Crank Angle and Engine Speed

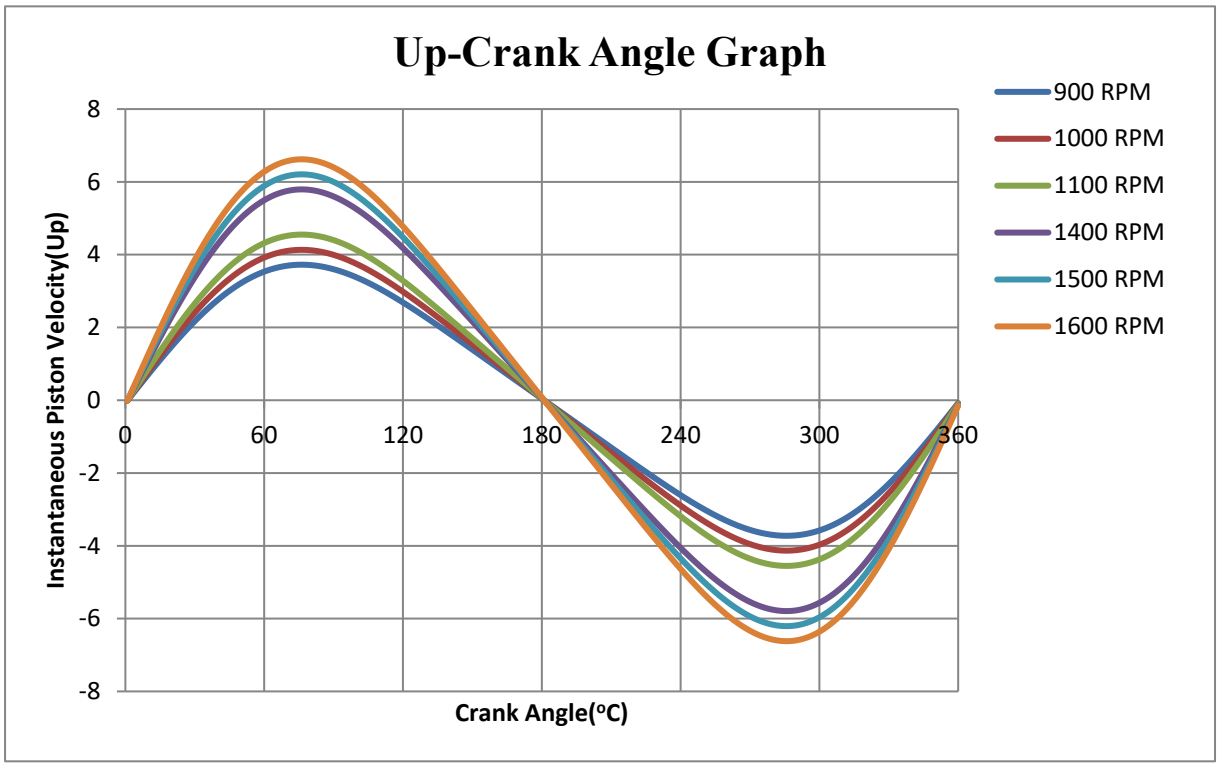

Figure 5.4. The Changing of Instantaneous Piston Velocity Depending on Crank Angle and Engine Speed

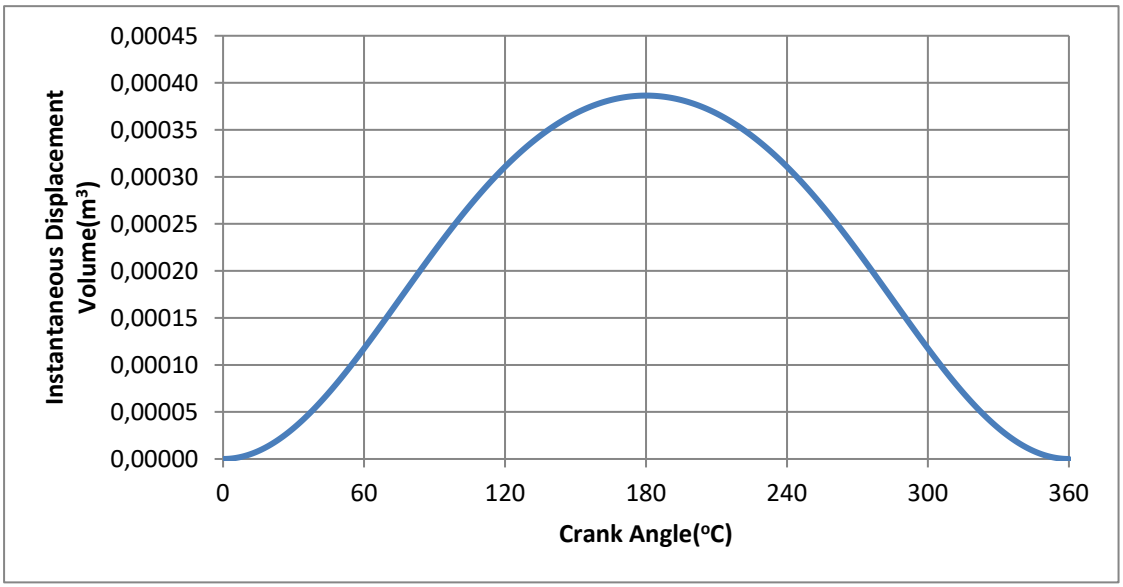

Figure 5.5. The Instantaneous Displacement Volume Depending on the Crank Angle

5.3 NUMERICAL RESULTS

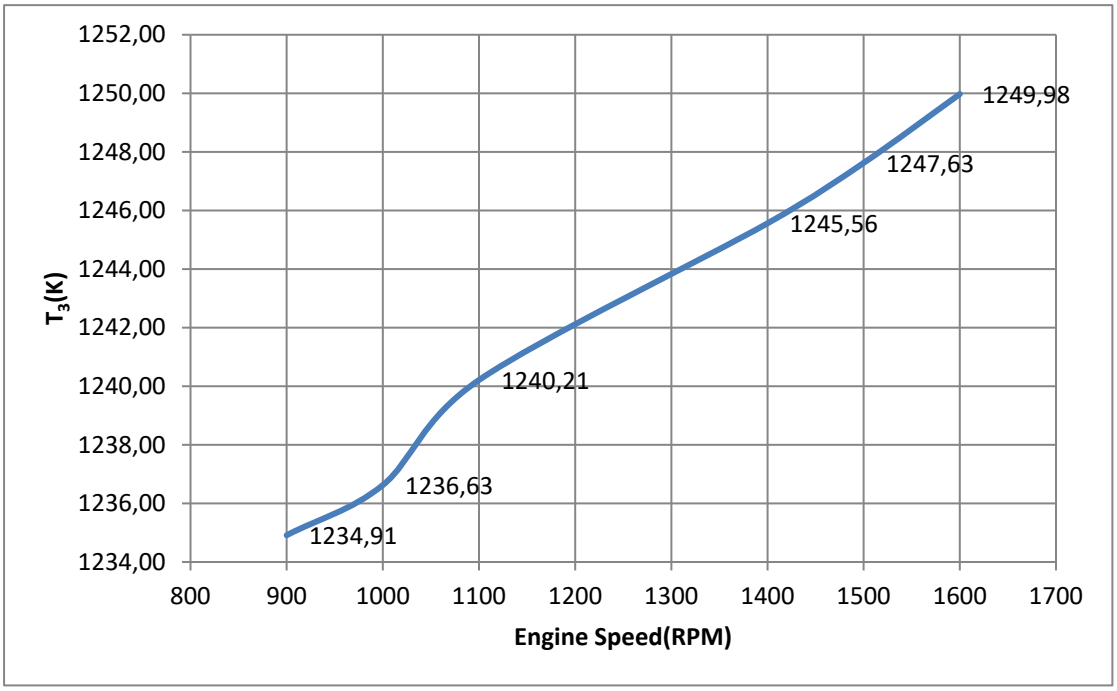

Figure 5.6 The Increasing of T_3 Value Depending on the Engine Speed

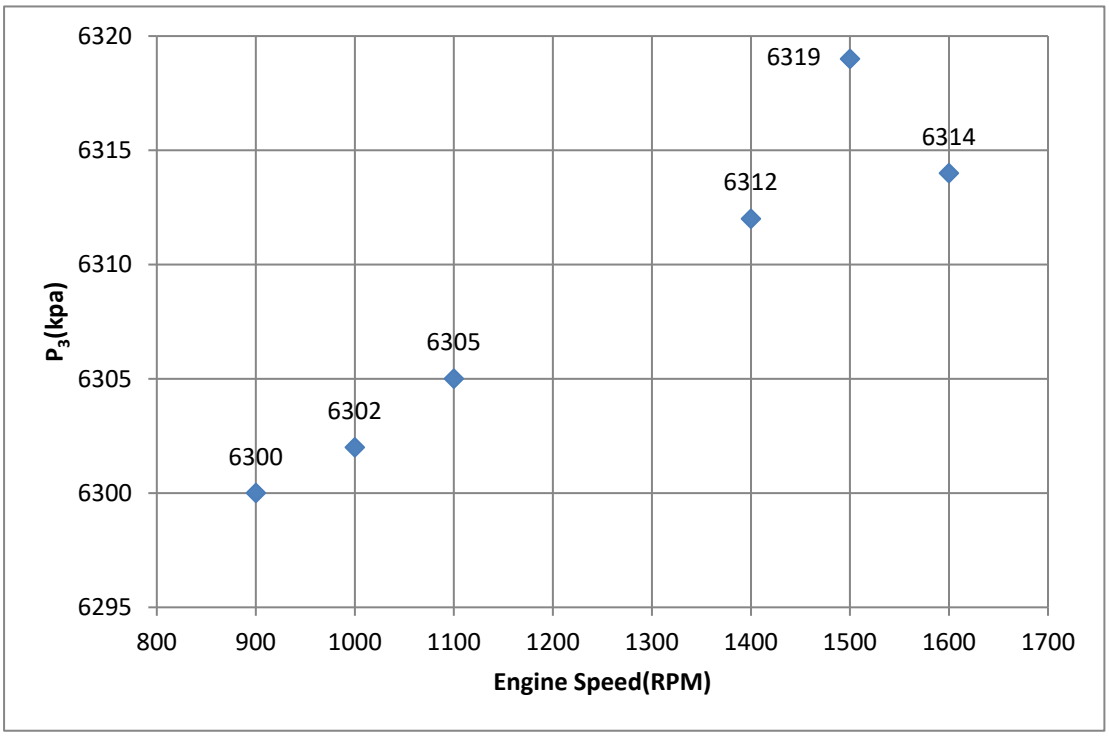

Figure 5.7. The Changing of P_3 Value Depending on the Engine Speed

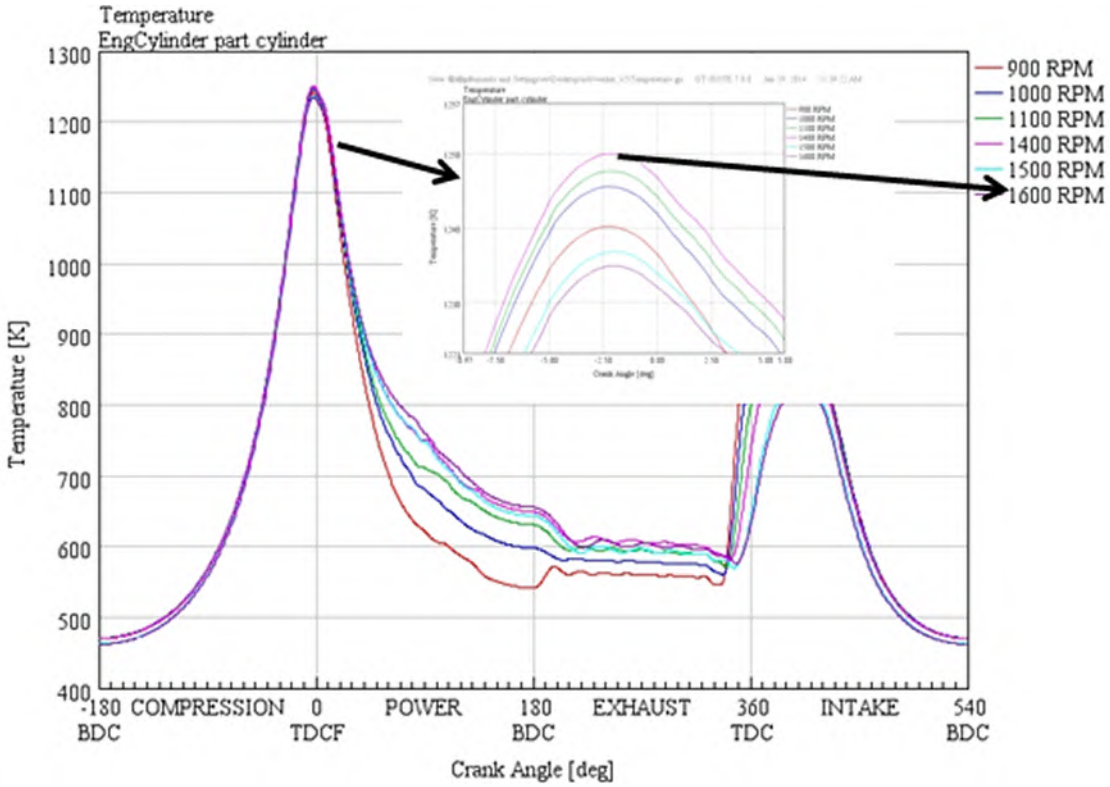

Figure 5.8. The Changing of Pressure Depending on Engine Speed and Crank Angle

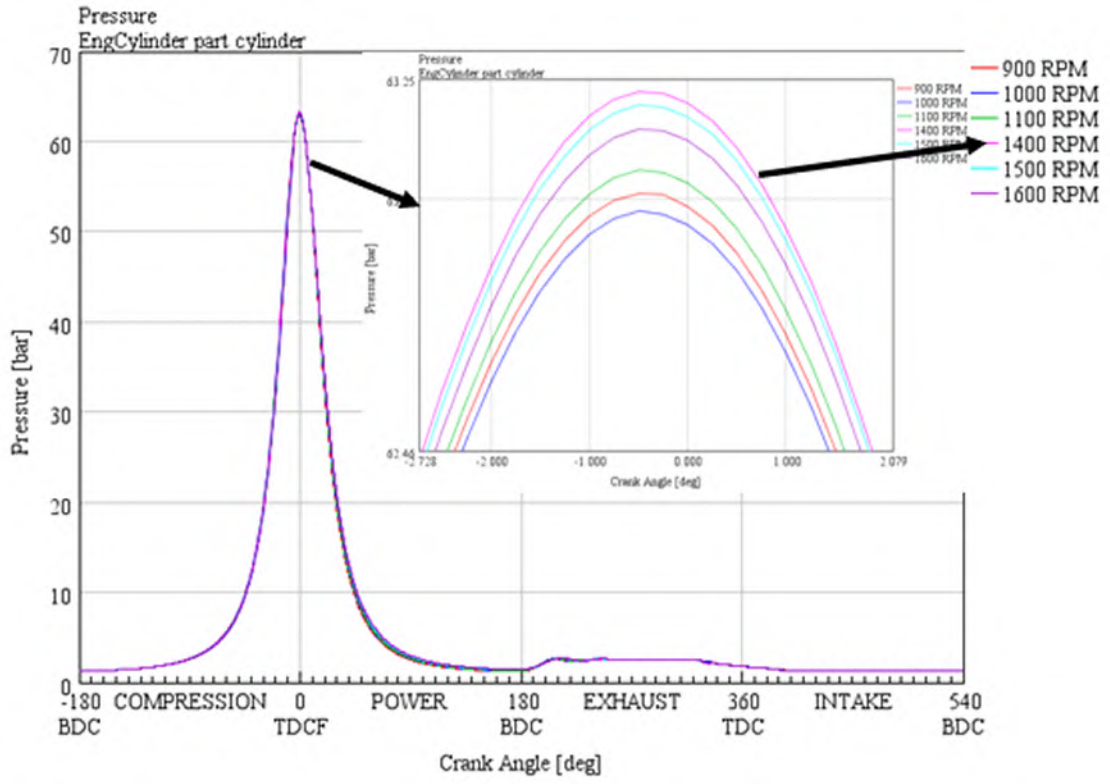

Figure 5.9. The Changing of Temperature Depending on Engine Speed and Crank Angle

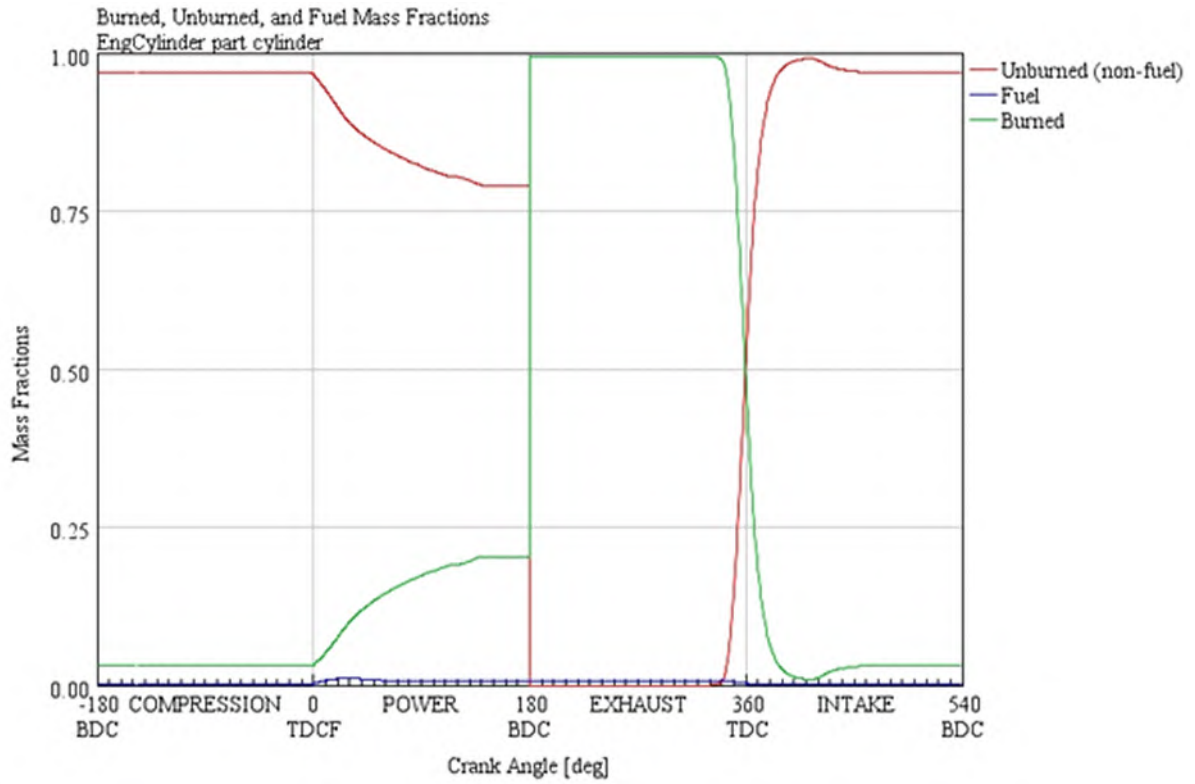

Figure 5.10. Changing of Burned, Unburned and Fuel Mass Fractions at 1400 RPM

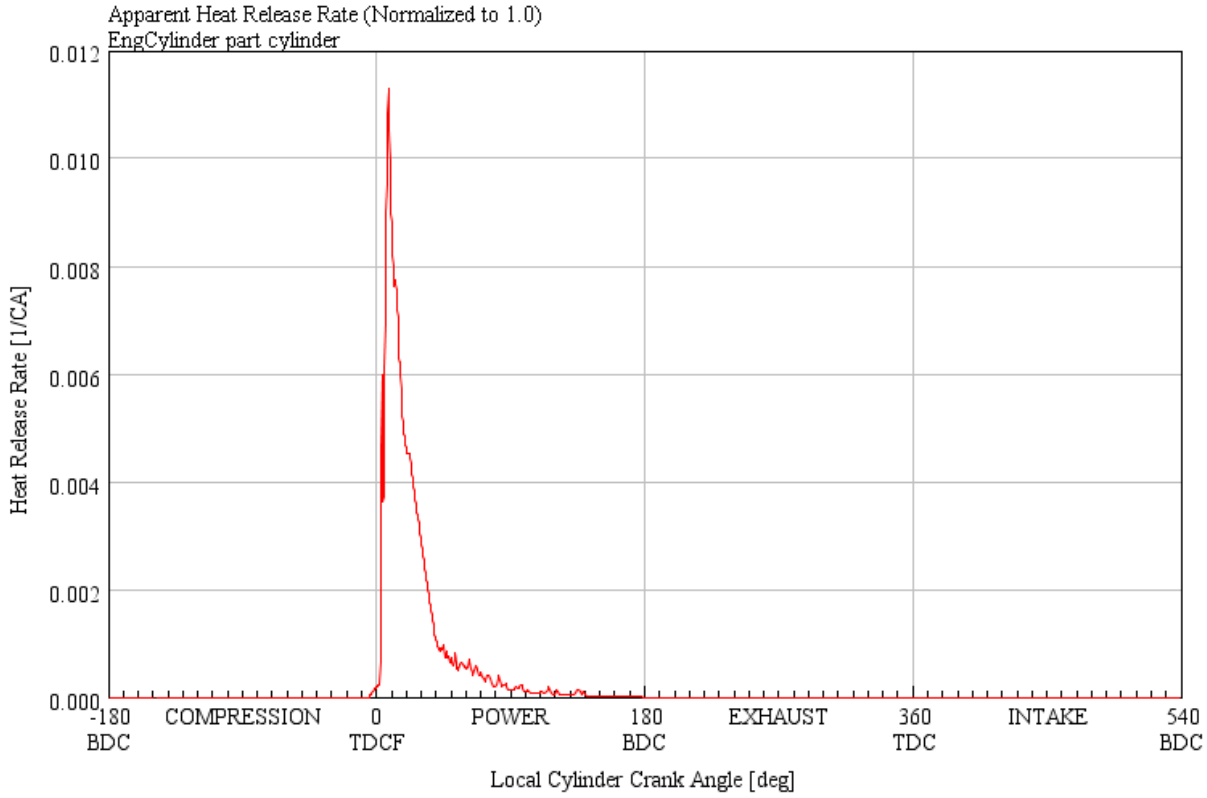

Figure 5.11. The Changing of Heat Release Rate at 1100 RPM

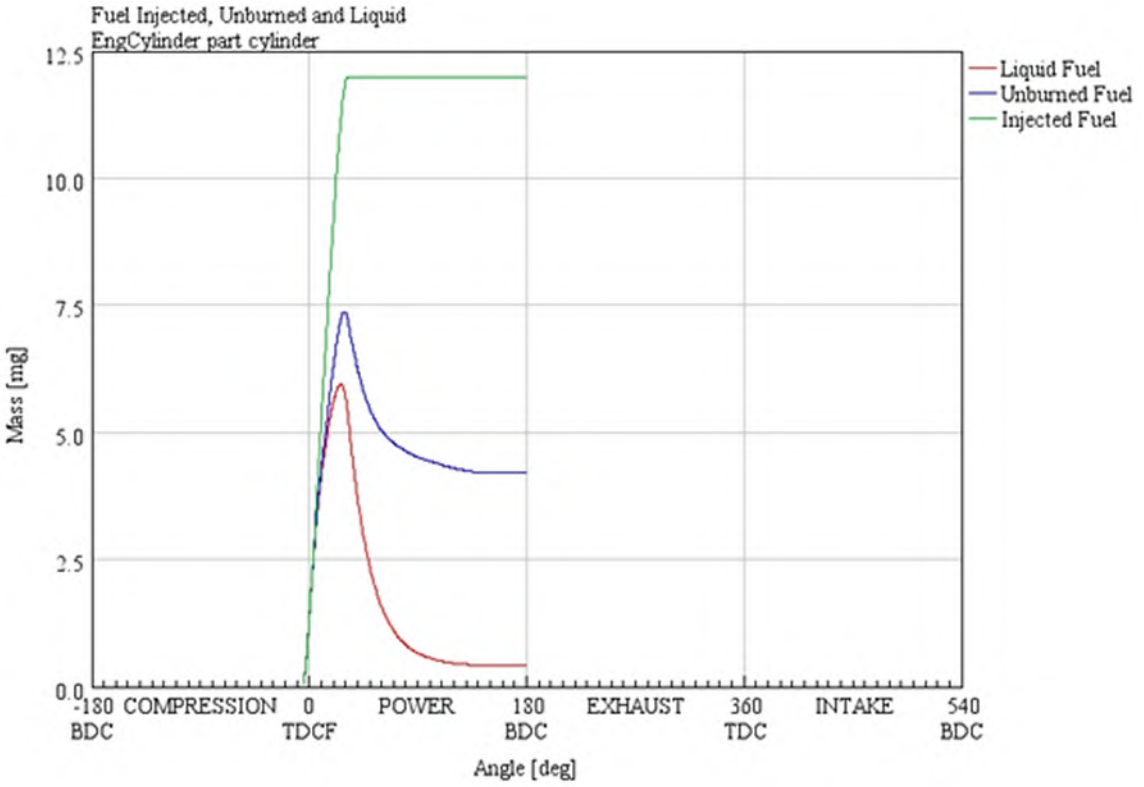

Figure 5.12. The Changing of Fuel Injected, Unburned and Liquid at the 1000 RPM

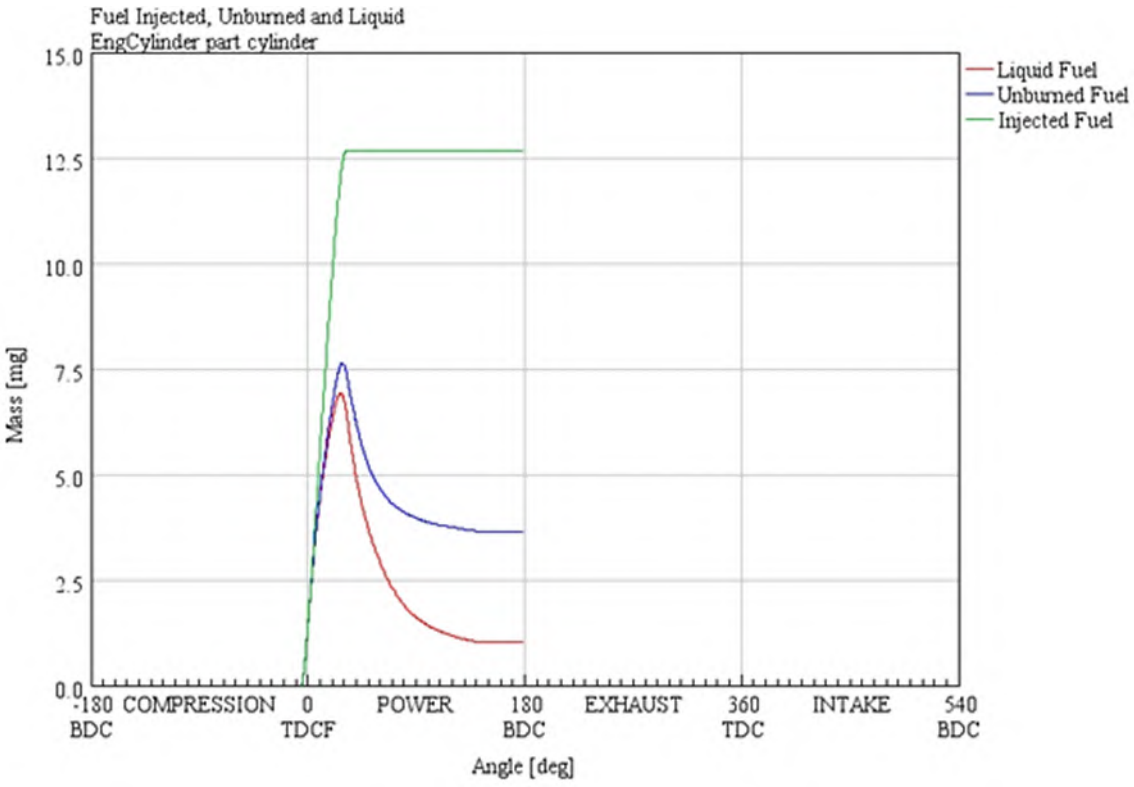

Figure 5.13. The Changing of Fuel Injected, Unburned and Liquid at the 1600 RPM

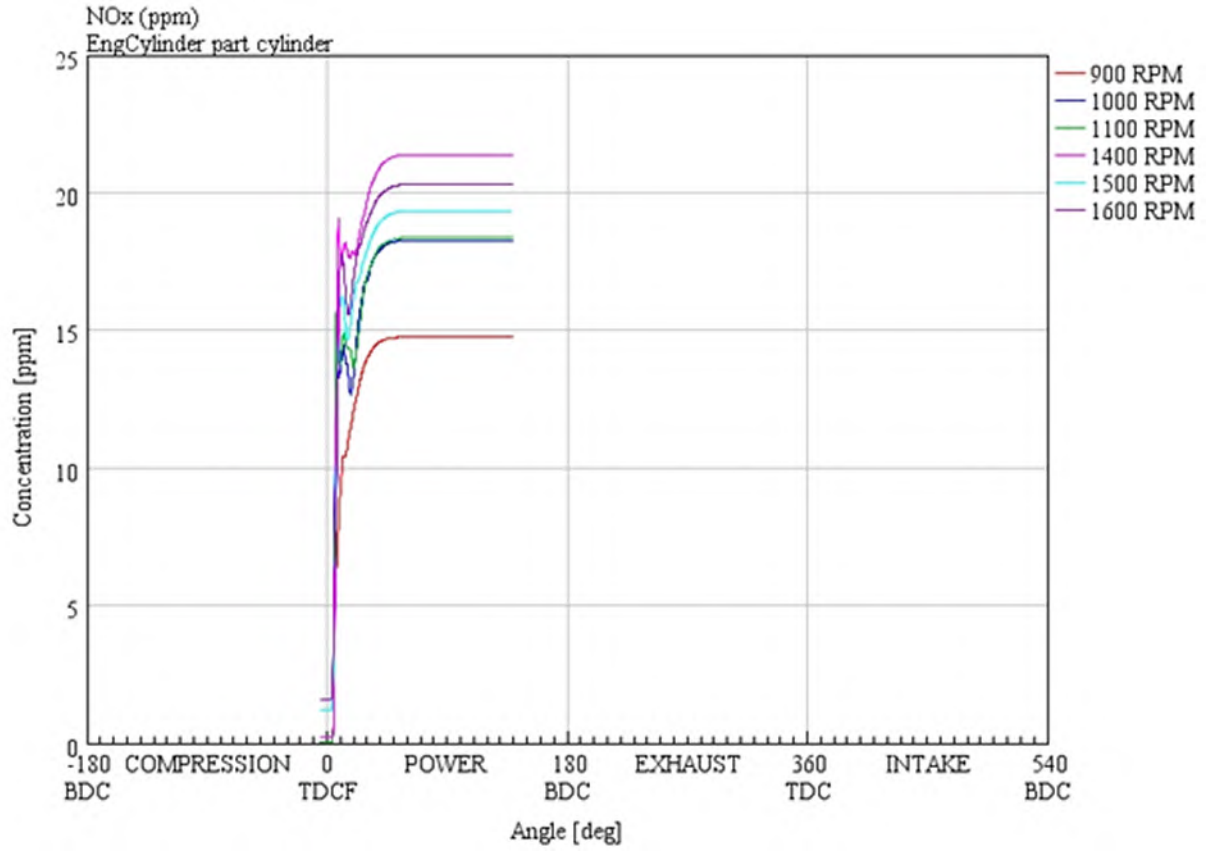

Figure 5.14. The Changing of NOx Concentration Depending on RPM and Crank Angle

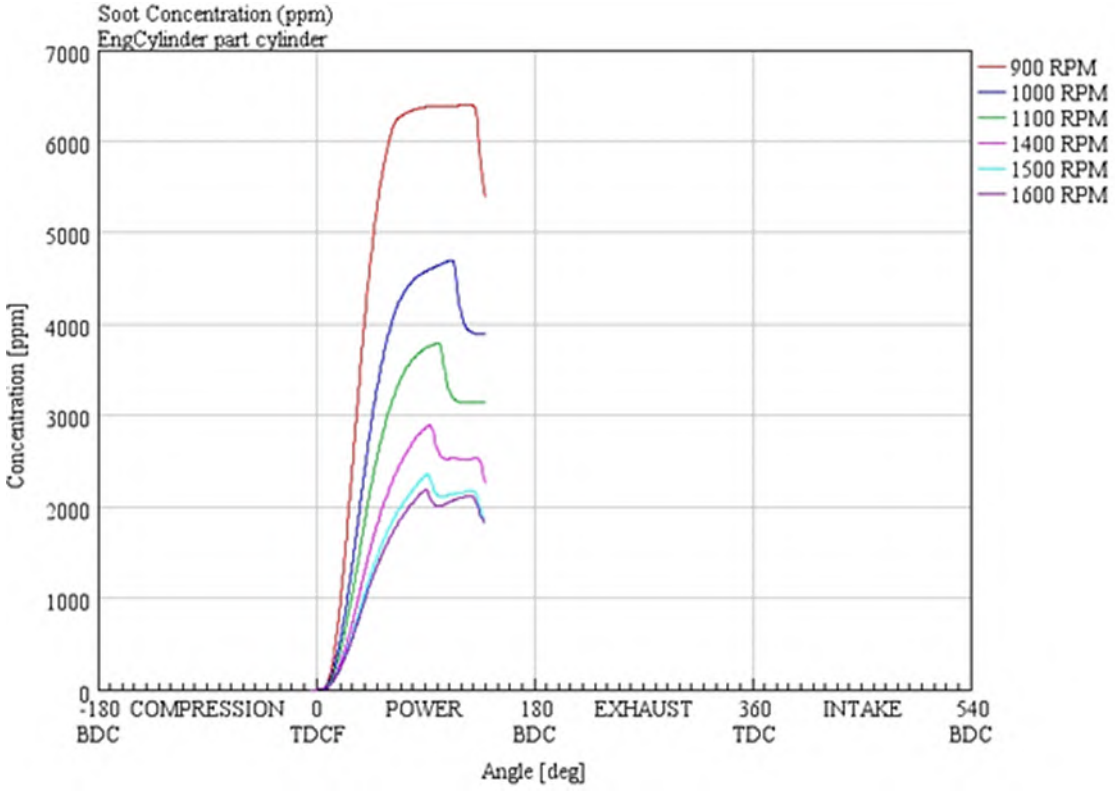

Figure 5.15. The Changing of Soot Concentration Depending on RPM and Crank Angle

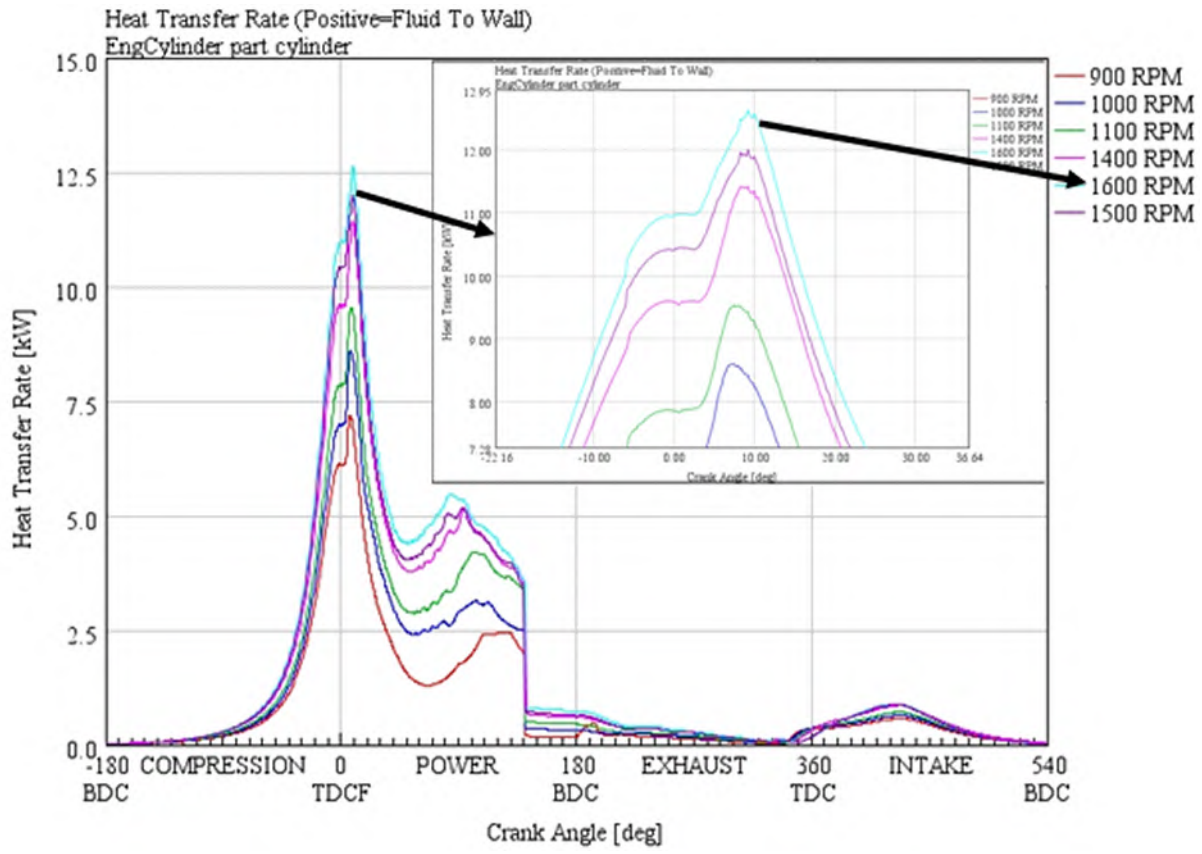

Figure 5.16. The Changing of Heat Transfer Rate Depending on RPM and Crank Angle

5.4 EXPERIMENTAL RESULTS

Engine Speed(RPM)	Rail Pressure (MPA)	Injected Fuel Quantity(kg/cycle)	Fuel Temperature (oC)	Oil Temperature (oC)	Air-mass(kg/cycle)
900	23	0,000025218	34,5	67	0,000457077
1000	23,4	0,000026701	39	76	0,000459477
1100	24	0,000026701	42	82	0,000460676
1400	25,4	0,000027443	45,4	85	0,000463076
1500	28,5	0,000027443	47	87	0,000470274
1600	32	0,000028185	49	88	0,000473873

Table 5.6. Rail Pressure, Injected Fuel Quantity, Fuel Temperature Oil Temperature and Air mass Depending on Engine Speed

Engine Speed(RPM)	Intake Air Temperature (oC)	Engine Coolant Temperature(oC)	Exhaust Gas Temperature (oC)T4	Intake Manifold Pressure(kpa)
900	32	72	132	130
1000	35	82	140	130
1100	37	84	143	130
1400	39	86	150	130
1500	40	87	155	130
1600	42	88	158	130

Table 5.7. Intake Air Temperature, Engine Coolant Temperature, Exhaust gas Temperature and Intake Manifold Pressure Depending on Engine Speed

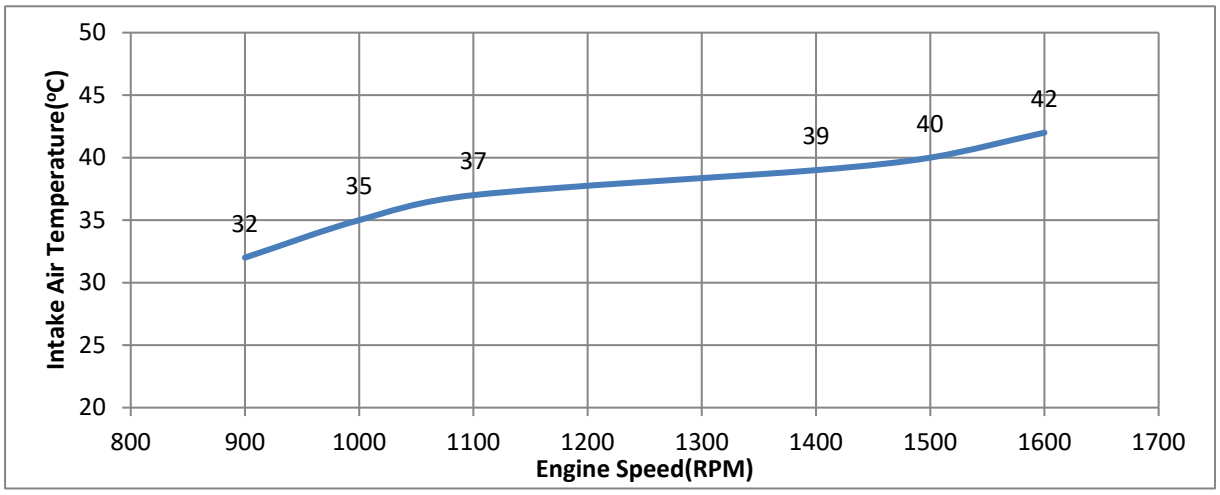

Figure 5.17. The Increasing of Intake Air Temperature(T_1) Depending on Engine Speed

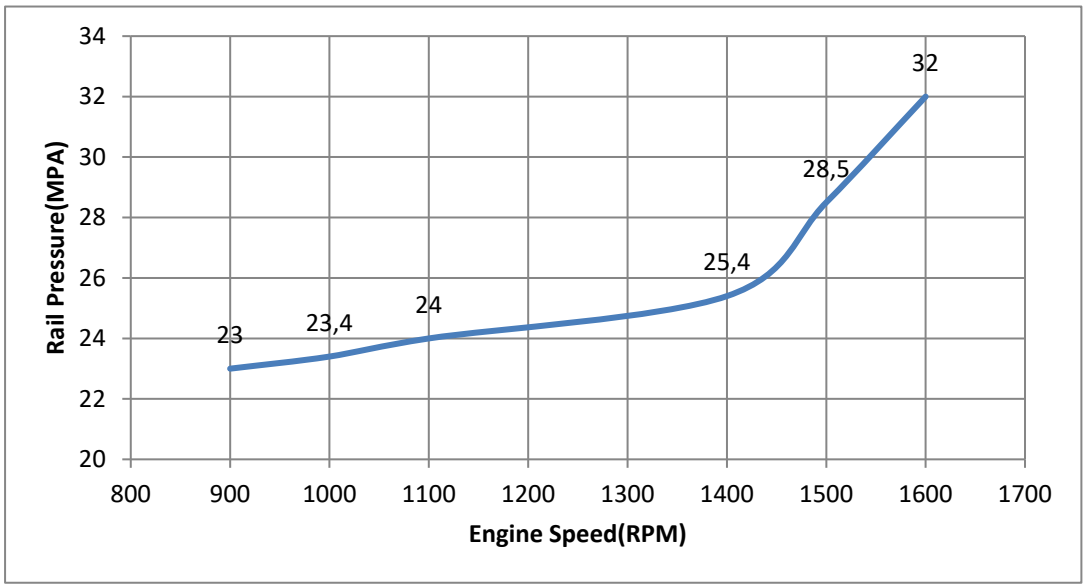

Figure 5.18. The Increasing of Rail Pressure Depending on Engine Speed

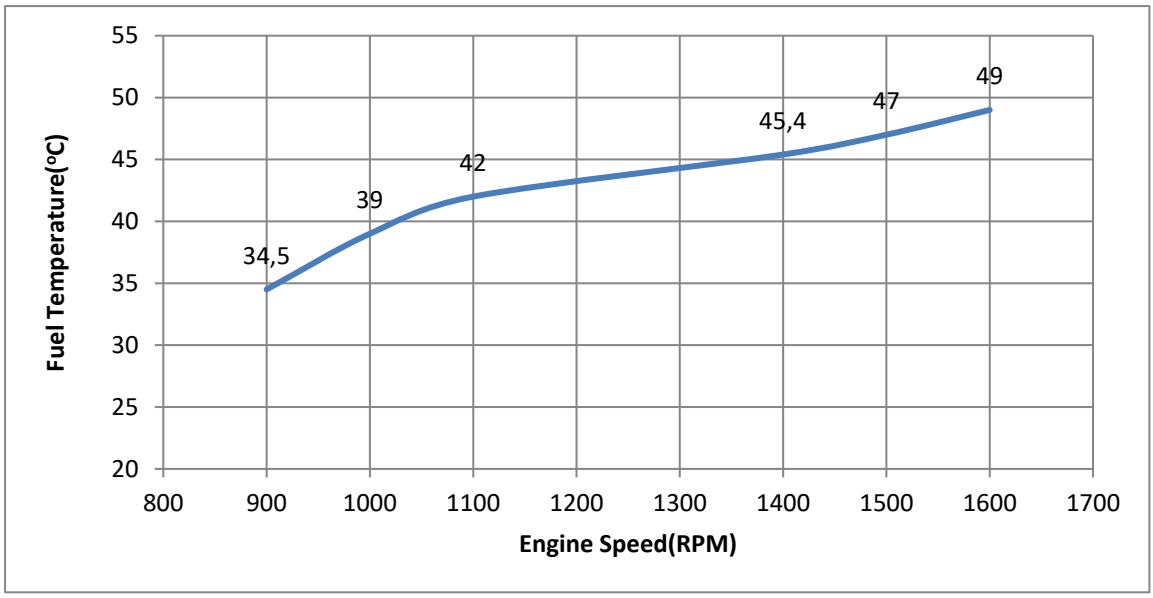

Figure 5.19. The Changing of Fuel Temperature Depending on Engine Speed

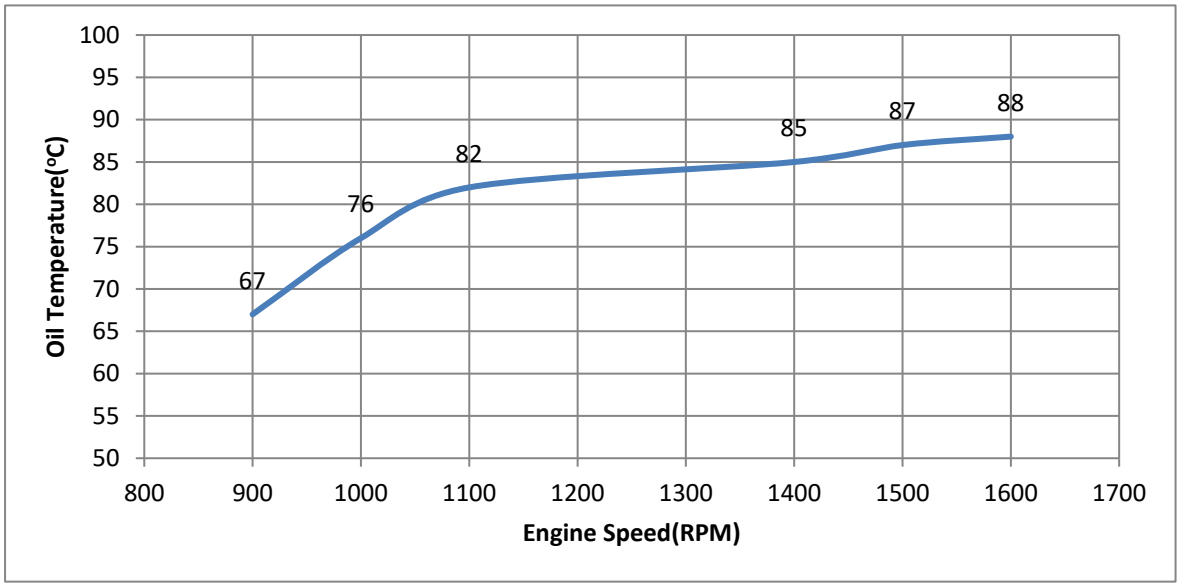

Figure 5.20. The Changing of Oil Temperature Depending on Engine Speed

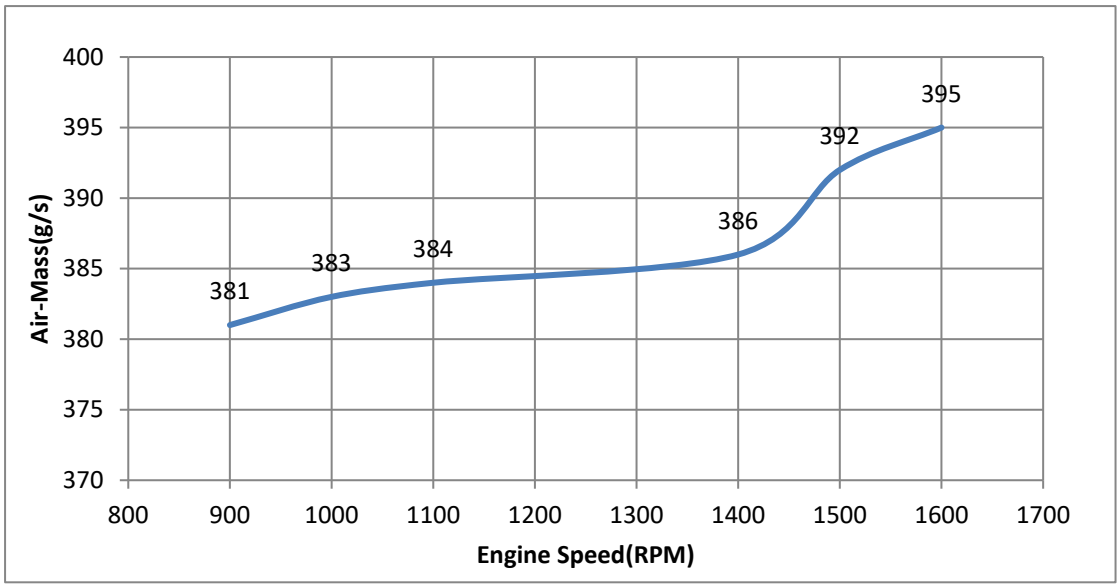

Figure 5.21. The Changing of Air- Mass Depending on Engine Speed

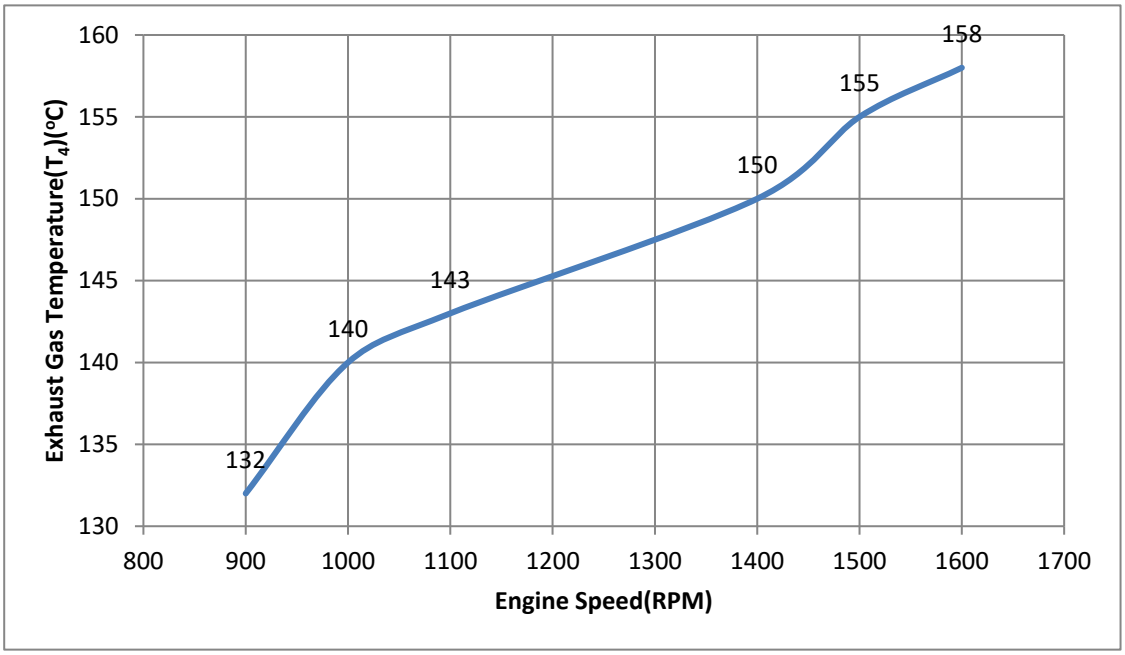

Figure 5.22. The Changing of Exhaust Gas Temperature Depending on Engine Speed

5.5 COMPARISON OF RESULTS

The comparison of exhaust temperature between the numerical, experimental and theoretical result;

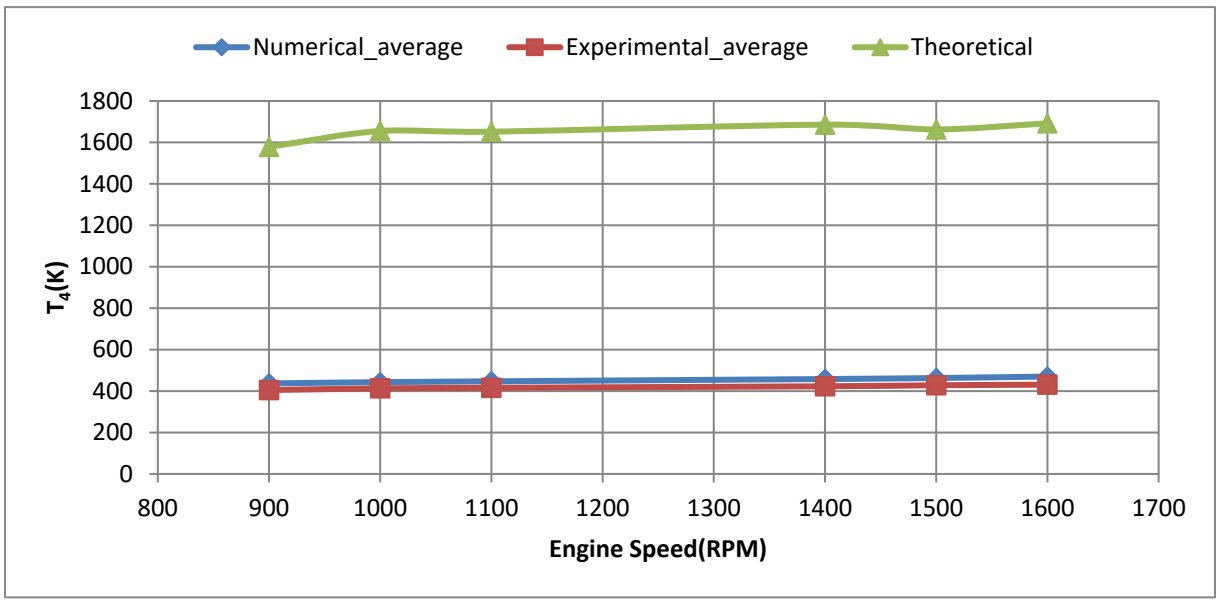

Figure 5.23. The Comparison of Numerical, Experimental and Theoretical Exhaust Gas Temperature

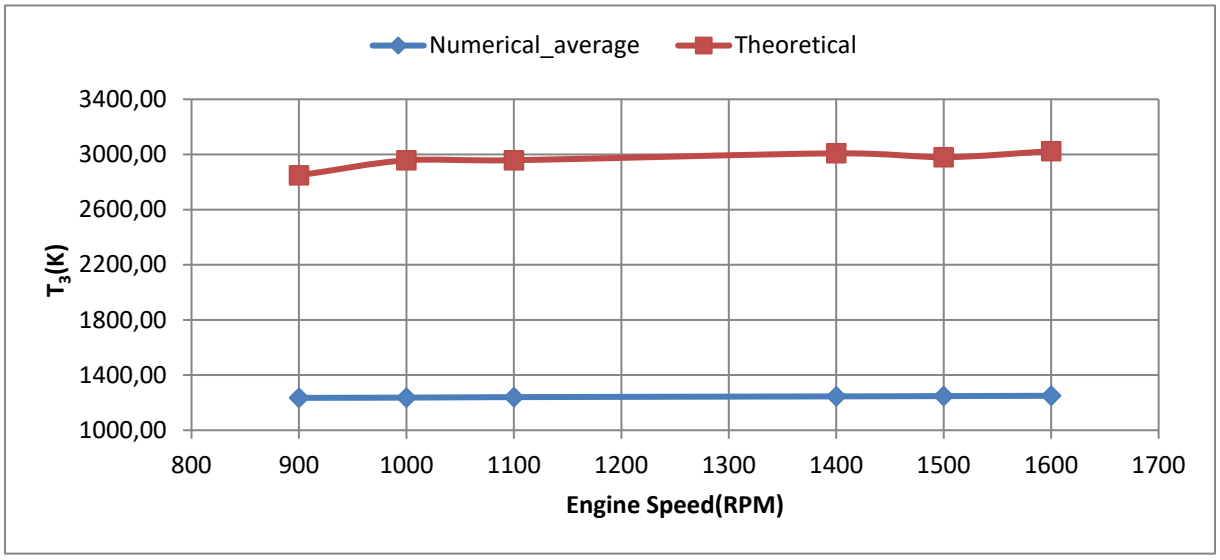

Figure 5.24. The Comparison of Theoretical and Numerical T_3 Temperature

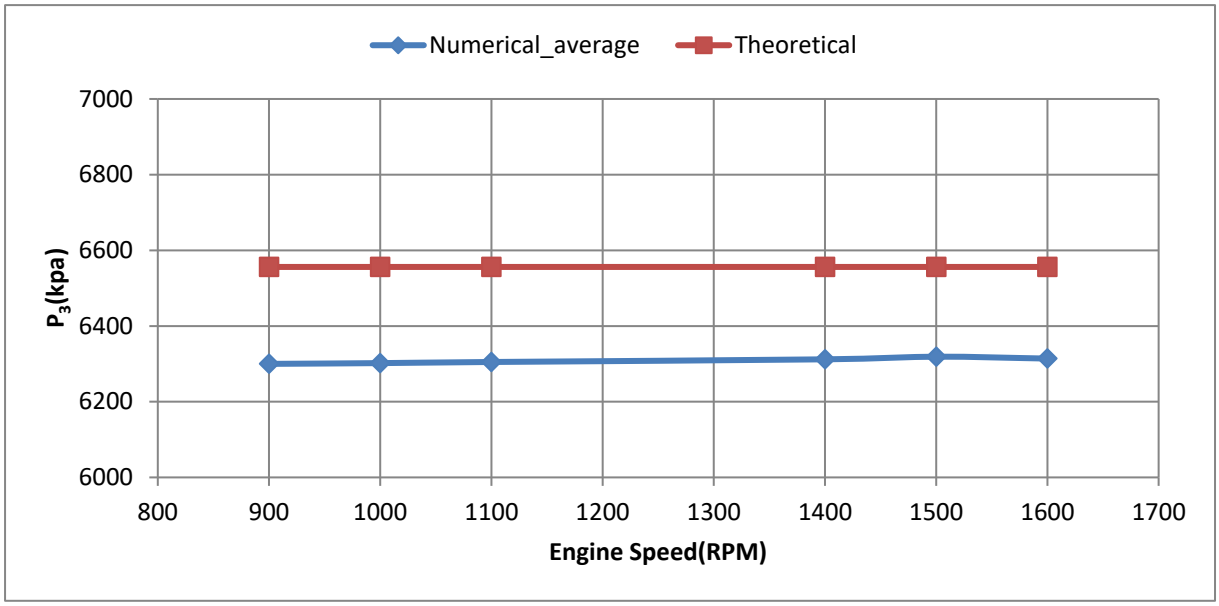

Figure 5.25. The Comparison of Theoretical and Numerical P_3 Pressure

6. CONCLUSIONS

In this study, the worked on four cylinder four stroke diesel engine experiment system. Seeing that rail pressure, injected fuel quantity, fuel temperature, oil temperature, air mass, intake air temperature, engine coolant temperature, exhaust gas temperature and intake manifold pressure with respect to six different engine speed values. Pressure sensor, thermocouple, encoder, internal combustion engine system and dynamometer system are learned and applied.

Another result was, the difference of 0D/1D-3D simulation are learned on the GT power program. Models (heat transfer model, combustion model, flow model) which used on GT power program are performed.

From the GT power, taken the graph of temperature, pressure, heat release rate, NOx concentration, soot concentration, burned, unburned fuel mass fraction, fuel injected unburned and liquid depending on the crank angle and engine speed.

Also, some graphs from experimental and theoretical results were obtained. Seeing that the values increase linearly according the engine speed. The temperature and pressure increase depending on the engine speed. Repeatly, according to the engine speed, other parameters also increase.

The experimental results more closely to numerical results and lower than theoretical results. But, experimental results more confidence than other data because of the experimental conditions are changeable.

Finally, the different the experimental, numerical and theoretical data were compared ın order to see the difference of these results.

REFERENCES

Aaron J. Reiter, Song-Charng Kong, “Combustion and emissions characteristics of compression-ignition engine using dual ammonia-diesel fuel”, Department of Mechanical Engineering, Iowa State University, USA, 2010

A.Henham and M. K. Makkar,”Combustion of simulated biogas in a dual-fuel diesel engine”,School of Mechanical and Materials Engineering, University of Surrey, 1998.

Antonio P. Carlucci, Domenico Laforgia, Roberto Saracino, Giuseppe Toto, “Combustion and emissions control in diesel–methane dual fuel engines: The effects of methane supply method combined with variable in-cylinder charge bulk motion”, Department of Engineering for Innovation, University of Salento, Lecce, Italy, 2010

AutoPSI Pressure Sensor User Manual OPTRAND Incorporated

A.P. Carlucci, A. de Risi, D. Laforgia, F. Naccarato, “Experimental investigation and combustion analysis of a direct injection dual-fuel diesel–natural gas engine”, Department of Engineering for Innovation, University of Salento, Italy, 11 December 2006.

Bade, Shrestha, S.O., Narayanan G., 2008. “Landfill gas with hydrogen addition – A fuel for SI engines”, **Fuel** 87 3616–3626.

B.B. Sahoo, N. Sahoo, U.K. Saha,”Effect of engine parameters and type of gaseous fuel on the performance of dual-fuel gas diesel engines”, Centre for Energy, Indian Institute of Technology, India Department of Mechanical Engineering, 7 January 2008.

Biogas as Vehicle Fuel, A European Overview, Trendsetter Report No 2003:3

Chang Sik Lee, Ki Hyung Lee, Dae Sik Kim, “Experimental and numerical study on the combustion characteristics of partially premixed charge compression ignition engine with dual fuel”,Department of Mechanical Engineering, Hanyang University, South Korea , Graduate School of Hanyang University, South Korea, 1 April 2002.

Cheikh Mansour, Abdelhamid Bounif, Abdelkader Aris, Françoise Gaillard, “Gas–Diesel (dual-fuel) modeling in diesel engine environment”,Université des Sciences et de la Technologie, Algeria, Centre National de la Recherche Scientifique, France, 2 December 1999.

Cohe, C. , Chauveau, C., Gokalp, İ., Kurtuluş, D. F., 2009. “CO2 addition and pressure effects on laminar and turbulent lean premixed CH4 air flames”, Proceedings of the Combustion Institute, 32: 1803–1810.

C.C.M. Luijten, E. Kerkhof,” Jatropha oil and biogas in a dual fuel CI engine for rural electrification”, Department of Mechanical Engineering, Eindhoven University of Technology, The Netherlands, 2010

Crookes, R. J., 2006. “Comparative bio-fuel performance in internal combustion Engines”, **Biomass and Bioenergy**, 30: 461–468.

D.B. Lata, Ashok Misra, “Theoretical and experimental investigations on the performance of dual fuel diesel engine with hydrogen and LPG as secondary fuels”, Department of Mechanical Engineering, Birla Institute of Technology, India, 16 September 2010

D.B. Lata, Ashok Misra, “Analysis of ignition delay period of a dual fuel diesel engine with hydrogen and LPG as secondary fuels”, Department of Mechanical Engineering, Birla Institute of Technology, India, 22 October 2010

Duff M., Towey J., “Two Ways to Measure Temperature Using Thermocouples Feature Simplicity, Accuracy, and Flexibility” October 2010

J.P. Holman Experimental Method for Engineers Mc Graw Hill

Febris v1.0 User manual NEL presto

Forsich, C., Lacknera, M., Winter, F., Kopecek, H., Wintner, E., 2004. “Characterization of laser-induced ignition of biogas–air mixtures”, **Biomass and Bioenergy,** 27: 299-312.

G. A. Karim, A.M.I, S. R. Klat, and N. P. W. Moore, M.I,” Knock in dual fuel engines”, 1966

Gezgin E., Ç., 2003. Enerji Yaşamın Çekirdeği, İnterteks İnşaat Fuarı, İstanbul,.

G.H. Abd Alla, H.A. Soliman, O.A. Badr, M.F. Abd Rabbo, **“**Effect of pilot fuel quantity on the performance of a dual fuel engine”, Zagazig University, Shoubra Faculty of Engineering, 21 December 1998.

Görez, T., Alkan, A., Türkiye’nin yenilenebilir enerji kaynakları ve hidroelektirik enerji potansiyeli,Dokuz Eylül Üniversitesi Mühendislik Fakültesi İnşaat Mühendisliği Bölümü, Tınaztepe-Buca, İzmir.

GT Post User’s Manual Version 7.0

Gümüş, M., “Dizel Motorlarında Tutuşma Gecikmesinin Silindir Basınç Seviyesine Etkisi”, Doktora Tezi, Marmara Üniversitesi, Fen Bilimleri Enstitüsü ,İstanbul, 2005

Haiyan Miao, Brian Milton,” Numerical simulation of the gas/diesel dual fuel engine in-cylinder combustion process”, School of Mechanical and Manufacturing Engineering, The University of New South Wales, Australia, 2005

Henham, A., and Makkar, M. K., 1998. “Combustion of simulated biogas in a dual-fuel diesel engine”, **Energy Convers. Mgmt** Vol, 39, No. 16-18: Pp. 2001-2009,.

H.E. Saleh, “Effect of variation in LPG composition on emissions and performance in a dual fuel diesel engine”, Department of Mechanical Power Engineering, Faculty of Engineering, Mattaria, Helwan University, 16 August 2007.

Huang, J, D., Crookes, R. J., 1998. “Assessment of simulated biogas as a fuel for the spark-ignition engine”, **Fuel**, 77(15):1793–801.

IEA, THE INTERNATIONAL ENERGY AGENCY; 2008. World Energy, http://www.oecd.org/ ,(Erişim tarihi: Ekim 2012).

IEA, The International Energy Agency, 2009. Global Renewable energy policies and measures, http://www.iea.org/ ,(Erişim tarihi: Ekim 2012).

Iván Darío Bedoya, Andrés Amell Arrieta, Francisco Javier Cadavid, “Effects of mixing system and pilot fuel quality on diesel–biogas dual fuel engine performance”, Gas Science and Technology Group, Faculty of Engineering, University of Antioquia, Colombia, 5 December 2008.

Jiang, Y., Xiong, S., Shi, W., He, W., Zhang, T., Lin, X., Gu, Y., Lu, Y., Qian, X., Ye Z., Wang, C., Wang, B., “Research of biogas as fuel for internal combustion engine”, http://ieeexplore.ieee.org/stamp/stamp.jsp, (erişim tarihi:Ekim 2012).

J. Patterson, A. Clarke and R. Chen**,** “Experimental Study of the Performance and Emissions Characteristics of a Small Diesel Genset Operating in Dual-Fuel Mode with Three Different Primary Fuels”**,** Loughborough University, UK, 2006

J Stewart, A Clarke, and R Chen, “An experimental study of the dual-fuel performance of a small compression ignition diesel engine operating with three gaseous fuels” Department of Aeronautical and Automotive Engineering, University of Loughborough, UK ,Wolfson School of Mechanical and Manufacturing Engineering, University of Loughborough, UK, 11 October 2006.

Kalyan K. Srinivasan, Pedro J. Mago, Sundar R. Krishnan, “Analysis of exhaust waste heat recovery from a dual fuel low temperature combustion engine using an Organic Rankine Cycle”, Department of Mechanical Engineering, Mississippi State University, Mississippi State, MS 39762, USA, 2009

Karim, G. A., Wierzba, I., 1992. “Methane–carbon dioxide mixtures as a fuel”, **SAE Special Publications**, No.927, No: 921557, pp. 81–91

KISTLER Piezoresistive High Pressure Sensor User Manual

Krisada Wannatong, Nirod Akarapanyavit, Somchai Siengsanorh, Somchai Chanchaona, “Combustion and Knock Characteristics of Natural Gas Diesel Dual Fuel Engine”,PTT Research & Technology Institute, PTT Public Company Limited and Department of Mechanical Engineering, King Mongkut’s University of Technology Thonburi, 2007

KUBLER by Turck works Incremental and absolute encoder

Kum. H., “Yenilenebilir enerji kaynakları: Dünya piyasalarındaki son gelismeler ve Politikalar”,**Erciyes Üniversitesi iktisadi ve idari Bilimler Fakültesi Dergisi**, 1999, Sayı: 33: ss.207-223

Liu Shenghua, Zhou Longbao,Wang Ziyan and Ren Jiang,” Combustion characteristics of compressed natural gas/diesel dual-fuel turbocharged compressed ignition engine”,Department of Automotive Engineering, Xi’an Jiaotong University, China, 16 December 2002.

M. G. Galal, M.M. Abdel Aal, M.A. Elkady, “A comparative study between diesel and dual-fuel engines: Performance and Emissions ”, Mechanical Engineering Department, Faculty of Engineering, Al-Azhar University, NasrCity, Cairo, Egypt, 29 May 2002.

M. Masood, M.M. Ishrat, “Computer simulation of hydrogen–diesel dual fuel exhaust gas emissions with experimental verification”, Mechanical Engineering Department, M.J. College of Engineering and Technology, Hyderabad, India, 2007

Mohamed Y.E. Selim,”Effect of engine parameters and gaseous fuel type on the cyclic variability of dual fuel engines”, Mechanical Engineering Department, Faculty of Engineering, United Arab Emirates University, 12 February 2004.

Mohamed Y.E. Selim, “Effect of exhaust gas recirculation on some combustion characteristics of dual fuel engine”, Department of Mechanical Engineering, Faculty of Engineering, United Arab Emirates University, 16 October 2001.

Mohamed Y.E. Selim,”Pressure–time characteristics in diesel engine fueled with natural gas”, Mech. Power Eng. Dept, Faculty of Engineering, Helwan University, Egypt, 17 February 2000.

Mohamed Y.E. Selim, ”Sensitivity of dual fuel engine combustion and knocking limits to gaseous fuel composition”, Department of Mechanical Engineering, Faculty of Engineering, United Arab Emirates University, United Arab Emirates, 26 December 2002.

Motest10 User Manual, TUZEKS Industrial Facility

N.R. Banapurmat, P.G. Tewari, ”Comparative performance studies of a 4-stroke CI engine operated on dual fuel mode with producer gas and Honge oil and its methyl ester (HOME) with and without carburetor”, Department of Mechanical Engineering, B.V.B. College of Engineering and Technology, India, 2008

O. Badr, G.A. Karim, B. Liu, “An examination of the flame spread limits in a dual fuel engine”, The University of Calgary, Department of Mechanical Engineering, 3 March 1998.

O. Mınwafor, “Knock characteristics of dual-fuel combustion in diesel engines using natural gas as primary fuel”, Department of Mechanical Engineering, Federal University of Technology, Nigeria, 2001

Phan Minh Duc, Kanit Wattanavichien," Study on biogas premixed charge diesel dual fuelled engine" ,Mechanical Engineering Department, Faculty of Engineering, Chulalongkorn University, Thailand, 22 July 2006.

Porpatham, E., Ramesh, A., Nagalingam, B., 2008. "Investigation on the effect of concentration of methane in biogas when used as a fuel for a spark ignition engine", **Fuel** 87: 1651–1659.

Rakopoulos, C. D., Michos, C. N., 2009. Generation of combustion irreversibilities in a spark ignition engine under biogas–hydrogen mixtures fueling, **Int. Journal of Hydrogen Energy,** 34; 4422 – 4437.

R.G. Papagiannakis, D.T. Hountalas, **"**Combustion and exhaust emission characteristics of a dual fuel compression ignition engine operated with pilot Diesel fuel and natural gas", Department of Mechanical Engineering, Thermal Engineering Section, National Technical University of Athens, 23 July 2003.

R.G. Papagiannakis, C.D. Rakopoulos, D.T. Hountalas, D.C. Rakopoulos, "Emission characteristics of high speed, dual fuel, compression ignition engine operating in a wide range of natural gas/diesel fuel proportions", Thermodynamic and Propulsion Systems Section, Aeronautical Sciences Department, Hellenic Air Force Academy, Greece. Internal Combustion Engines Laboratory, Thermal Engineering Department, School of Mechanical Engineering, National Technical University of Athens, Greece, 29 September 2009.

R.G. Papagiannakis, D.T. Hountalas, "Experimental investigation concerning the effect of natural gas percentage on performance and emissions of a DI dual fuel diesel engine", Internal Combustion Engines Laboratory, Thermal Engineering Section, Mechanical Engineering Department, National Technical University of Athens, Greece, 12 January 2002.

Saiful Bari, "Effect of carbon dioxide on the performance of biogas diesel duel-fuel engine" School of Mechanical Engineering, Universiti Sains Malaysia, 1996.

Saygın, H., 2004. Sürdürülebilir gelişme gündeminde nükleer enerjinin sorunları, **Elektrik Mühendisliği Dergisi**, Kasım (423): ss.32-40.

Seung Hyun Yoon, Chang Sik Lee, "Experimental investigation on the combustion and exhaust emission characteristics of biogas–biodiesel dual-fuel combustion in a CI engine", Graduate School of Hanyang University, Republic of Korea and School of Mechanical Engineering, Hanyang University, Republic of Korea, 2011

Siripornakarachai, S., Sucharitakul, T., 2007. "Modification and tuning of diesel bus engine for biogas electricity production", **Mj. Int. J. Sci. Tech**., 01(2): 194-207.

S Singh, L Liang, S-C Kong, and R D Reitz, “Development of a flame propagation model for dual-fuel partially premixed compression ignition engines”, Engine Research Center, The University of Wisconsin, USA, 2005

Stone, C. R., Gould, J. nd Ladommatos, N., 1993. “Analysis of biogas combustion in sparkignition engines, by means of experimental data and a computer simulation”, **J.Inst. Energy**, vol. 66, pp. 180-187.

T. Korakianitis, A.M. Namasivayam, R.J. Crookes, “Diesel and rapeseed methyl ester (RME) pilot fuels for hydrogen and natural gas dual-fuel combustion in compression–ignition engines”, School of Engineering and Materials Science, Queen Mary University of London, UK, 2011

T. Lakshmanan, G. Nagarajan, “Experimental investigation on dual fuel operation of acetylene in a DI diesel engine”, Department of Mechanical Engineering, Rajarajeswari Engineering College, India and Internal Combustion Engineering Division, College of Engineering, Anna University, India, 2009

T. Lakshmanan, G. Nagarajan, “Experimental investigation of timed manifold injection of acetylene in direct injection diesel engine in dual fuel mode”, Department of Mechanical Engineering, Rajarajeswari Engineering College, India and Internal Combustion Engineering Division, College of Engineering, Anna University, India, 2010

Turkcan A., “Bir Dizel Motorun Performans Parametrelerinin Deneysel Tespiti”, Kocaeli Üniversitesi Fen Bilimleri Enstitüsü Makine Eğitimi, 2006

Uyarel A.Y., Erşan K., 1987. “İçten yanmalı motorlarda biyogaz kullanımı ve motor performansına etkisi”, **Gazi Üniversitesi Teknik Eğitim Fakültesi Dergisi** Cilt 1, 7 –61,

V. Pirouzpanah, R. Khoshbakhti Saray, A. Sohrabi, A. Niaei, “Comparison of thermal and radical effects of EGR gases on combustion process in dual fuel engines at part loads” Faculty of Mechanical Engineering, University of Tabriz, Iran, Faculty of Mechanical Engineering, University of Amirkabir, Iran, Chemical Engineering Department, University of Tabriz, Iran, 2007

www.reotemp.com

www.car-engineer.com

Willard W. Pulkrabek Engineering Fundamentals of the Internal Combustion Engine

wikipedia.org

Z Liu and G A Karim," Simulation of combustion processes in gas-fuelled diesel engines**",**Department of Mechanical Engineering, The University of Calgary, Canada, 4 April 1996.